

# Atomic Spectroscopy

---

May/June 2004

Volume 25, No. 3

## In This Issue:

Determination of Pt in Biological Fluids With ICP-MS: Evaluation of Analytical Uncertainty

**M. Bettinelli, S. Spezia, A. Ronchi, and C. Minoia** ..... 103

Determination of Selected Trace Elements in Raw Clams and Commercial Clam Meats From the State of Miranda (Venezuela) Employing ICP-OES, GF-AAS, and WD-XRF

**John J. LaBrecque, Zully Benzo, Juan A. Alfonso, Perdo R. Codoves, Manuelita Quintal, Clara V. Gomez, and Eunice Marcano** ..... 112

Characterization of Hyphenated HPIC/ICP-OES System Response for Iron Speciation in Natural Waters

**Sanda Roncevic and Ilse Steffan** ..... 125

Evaluation of Sample Treatment for the Simultaneous Flow Injection Hydride Generation and Determination of As, Bi, Sb and Se by GFAAS

**Carolina D. Freschi, Gian Paulo G. Freschi, and José A. Gomes Neto**..... 133

Determination of Al, Cd, and Pb in Brazilian Sugar Cane Spirit, Cachaça, by ETAAS Using Matrix-matched Calibration

**Marcus H. Canuto, Helmuth G. L. Siebald, Milton Batista Franco, and José Bento Borba Silva** ..... 140

Flow Injection On-line Sorption Preconcentration Coupled With Cold Vapor Atomic Fluorescence Spectrometry and On-line Oxidative Elution for the Determination of Trace Mercury in Water Samples

**Li-Ping Yu and Xiu-Ping Yan** ..... 145

---

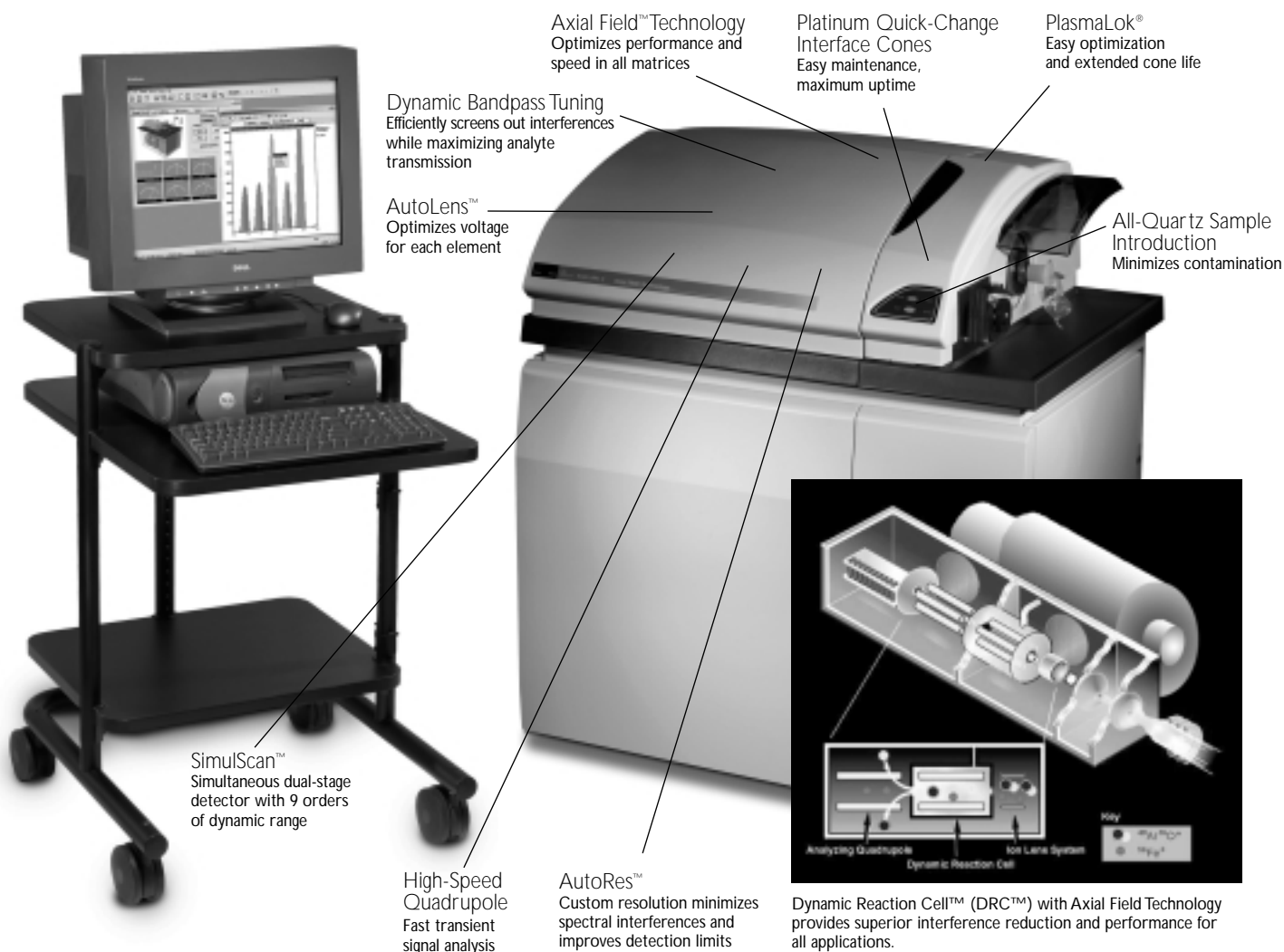
ASPND7 25(3) 103–156 (2004)  
ISSN 0195-5373

Issues also  
available  
electronically.

(see inside back cover)



**PerkinElmer**<sup>®</sup>  
precisely.



## Eliminates interferences COMPLETELY

When your applications extend beyond the capabilities of conventional ICP-MS, you need the power of the innovative ELAN® DRC II. The DRC II combines the power of patented Dynamic Reaction Cell (DRC) technology with performance-enhancing Axial Field Technology, providing uncompromised sensitivity and performance in all matrices for even the toughest applications. Unlike collision cell, high-resolution, or cold plasma systems, the DRC II completely eliminates polyatomic interferences providing ultratrace-level detection limits.

The DRC II uses chemical resolution to eliminate plasma-based polyatomic species before they reach the quadrupole mass spectrometer. This ion-molecule chemistry uses a gas to “chemically scrub” polyatomic or isobaric species from the ion beam before they enter the analyzer, resulting in improved detection limits for elements such as Fe, Ca, K, Mg, As, Se, Cr, and V.

Unlike more simplistic collision cells, patented DRC technology not only reduces the primary interference; it eliminates sequential side reactions that create new interferences. Unless kept in check by DRC technology, these uncontrolled reactions increase spectral complexity and create unexpected interferences.

# Determination of Pt in Biological Fluids With ICP-MS: Evaluation of Analytical Uncertainty

\*M. Bettinelli, S. Spezia, A. Ronchi, and C. Minoia  
Laboratory for Environmental and Toxicological Testing  
S. Maugeri Foundation, Via Ferrata 8, 29100 Pavia, Italy

## INTRODUCTION

Chrysotherapy with Pt-based drugs is gaining increasing importance, especially in the treatment of solid tumors, testicular and ovarian tumors, head, neck, and bladder carcinomas, and brain malignancies (1,2).

A variety of oral analogues of known antitumor agents have been developed in the past few years for economic, pharmacological, and practical reasons. To merit further clinical development, the oral analogue should have a preclinical antitumor activity and toxicity comparable to those of parent compound, with only limited gastrointestinal toxicity, acceptable bioavailability, safe and reproducible pharmacokinetic profile.

A series of ammine/amine Pt(IV) dicarboxylates of higher lipophilicity and stability than cisplatin and carboplatin have been developed in an effort to improve absorption and decrease the metabolic activation through processes in the gastrointestinal track (3).

From this point of view, it is essential to correctly interpret the mechanism by which platinum compounds act in order to optimize the therapies that have been proposed to date and to develop adequate analytical methods for monitoring the Pt levels in biological fluids.

Method validation is the process of proving that an analytical method is acceptable for its intended purpose. For pharmaceutical methods, guidelines from United States Pharmacopeia (USP) (4), International Conference on

## ABSTRACT

Estimation of the uncertainty associated with analytical methods is necessary in order to establish comparability of the results. Methods of Pt determination in biological fluids very often lack of information about the uncertainty of results. This has implications when results are used to interpret the mechanism of platinum compounds, or when the results are considered to optimize clinical therapies.

An ICP-MS method for the determination of Pt in biological fluids (plasma, ultrafiltrate, and urine) of patients treated with antitumor agents has been developed and validated. The limits of quantification (LOQ) in the three matrices were 1.0, 0.1, and 2.0  $\mu\text{g L}^{-1}$ , respectively.

Intra-day and inter-day precision and accuracy were in good agreement with the FDA criteria for validation of the analytical methods. The validation study was implemented by assessing the uncertainty evaluation for Pt determination in the different matrices according to the EURACHEM/CITAC Guide.

Harmonization (ICH) (5), and the Food and Drug Administration (FDA) (6) provide a framework for performing such validations. In general, methods for regulatory submission must include studies on specificity, linearity, accuracy, precision, range, detection limit, quantitation limit, and robustness.

Today, it is generally acknowledged that the fitness of an analytical result cannot be assessed without some estimate of the measurement uncertainty for comparison with the confidence required. The Guide to the Expression of

Uncertainty in Measurement (GUM) published by ISO (7) establishes general rules for evaluating and expressing uncertainty for a wide range of measurements. The guide was interpreted for analytical chemistry by EURACHEM in 2000 (8). The approach described in the GUM requires the identification of all possible sources of uncertainty associated with the procedure, the estimation of their magnitude from either experimental or published data, and the combination of these individual uncertainties to give standard and expanded uncertainties for the procedure as a whole. However, the GUM principles are significantly different from the methods currently used in analytical chemistry for estimating uncertainty which generally make use of "whole method" performance parameters, such as precision, recovery, and ruggedness. The purpose of this paper is to underline that if validation studies are properly planned and executed, the data produced can easily be handled in the uncertainty estimation process.

## EXPERIMENTAL

### Instrumentation

The PerkinElmer SCIEX ELAN<sup>®</sup> 5000 Inductively Coupled Plasma Mass Spectrometer (PerkinElmer SCIEX, Concord, Ontario, Canada) was designed for routine and rapid multielement quantitative determinations of trace and ultratrace elements and isotopes (6).

An IBM<sup>®</sup> PS/2 Model 70 386, equipped with an operating system Xenix<sup>®</sup> 386 (Version 2.3.4) and an Intel<sup>®</sup> 80386 microprocessor, controls the ELAN ICP-MS.

The instrument is equipped with a Cool Flow CFT-75 NESLAB chiller (Neslab, Portsmouth, New Hampshire,

\*Corresponding author.  
E-mail: mbettinelli@fsm.it

USA) and a Model AS-90 Autosampler (PerkinElmer Life and Analytical Sciences, Shelton, CT, USA).

To optimize the ICP-MS signal, a standard solution (Number N812-2014) containing 10 µg/L of three elements that covered the entire mass range (for example, <sup>24</sup>Mg, <sup>103</sup>Rh, and <sup>208</sup>Pb) was used. A fourth isotope, <sup>197</sup>Au, was used to monitor background noise in the system. Typically, the intensity values obtained for 10 µg/L were as follows: <sup>24</sup>Mg ≥ 5,000 ions/sec., <sup>103</sup>Rh ≥ 30,000 ions/sec., <sup>208</sup>Pb ≥ 5,000 ions/sec., and <sup>197</sup>Au ≤ 20 ions/sec.

The instrumental specifications and the analytical conditions are reported in Table I.

#### Reagents and Standard Solutions

- Platinum (PtCl<sub>2</sub>, 10% HCl) and iridium (IrCl<sub>3</sub>·3H<sub>2</sub>O, 10% HCl) were provided by BDH Laboratory Supplies, England.

- Nitric acid 65% (m/v) Suprapur™ was provided by Merck, Darmstadt, Germany.

- Water used for the ICP-MS analysis was prepared in-house using a Milli-RO 10 PLUS, Milli-Q™

185 PLUS purifier (Millipore, Bedford, MA, USA).

A platinum chloride stock solution of 1 g/L was diluted (1:10 v/v) in ultrapure water (Milli-RO 10 PLUS, Milli-Q 185 PLUS, Millipore) to obtain working solutions for the preparation of calibration curves and quality control samples.

In order to reduce the matrix effect, <sup>193</sup>Ir was used as an internal standard. The iridium chloride stock solution of 1 g L<sup>-1</sup> was diluted (1:10 v/v) in ultrapure water to obtain the working solution.

#### Preparation of Calibration Curves and Quality Control Samples

Aliquots of the working solutions were spiked into blank pooled human plasma [diluted 1:30 (v/v) with 1% HNO<sub>3</sub> (v/v)] to reproduce concentrations of 1, 10, 50, 100, 200 µg L<sup>-1</sup>, and into plasma ultrafiltrate samples [diluted 1:30 (v/v) with 1% HNO<sub>3</sub> (v/v)] to reproduce concentrations of 0.01, 0.1, 1, 10, 20 µg L<sup>-1</sup>. These samples were used as calibration standards.

The same working solutions were used for the preparation of the quality control samples (QC) at three different concentrations: 2, 41, 152 µg L<sup>-1</sup> for blank human plasma and 0.02, 6, 18 µg L<sup>-1</sup> for blank plasma ultrafiltrate.

One µg L<sup>-1</sup> Ir was used as an internal standard and was added to all samples employed for the preparation of calibration curves and quality control samples.

Aliquots of the working solutions were spiked into blank pooled human urine [diluted 1:50 (v/v) with 1% HNO<sub>3</sub> (v/v)] to reproduce concentrations of 2, 10, 50, 100, 200 µg L<sup>-1</sup>. These samples were used as calibration standards.

The same working solutions were used for the preparation of the quality control samples (QC) at

three different concentrations: 5, 40, 160 µg L<sup>-1</sup>; 3 µg L<sup>-1</sup> Ir used as an internal standard was added to all the samples employed for the preparation of calibration curves and quality control samples.

#### Sampling Procedure

Five-mL blood samples were collected in a tube containing EDTA at the following times: T = 0, 0.5, 1, 2, 3, 4, 6, 8, 12, 24 hours; all blood samples were immediately centrifuged at 2000 rpm for 15 min at 4°C and the plasma removed.

The plasma was separated and divided in two portions: one for the determination of total Pt (TPt) and the other for the preparation of free Pt species (UPt, unbound Pt). Separation of UPt species was performed by centrifugal ultrafiltration using a modified version of the method of Bannister et al. (6).

A portion of 2 mL from each plasma sample was placed into a microconcentrator Centricon-10 (Amicon Corp., Dan, MA, USA) having a cut-off value of 30000 daltons, and was centrifuged at 2000 rpm for 30 min at 4°C.

Two urine samples (fraction 0–8 hours and 8–24 hours) were collected during the treatment on days 1 and 14, the volume measured and stored at -20°C until analysis.

#### Sample Handling

Plasma, ultrafiltrate, and urine samples were thawed in a warm bath immediately before analysis.

Plasma and ultrafiltrate samples were diluted [1:30 (v/v)] in polypropylene tubes, with 1% HNO<sub>3</sub> (v/v). After addition of 1 µg L<sup>-1</sup> Ir as an internal standard, the samples were analyzed by ICP-MS. The sample uptake rate was of 1.0 mL/min.

Urine samples were diluted [1:50 (v/v)] in polypropylene tubes, with 1% HNO<sub>3</sub> (v/v). After addition of 3 µg L<sup>-1</sup> Ir as internal standard,

TABLE I

#### Instrumental Specifications and Analytical Conditions

Element/mass	<sup>195</sup> Pt
Internal standard	<sup>193</sup> Ir
Replicate time	900 ms
Dwell time	300 ms
Scanning mode	Peak hopping
Sweeps/reading	3
Number of replicates	10
Points/spectral peak	1
Resolution	Normal
Power	1100 W
Plasma argon	12 L/min
Auxiliary argon	0.80 L/min
Nebulizer argon	0.99 L/min

the samples were analyzed by ICP-MS. The sample uptake rate was of 1.0 mL/min.

## RESULTS AND DISCUSSION

### Specificity

The two major sources of analytical inaccuracy during ICP-MS analyses are matrix-induced signal suppression and spectral interferences.

In the case of matrix-induced signal suppression, the ion intensity of an analyte element is somewhat dependent upon the total composition of the sample. For a matrix of unknown composition, the method of standard addition calibration, in which known concentrations of standards are added directly to a sample solution, compensate for the difference in sensitivity between samples and standards.

Spectral interferences may originate from several sources: isobaric overlaps, plasma-induced polyatomic ions, matrix solvent-induced polyatomic ions, and matrix-induced polyatomic ions (7). Considering the natural abundance and potential interferences of Pt isotopes reported in Table II and preliminary studies not reported in the present paper, the  $^{195}\text{Pt}$  was identified as the isotope with the lowest number of interferences.

Under the described experimental conditions, no significant interference on Pt in human urine, plasma and ultrafiltrate matrix was observed in the drug-free samples, as shown for plasma by a representative ICP-MS spectrum (Figure 1).

An ICP-MS spectrum of the "blank" plasma sample enriched with 10  $\mu\text{g/L}$   $\text{PtCl}_2$  is given in Figure 2; Pt-measured isotopes correspond to the signal at 194, 195 and 196 amu.

Figure 3 shows a spectrum of a real sample obtained from a subject treated with an anticancer agent.

**TABLE II**  
**Natural Abundance and Potential Interferences of Pt Isotopes**

Pt Mass	Abundance	Potential Interferences
189.961	0.013%	Os, YbO, HfO
191.961	0.780%	Os, YbO, HfO, LuO
193.961	32.900%	YbO, HfO
194.961	33.800%	HfO
195.969	25.300%	Hg, HfO, WO, TaO
197.969	7.210%	Hg, HfO, WO, TaO

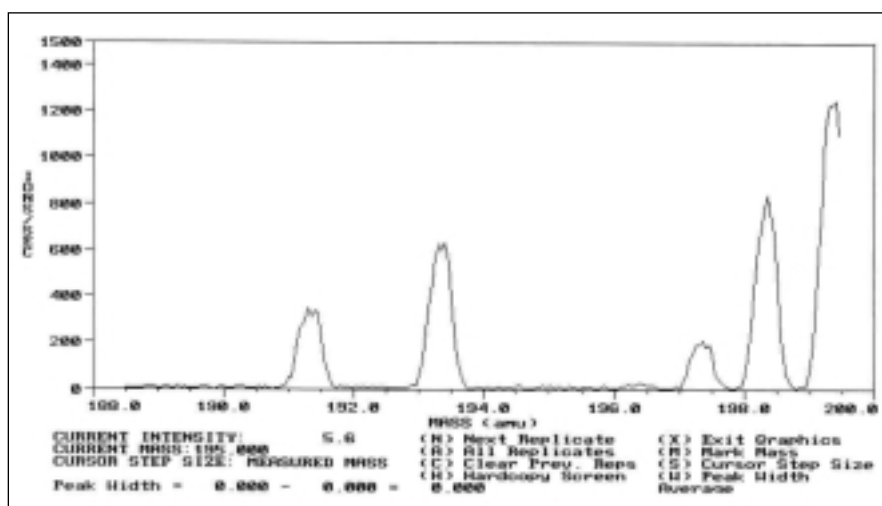


*Fig. 1. Spectrum of human blank plasma sample spiked with 1  $\mu\text{g/L}$  Ir. No interfering signal was present in the mass range of interest (194 – 196 amu).*

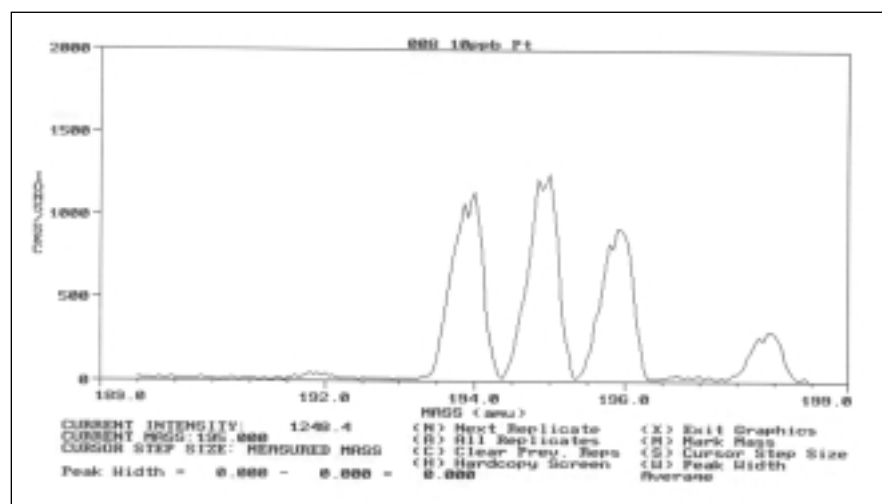


*Fig. 2. Spectrum of human blank plasma sample enriched with 10  $\mu\text{g/L}$  Pt.*

## Linearity

The standard addition method was used for plasma, ultrafiltrate, and urine matrices.

The calibration curves were established by plotting the current intensity (ions/sec) ratio between  $^{195}\text{Pt}$  and the internal standard ( $^{193}\text{Ir}$ ) against the concentration of Pt. Slopes and intercepts were determined by linear regression analysis.

## Accuracy and Precision

As CRMs are not available for Pt determination in blood and urine matrices, the accuracy and precision were evaluated on spiked samples at three different concentrations.

Intra-day and inter-day precision and accuracy were assessed by replicate determinations of Pt concentration added as  $\text{PtCl}_2$  to the blank human plasma, human plasma ultrafiltrate, and the urine on the same day and on three different days, respectively. The precision of the method was calculated as the coefficient of variation of the mean value found at each concentration level (one near the lower limit of quantitation, one near the middle, and one near the upper boundary of the calibration curve). The accuracy, expressed as the percent of recovery, was calculated as the ratio of the concentration found to the spiked concentration value.

## Limit of Detection (LOD) and Limit of Quantification (LOQ)

The instrumental detection limit (LOD) was evaluated on the basis of the  $3\sigma$  criterion by analyzing five "blanks" of plasma, ultrafiltrate, and urine on three non-consecutive days.

For the LOQ, we adopted the criterion reported by the FDA (8) "as the lowest concentration that can be determined with a satisfac-

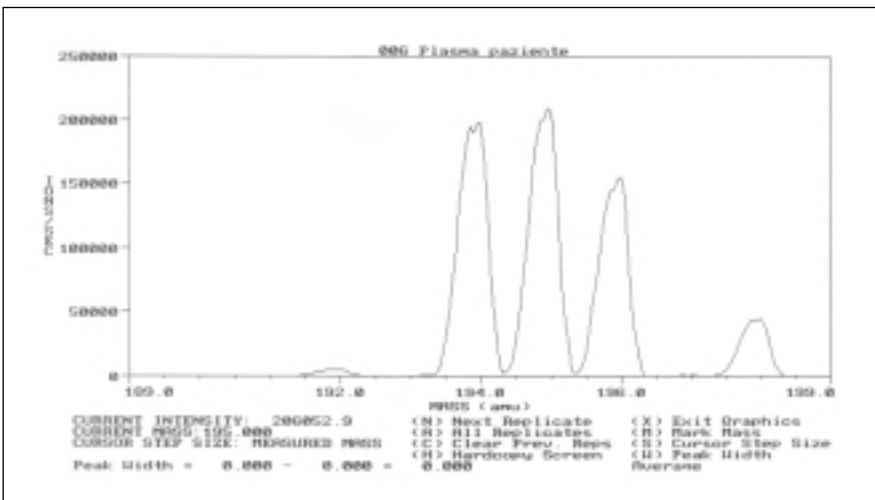


Fig. 3. Spectrum of real human plasma sample obtained from a subject treated with anticancer agent.

tory degree of accuracy (deviation from nominal value  $\leq 20\%$ ) and precision ( $\text{CV} \leq 20\%$ ) to provide pharmacokinetically useful results." In the case of plasma and urine analysis, considering that the concentrations of interest were one order of magnitude higher than those in ultrafiltrate, the LOQ was set at 1 and  $2 \mu\text{g L}^{-1}$ , respectively.

## Plasma and Ultrafiltrate

Matrix-matched calibration was achieved by adding dilute Pt standard solution to pooled plasma or ultrafiltrate samples and kept at  $-20^\circ\text{C}$  until use.

For plasma, the mean slope and intercept values of the calibration curves ( $0\text{--}200 \mu\text{g L}^{-1}$ ) obtained over a three-day validation period were: slope =  $0.199 \pm 0.008$  ( $\text{CV} = 3.86\%$ ) and intercept =  $-0.055 \pm 0.043$  with a correlation coefficient better than 0.9996.

For ultrafiltrate plasma, the statistical parameters for the calibration curves ( $0\text{--}20 \mu\text{g L}^{-1}$ ) obtained over a three-day validation period were: slope =  $0.376 \pm 0.042$  ( $\text{CV} = 11.1\%$ ) and intercept =  $-0.005 \pm 0.006$  with a correlation coefficient better than 0.9989.

Intra-day and inter-day accuracy and precision of the method for the determination of platinum in human plasma and ultrafiltrate samples are reported in Tables III and IV, respectively.

Intra-day precision and accuracy for Pt determination in human plasma samples ranged, respectively, between 0.14 and 2.01, and 99.7 and 103.2 (C.V.%), whereas in the ultrafiltrate they ranged between 0.03 and 5.22, and 97.5 and 108.0 (C.V.%). Slightly better ranges of inter-day precision and accuracy were achieved for plasma with respect to ultrafiltrate, probably due to the higher Pt concentrations investigated.

The instrumental detection limit (LOD) was  $0.002 \mu\text{g L}^{-1}$  with a minimum quantifiable platinum concentration (LOQ) for ultrafiltrate equal to  $0.01 \mu\text{g L}^{-1}$ . In the case of plasma analysis, the concentrations of interest were one order of magnitude higher than those in ultrafiltrate samples; therefore, the LOQ was set at  $1 \mu\text{g L}^{-1}$ .

**TABLE III**  
**Accuracy and Precision in the Determination of Pt in Human Plasma Samples,**  
**Evaluated on Three Different Days**

Nominal Concentration ( $\mu\text{g L}^{-1}$ )	QC1 (2 $\mu\text{g L}^{-1}$ )	QC2 (41 $\mu\text{g L}^{-1}$ )	QC3 (152 $\mu\text{g L}^{-1}$ )	LOQ (1 $\mu\text{g L}^{-1}$ )
<u>1st day</u>				
Found Concentrations ( $\mu\text{g L}^{-1}$ )				
Intra-day Mean $\pm$ S.D.	2.06 $\pm$ 0.02	41.14 $\pm$ 0.29	152.16 $\pm$ 0.55	1.032 $\pm$ 0.005
Intra-day C.V. (%)	0.87	0.70	0.36	0.46
Intra-day Accuracy (%)	103.2	100.3	100.1	103.2
<u>2nd day</u>				
Intra-day Mean $\pm$ S.D.	2.01 $\pm$ 0.04	40.88 $\pm$ 0.06	152.14 $\pm$ 0.32	1.032 $\pm$ 0.028
Intra-day C.V. (%)	2.01	0.14	0.21	2.69
Intra-day Accuracy (%)	100.5	99.7	100.1	103.2
<u>3rd day</u>				
Intra-day Mean $\pm$ S.D.	1.99 $\pm$ 0.03	41.17 $\pm$ 0.70	151.93 $\pm$ 0.50	1.037 $\pm$ 0.017
Intra-day C.V. (%)	1.57	1.70	0.33	1.64
Intra-day Accuracy (%)	99.7	100.4	99.9	103.7
<u>Inter-day Accuracy and Precision</u>				
Mean ( $\mu\text{g L}^{-1}$ )	2.02 $\pm$ 0.04	41.06 $\pm$ 0.40	152.08 $\pm$ 0.42	1.034 $\pm$ 0.017
C.V. (%)	2.05	0.98	0.28	1.61
Accuracy (%)	101.1	100.2	100.1	104.6

**TABLE IV**  
**Accuracy and Precision in the Determination of Pt in Human Plasma Ultrafiltrate Samples,**  
**Evaluated on Three Different Days**

Nominal Concentration ( $\mu\text{g L}^{-1}$ )	QC1 (0.02 $\mu\text{g L}^{-1}$ )	QC2 (6 $\mu\text{g L}^{-1}$ )	QC3 (18 $\mu\text{g L}^{-1}$ )	LOQ (0.001 $\mu\text{g L}^{-1}$ )
<u>1st day</u>				
Found Concentrations ( $\mu\text{g L}^{-1}$ )				
Intra-day Mean $\pm$ S.D.	0.019 $\pm$ 0.001	6.024 $\pm$ 0.142	17.78 $\pm$ 0.01	0.0098 $\pm$ 0.0008
Intra-day C.V. (%)	3.36	2.36	0.03	8.10
Intra-day Accuracy (%)	97.50	100.40	98.78	98.0
<u>2nd day</u>				
Intra-day Mean $\pm$ S.D.	0.022 $\pm$ 0.001	5.975 $\pm$ 0.070	18.02 $\pm$ 0.14	0.0108 $\pm$ 0.0007
Intra-day C.V. (%)	5.22	1.18	0.77	6.52
Intra-day Accuracy (%)	108.00	99.59	100.13	107.7
<u>3rd day</u>				
Intra-day Mean $\pm$ S.D.	0.0201 $\pm$ 0.0003	5.981 $\pm$ 0.061	18.06 $\pm$ 0.24	0.0108 $\pm$ 0.0006
Intra-day C.V. (%)	1.55	1.02	1.33	5.56
Intra-day Accuracy (%)	103.83	99.69	100.31	108.0
<u>Inter-day Accuracy and Precision</u>				
Mean $\pm$ S.D.	0.021 $\pm$ 0.001	5.993 $\pm$ 0.088	17.95 $\pm$ 0.19	0.0105 $\pm$ 0.0008
C.V. (%)	5.51	1.47	1.06	7.49
Accuracy (%)	103.11	99.89	99.74	104.6

**TABLE V**  
**Accuracy and Precision in the Determination of Pt in Human Urine Samples,**  
**Evaluated on Three Different Days**

Nominal Concentration ( $\mu\text{g L}^{-1}$ )	QC1 (5 $\mu\text{g L}^{-1}$ )	QC2 (40 $\mu\text{g L}^{-1}$ )	QC3 (160 $\mu\text{g L}^{-1}$ )	LOQ (2 $\mu\text{g L}^{-1}$ )
<u>1st day</u>				
Found Concentrations ( $\mu\text{g L}^{-1}$ )				
Intra-day Mean $\pm$ S.D.	5.037 $\pm$ 0.010	40.07 $\pm$ 0.09	160.12 $\pm$ 0.42	2.091 $\pm$ 0.012
Intra-day precision (C.V.%)	0.19	0.23	0.26	0.58
Intra-day Accuracy (mean found/added %)	100.7	100.2	100.1	104.6
<u>2nd day</u>				
Intra-day Mean $\pm$ S.D.	5.009 $\pm$ 0.004	40.05 $\pm$ 0.05	159.96 $\pm$ 0.94	2.068 $\pm$ 0.017
Intra-day precision (C.V.%)	0.08	0.11	0.59	0.81
Intra-day Accuracy (mean found/added %)	100.2	100.1	99.9	103.4
<u>3rd day</u>				
Intra-day Mean $\pm$ S.D.	5.021 $\pm$ 0.083	39.98 $\pm$ 0.08	159.94 $\pm$ 0.33	2.119 $\pm$ 0.012
Intra-day precision (C.V.%)	1.66	0.21	0.21	0.57
Intra-day Accuracy (mean found/added %)	100.4	99.9	100.0	105.9
<u>Inter-day Accuracy and Precision</u>				
Mean $\pm$ S.D.	5.023 $\pm$ 0.044	40.032 $\pm$ 0.078	160.01 $\pm$ 0.55	2.093 $\pm$ 0.025
Precision (C.V.%)	0.87	0.20	0.34	1.20
Accuracy (mean found/added %)	100.46	100.08	100.00	104.6

### Urine

Matrix-matched calibration was achieved by adding dilute Pt standard solution to pooled urine samples, previously centrifuged to remove the sediment, and kept at  $-20^{\circ}\text{C}$  until use.

The mean slope and intercept values of the calibration curves (0–200  $\mu\text{g/L}$ ) obtained over a three-day validation period were: slope =  $0.128 \pm 0.04$  (CV= 2.97%) and intercept =  $0.033 \pm 0.041$  with a correlation coefficient better than 0.9999.

The detection limit (LOD) was  $0.002 \mu\text{g L}^{-1}$  with a minimum quantifiable platinum concentration (LOQ) set at  $2 \mu\text{g L}^{-1}$ .

Intra-day and inter-day accuracy and precision of the method for the determination of platinum in human urine samples are reported in Table V.

Intra-day precision, expressed as CV%, ranged between 0.08 and

0.59 (with only one value higher than 1%), and intra-day accuracy, calculated as the percentage recovery of the spiked samples, ranged on average between 99.9 and 100.7%. Precision lower than 1% and accuracy very close to 100% were achieved during the inter-day evaluation. Accuracy and precision for urine samples at the LOQ concentration are reported in Table V.

The results obtained in the present study meet to the FDA criteria for the validation of analytical methods (3). For each concentration level, the mean value is within  $\pm 15\%$  of the nominal value (at the LOQ within  $\pm 20\%$ ), and the coefficient of variation (CV) around the mean value is lower than  $\pm 15\%$  (at the LOQ  $\pm 20\%$  for the CV is accepted).

These results prove that, in keeping with international standards, the method is adequate for the assay of platinum in human plasma and urine samples.

### Uncertainty Evaluation From Validation Data

The validation study of the present assay was implemented by assessing the uncertainty evaluation for Pt in the different matrices at the four levels of concentration. According to the EURACHEM/CITAC Guide (23), the combined uncertainty ( $u_{\text{combined}}$ ) has been calculated by estimating the components associated with the repeatability ( $u_{\text{repeatability}}$ ), the instrumental calibration ( $u_{\text{calibration}}$ ), and the sampling ( $u_{\text{sampling}}$ ). The uncertainty component due to the recovery ( $u_{\text{recovery}}$ ) was not considered because the calibration curve was performed by standard addition method (in the same matrix as the sample), determining the analytes according to the procedure described in the Experimental section.

Consequently, the equation that best represents the mathematical model upon which the relative



uncertainty is evaluated is taken to be:

$$u_{(Comb.)} = \sqrt{\frac{(u_{(Repeat.)})^2 (u_{(Calib.)})^2 (u_{(Samp.)})^2}{(Repeat.) (Calib.) (Samp.)}}$$

$$u_{(Comb.)} = \sqrt{(u_{(Repeat.)})^2 + (u_{(Calib.)})^2 + (u_{(Samp.)})^2}$$

where:

$u_{(Comb)}$  = combined relative uncertainty

$u_{(Repeat.)}$  = relative uncertainty of repeatability

$u_{(Calib.)}$  = relative uncertainty of calibration

$u_{(samp.)}$  = relative uncertainty of sampling

In order to investigate the contributions of all components to the combined relative uncertainty as a function of Pt concentration (in plasma, ultrafiltrate, and urine), these uncertainties were evaluated and plotted in Figures 4, 5, and 6, respectively.

With respect to Pt in plasma and urine, the graphs show that the relative uncertainty ranges from 4–7% at 1–2  $\mu\text{g L}^{-1}$  and go down to 2–3% for the higher concentrations (40–150  $\mu\text{g L}^{-1}$ ).

While the uncertainty component associated with the repeatability is constant (0.5–2%), overall the different concentration levels and the different days, the component due to the instrumental calibration increases significantly (7–8%) relative to the lowest concentrations of analyte.

With respect to Pt in the plasma ultrafiltrate, Figure 5 shows that the relative uncertainty ranges from 4–5% at 8–16  $\mu\text{g L}^{-1}$  and increases up

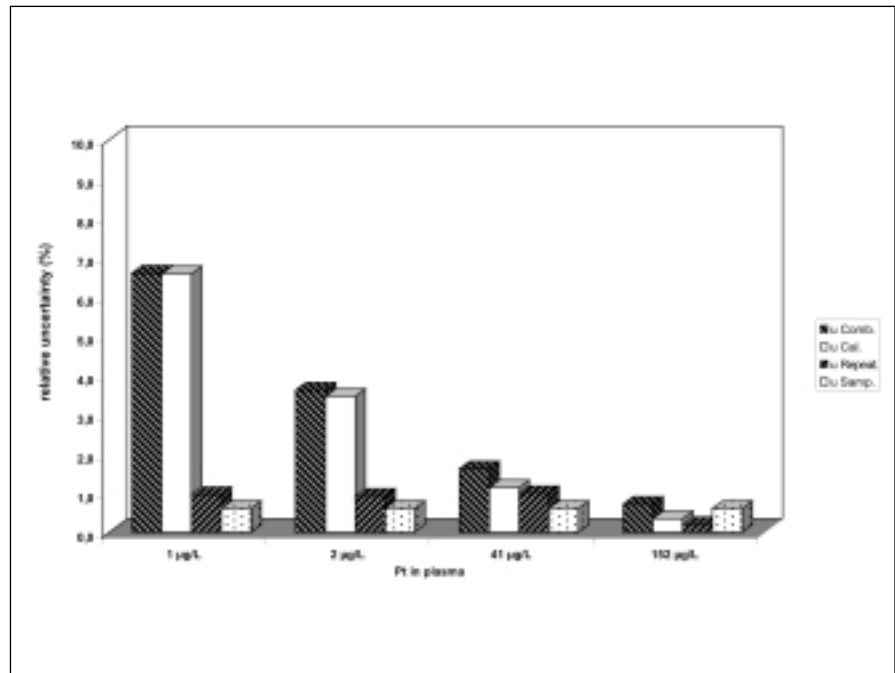


Fig. 4. Relative Uncertainty Values (%) obtained at different concentration levels for Pt in human plasma.

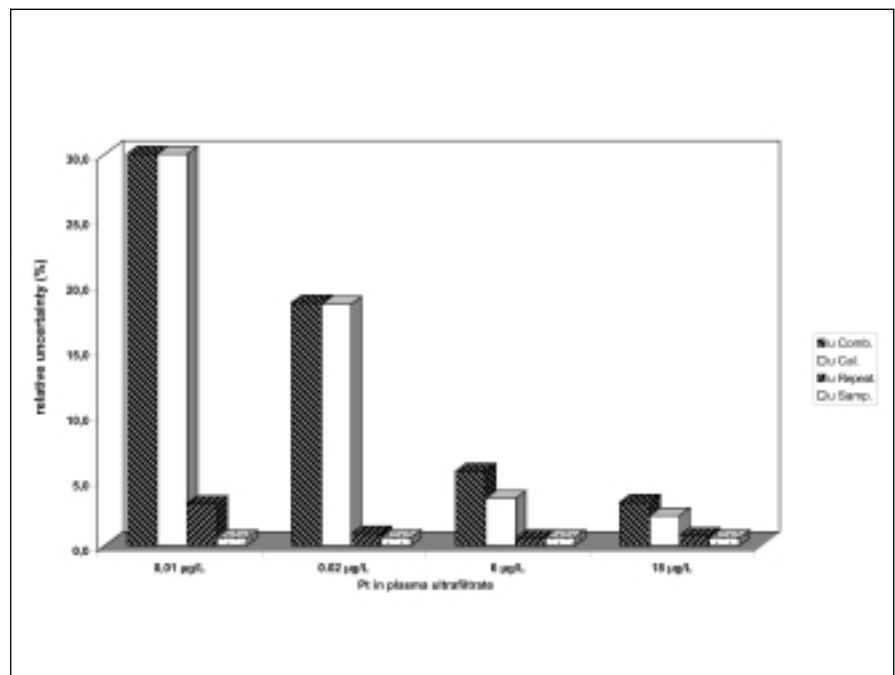


Fig. 5. Relative Uncertainty Values (%) obtained at different concentration levels for Pt in human plasma ultrafiltrate.

to 20–30% for the lower concentrations (at 0.01–0.02  $\mu\text{g L}^{-1}$ ).

This occurrence means that the quantitative determination of low concentrations of Pt in the ultrafiltrate is greatly affected by the uncertainty assignable to the instrumental calibration as done in the present study (0–20  $\mu\text{g L}^{-1}$ ). Further tests performed show that by reducing the calibration range but keeping the same number of concentration levels (n=6) gives better values of combined uncertainty as a consequence of a significant improvement of the uncertainty component due to calibration. The mathematical function (9) used for the calculation of uncertainty of ( $x_{\text{pred}}$ ) due to calibration is the following:

$$u(x_{\text{pred}}) = \frac{s^2_{y/q} \sqrt{\frac{1}{m} + \frac{1}{n} + \frac{(x_{\text{pred}} - \bar{x}_{\text{Cal}})^2}{\sum (x_i - \bar{x}_{\text{Cal}})^2}}}{b}$$

where:

$s^2_{y/q}$  is the residual variance of the regression model

b is the slope of the regression curve

m is the number of repetitions from which is derived the predicted value

n is the number of calibration points on the regression line

$x_{(\text{pred})}$  is the predicted value

$\bar{x}_{(\text{Cal})}$  is the mean value of the concentration levels used in the calibration curve

Inspection of the previously reported equation confirms that as  $x_{\text{pred}}$  approaches  $\bar{x}_{\text{Cal}}$ , the third term under the square root  $u(x_{\text{pred}})$  approaches zero and thus approaches a minimum value. In a practical analysis, therefore, a calibration of this type will give the most precise results when the measured instrument signal corresponds to a point close to the centroid of the regression line ( $\bar{x}_{\text{Cal}}, \bar{y}_{\text{Cal}}$ ). In

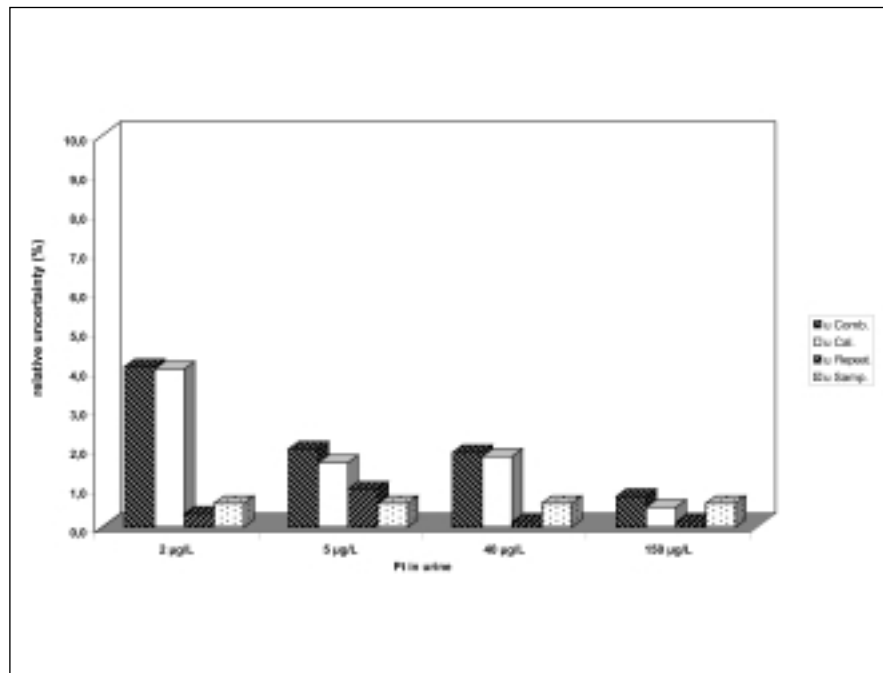


Fig. 6. Relative Uncertainty Values (%) obtained at different concentration levels for Pt in human urine.

our study, with a calibration range of 0–20  $\mu\text{g L}^{-1}$  and a centroid corresponding to (5.18; 1.84), the  $u(\text{Calib.})$  for a predicted mean value of 0.36  $\mu\text{g L}^{-1}$  Pt in the ultrafiltrate (n=3 replicates) was about 21.9%; the same results became lower (0.22%) when the calibration range was set at 0–2  $\mu\text{g L}^{-1}$  with the same number of calibration points and with a centroid corresponding to (0.527, 0.163).

These results show the importance of calibration in evaluating the measurement uncertainty of low Pt concentrations in biological fluids. Keeping the repeatability of measurements constant as, in the case of a wider calibration range, we should accept larger uncertainty of calibration which will reflect significantly on the combined uncertainty.

If we wished to improve (i.e., narrow) the confidence limits of calibration, we could reduce the calibration range, increase the number of calibration points on the

regression line or make more than one measurement and use the mean value in the calculation of the predicted value.

### Analysis of Real Samples

The present method was employed to determine the pharmacokinetic profiles of total Pt and ultrafiltrable Pt in patients who received JM216 (an oral bis(acetate) amine dichloro cyclohexylamine platinum (IV) analogue) brought into clinical development for phase II evaluation. Forty-six patients were treated at doses ranging from 10  $\text{mg/m}^2/\text{d}$  to 50  $\text{mg/m}^2/\text{d}$  and 39 patients were evaluated for hematologic toxicity over 74 cycles. The pharmacokinetics of total and ultrafiltrable Pt were studied on days 1 and 14 of the first cycle, and the results were recently published by Sessa (3). Figure 7 shows, as example, the pharmacokinetics profiles of four patients who received 45  $\text{mg/m}^2/\text{d}$  of agent.

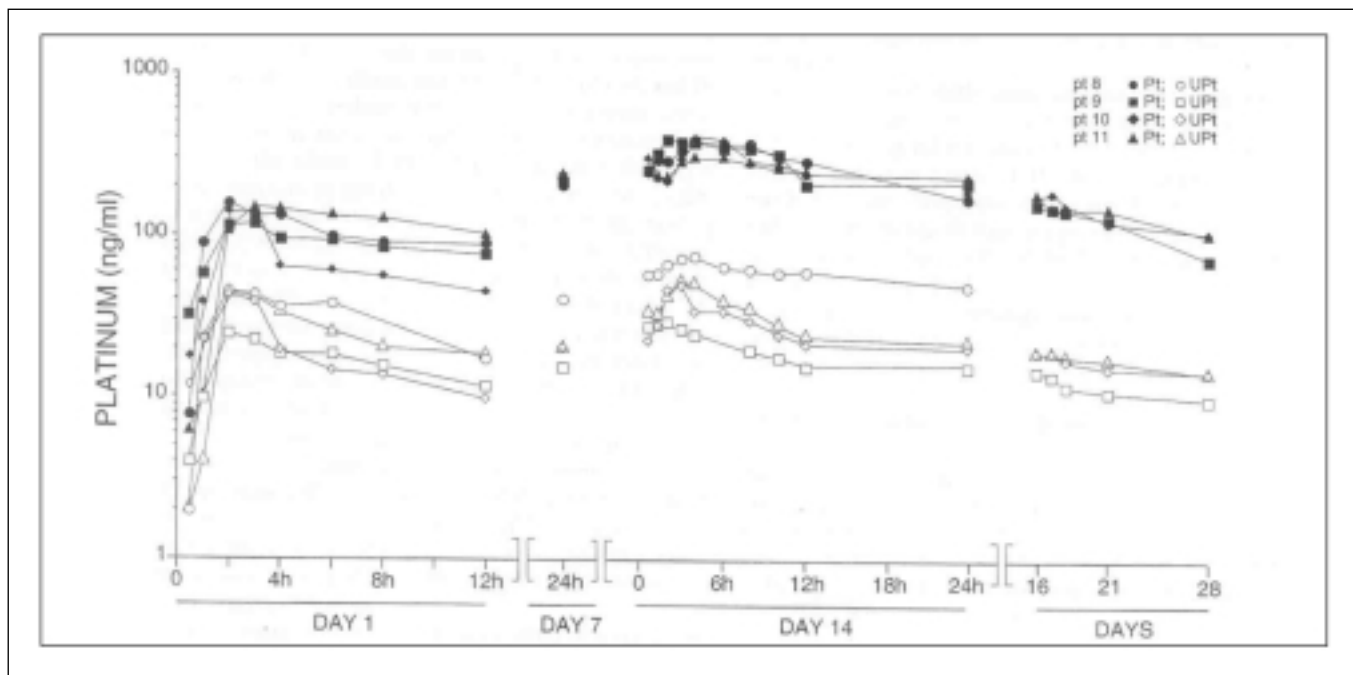


Fig. 7. Pharmacokinetics profiles of four patients treated with 45 mg/m<sup>2</sup>/d of agent. Plasma levels of total platinum (Pt) and plasma ultrafiltrate platinum (Upt).

JM216 was rapidly absorbed, with Pt and UPt detectable in plasma as early as 30 min after the administration. On day 1, Pt and UPt peak levels were achieved in most cases within 3 hours with median  $T_{max}$  values of 2.5 and 2, respectively. Elimination was variable and slow with Pt and UPt concentrations of, respectively, 100  $\mu\text{g L}^{-1}$  and 20  $\mu\text{g L}^{-1}$  and still detectable two weeks after the last dosing.

## CONCLUSION

An ICP-MS method for the determination of Pt in biological fluids (plasma, ultrafiltrate, and urine) of patients treated with antitumor agents has been developed and validated. The limits of quantification (LOQ) in the three matrices were 1.0, 0.1, and 2.0  $\mu\text{g L}^{-1}$ , respectively.

Intra-day and inter-day precision and accuracy was in good agreement with the FDA criteria for the validation of analytical methods.

The present study was implemented by assessing the uncertainty evaluation for Pt determination in the different matrices according to the EURACHEM/CITAC Guide. The combined uncertainty, calculated by estimating the components associated with the repeatability, the instrumental calibration and the sampling, was always lower than 10% for Pt concentrations higher than 1  $\mu\text{g/L}$ .

While the uncertainty component associated to the repeatability was constant overall, the different concentration levels and the sampling uncertainty was negligible, the component due to the instrumental calibration increased significantly in relation to the lowest concentrations of analyte.

Received December 23, 2003.

## REFERENCES

1. J.A. Gottlieb and B. Drewinko, *Cancer Treat. Rep.* 59, 621 (1975).
2. A.B. Khan, B.J. D'Souza, M.D. Wharam, L.A.A. Champion, L.F. Sinks, S.Y. Woo, D.C. McCullough, and B.C. Leventhal, *Cancer Treat. Rep.* 66, 2013 (1982).
3. C. Sessa, C. Minoia, A. Ronchi, M. Zucchetti, J. Bauer, M. Corner, M., J. de Jongh, O. Pagani, J. Renard, C. Weil, C., and M. D'Áfincalci, *Annals of Oncology* 9, 1315 (1988).
4. U.S. Pharmacopeia 23, 1982-84, United States Pharmacopeial Convention, Inc., (1994).
5. International Conference on Harmonization, Draft Guidance on Validation of Analytical Procedures: Definitions and Terminology, Federal Register, Volume 60, pp. 1260 (March 1, 1995).
6. FDA - Guidance for Industries, Bioanalytical Method Validation, U.S. Department of Health and Human Services Food and Drug Administration (May 2001).
7. ISO, Guide to the Expression of Uncertainty in Measurement, International Standards Organization, Geneva, Switzerland (1993).
8. EURACHEM/CITAC Guide (2000), Quantifying Uncertainty in Analytical Measurement, 2nd Edition.
9. S.J. Bannister, Y. Chang, L.A. Sterson, and A.J. Repta, *Clin. Chem* 24, 877 (1978).
10. E.H. Evans and J.J. Giglio, *J. Anal. At. Spectrom.* 8, 1 (1993).
11. V.J. Berwick and S.L.R. Ellison, *Accred. Qual. Assur.* 5, 47 (2000).

# Determination of Selected Trace Elements in Raw Clams and Commercial Clam Meats From the State of Miranda (Venezuela) Employing ICP-OES, GF-AAS, and WD-XRF

John J. LaBrecque, Zully Benzo, \*Juan A. Alfonso, Perdo R. Codoves, Manuelita Quintal, Clara V. Gomez, and Eunice Marcano

Instituto Venezolano de Investigaciones Cientificas (IVIC)  
Apartado 21827, Caracas, 1020A, Venezuela

## INTRODUCTION

In recent years, the abundance of clams (*Tivela mactroidea*) along the coast of Venezuela between Higuerote and Tacarigua de la Laguna (State of Miranda, Venezuela) has increased greatly. The clams and their processed meats are available throughout the year and in large quantities. As a result, many of the local inhabitants and regular beach goers have included clams and/or clam meat in their diet, especially since clams are easily obtained and commercial clam meat is very economical, less than \$1.00 per kilogram.

The processing of raw clams into commercial clam meat is a very simple and crude method performed directly on the beach (see Figure 1). First, the clams are collected with a metal basket using either a metal or plastic screen as shown in Figure 1A, transferred to a plastic box (usually an old beer bottle container with a metal or plastic screen replacing the bottom) (see Figure 1B), and then rinsed with the seawater to eliminate (or separate) the marine sediments. The semi-clean clams are then transferred to old metal buckets or large cans (Figures 1C and 1D) and cooked over an open fire with little or no seawater added until the shells open. The cooked clams are transferred to the same or similar plastic box with a screen attached to the bottom, as was used

## ABSTRACT

The trace elements Fe, Cu, and Zn were originally determined by WD-XRF and compared with ICP-OES analysis of raw clams and their processed meats for nutritional purposes. Since the accuracy of the ICP-OES method was much superior to the WD-XRF method, we decided to employ ICP-OES, even though the WD-XRF method did not require a costly and time-consuming sample dissolution procedure. Chromium, Ni, and Cd were also determined from the same sample digest by ICP-OES, as well as Pb and V by GF-AAS.

The oven-drying procedure was checked by a freeze-drying method to ensure that no trace element content was lost in this process. A comparison of the trace element content in raw clams and their respective clam meats showed only one case of contamination at the five different processing sites, even though the process is performed in an unclean environment. Additional marine sediment was suggested as the main source of contamination. Monitoring of the trace element content of commercial clam meats sold at the Rio Chico marketplace over a 14-months' period showed no significant difference even though their supply did not always come from the same site. The only trace element determined to be a health risk was vanadium; the values were between 2.4 and 5.2  $\mu\text{g/g}$ , far above the 1- $\mu\text{g/g}$  level suggested by the U.S. EPA. It should be noted that some of the trace element content is due to contamination of the clam material by marine sediments. The effect of marine sediment contamination in the digests was also studied.

to rinse off the marine sediment. The box is shaken vigorously so that the clam meat passes through the screen and falls onto a large plastic sheet, leaving most of the shells and other foreign material in the box. Finally, the clam meat is placed in a large plastic bag for transport to a local market or is divided up into approximately one-quarter or one-half kilogram portions and placed into small plastic bags ready to be sold (see Figure 1E). Since, this process is performed in an unclean manner and environment, we shall compare the values of the selected trace elements of the raw clams (starting material) with their respective processed meats (at different sites and on different days) to study the possibility of contamination of the clam meats during their processing, as well as to assess their health risk for human consumption.

There are many publications (e.g., 1–4) on the determination of trace elements in shellfish (clams, mussels, oysters, etc.) and the quality of marine water, since shellfish can accumulate trace elements up to 105 times higher than the levels observed in the water they live. Some species concentrate some trace elements relatively better than others, probably as a consequence of their different feeding habits. There are only a few publications (5–7) available on the determination of trace elements in shellfish in order to assess their health risk for human consumption. However, most of these studies have neglected to determine vanadium, probably due to the lack of simple methods with sufficient sensitivity. But recently, vanadium has been

\*Corresponding author.

E-mail: jalfonso@ivic.ve

Fax: +58-212-504-1115

Mailing Address:

Centro de Quimica, 8424 NW 56th Street,  
Suite CCS 00204, Miami, FL 33166, USA

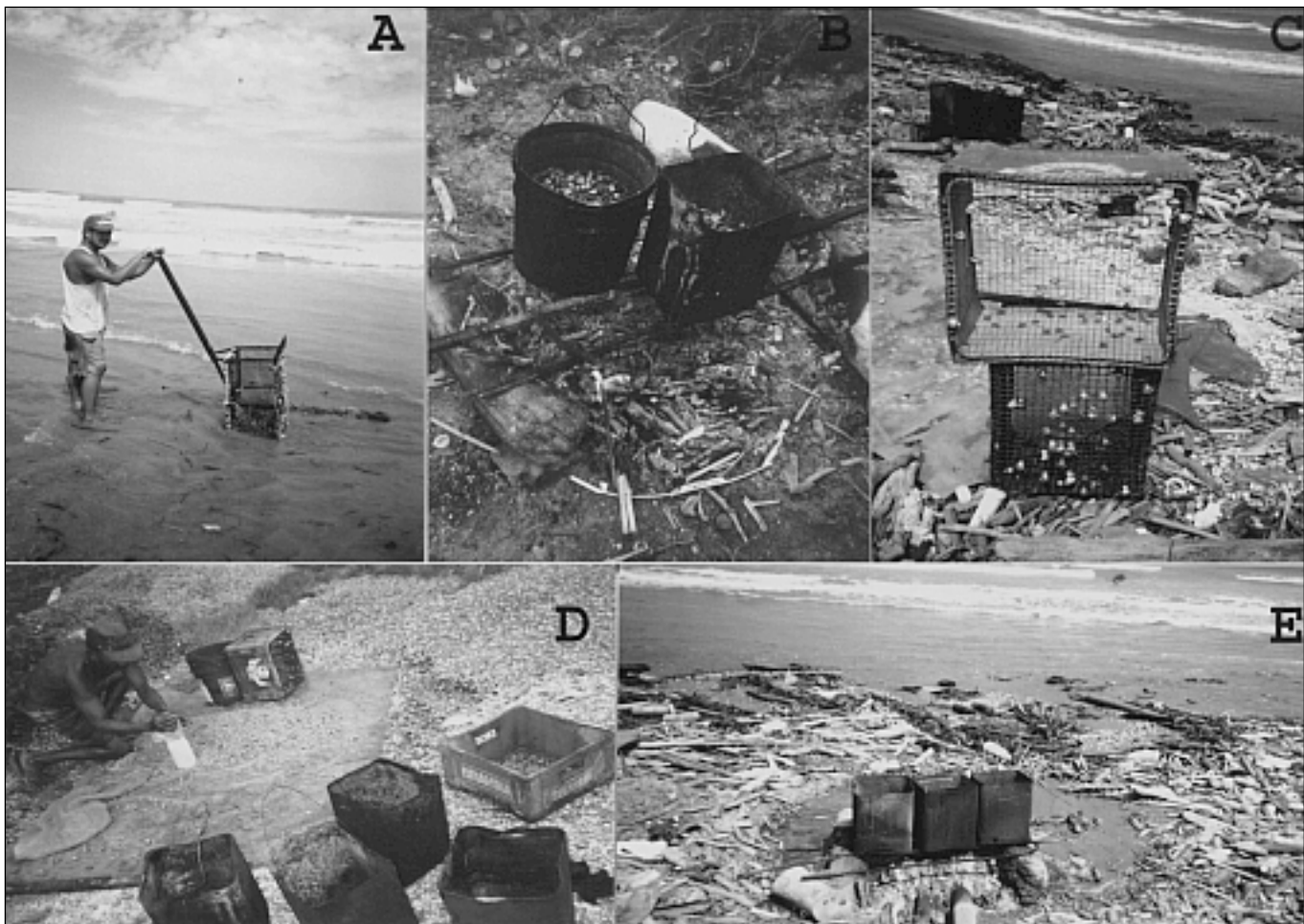


*Fig.1. Clam meat process: A) the collection of the raw clams with a metal basket; B) the cooking of the clams; C) the boxes used to rinse off the marine sediment before cooking and to separate the shells from the cooked meat afterwards; D) the packing of the clam meat that was sieved on to a large plastic sheet and; E) another picture of the containers and the environment where the clam meats are processed.*

determined in shellfish by ICP-OES (1) and GF-AAS (5), and in both cases it was the only trace element to surpass the risk assessment level of the U.S. Environmental Protection Agency (US EPA) (2).

Iron, copper, and zinc are considered important nutritional trace elements, which must be part of the human daily diet to ensure normal biological functions. Originally, we only planned to study these three trace elements by XRF, since their concentration ranges were high enough for their quantification and to compare some of their values with an ICP-OES method,

which is much more sensitive but requires a costly and time-consuming sample digestion procedure. But we extended our study to other essential trace elements also toxic at high concentrations such as Cr, Ni, and V as well as Pb and Cd.

It is well known that atomic spectrometry (atomic absorption, atomic emission X-ray fluorescence, etc.) has emerged as a very powerful technique for the determination of trace elements in shellfish (8-10) as well as other environmental samples (11-15). In general, these different techniques and methods are used for multi-element analysis

(some are even simultaneous element analysis methods), cover a wide concentration range, and have good detection limits, but each has its own advantages and limitations. For example, inductively coupled plasma optical emission spectrometry (ICP-OES) and graphite furnace atomic absorption spectrometry (GF-AAS) methods prefer liquid samples with small samples sizes in the range of milligrams. Thus, solid samples require a costly and time-consuming dissolution procedure, which results in measuring solutions with large dilution factors, but the detection limits are

generally very low, in the range of a few  $\mu\text{g}/\text{kg}$ . Wavelength dispersive X-ray fluorescence (WD-XRF) methods prefer solid samples, with sample sizes generally in the range of grams, requiring no dissolution procedure, but the detection limits are much higher, in the range of tens to hundreds of  $\mu\text{g}/\text{g}$ .

In the past, methods were investigated and developed for liquid samples for WD-XRF analysis, for example for water samples, using various chemical preconcentration procedures (16,17). These methods offered similar detection limits for specific elements as with ICP-OES and GF-AAS, but the preconcentration procedures were very time-consuming and costly, and required larger sample sizes. Similarly, ICP-OES and GF-AAS methods are used to analyze solid samples and are based on slurries (18–24) and emulsions (25–27), which requires special preparation and sample insertion techniques which are time-consuming. It can be seen that these different techniques can be employed for both liquid and solid samples, when the appropriate taken into consideration.

In this work, we compared the values of Fe, Cu, Ni, Zn, Cr, V, Cd, and Pb in raw clams and their respective processed meats from various sites employing ICP-OES, GF-AAS, and WD-XRF. We compared a simple oven-drying method with a freeze-drying method for sample preparation. And finally, over a one-year period, we routinely monitored the values in commercially sold clam meats at the local marketplace in Rio Chico, the major town between Higuero and Tacarigua de la Laguna.

## EXPERIMENTAL

### Instrumentation

A PerkinElmer® (PerkinElmer Life and Analytical Sciences, Shelton, CT, USA) Model Optima

3000™ ICP optical emission spectrometer was employed for the determination of Fe, Ni, Cu, Zn, Cr, and Cd in clams and clam meats. It was operated with a radio frequency generator at 40 MHz and 1400 W. The sample digests were delivered from a peristaltic pump to a Meinhard nebulizer via a Scott-type spray chamber. The nebulizer flow rate was 1.0 L/min, the plasma gas flow rate was 12 L/min, and the auxiliary gas (argon) flow rate was 0.6 L/min. The emission measurements were taken 8 mm above the radio frequency coil. The spectrometer was equipped with a Hewlett-Packard® Vectra computer system. It was run in automatic mode with background correction by an ICP-WinLab™ Optima 3000 software package.

A Varian-Techtron Model 875 atomic absorption spectrometer and a Varian GTA-95 graphite furnace equipped with a GTA sample dispenser was used to determine Pb (283.3 nm) (Varian Techtron Pty Limited, Mulgrave, Victoria, Australia). A PerkinElmer Zeeman 5100PC atomic absorption spectrometer equipped with a THGA™ 5100 ZL graphite furnace and AS-71 furnace auto sampler was employed for the vanadium (318.5 nm) determinations.

Freeze Dry System, Labconco Model Lyph Lock 6 was used for freeze-drying the samples at  $-46^{\circ}\text{C}$  and under a vacuum of  $8 \times 10^{-3}$  mBars for 48–72 hours (Labconco Corporation, Kansas City, MO, USA).

A Siemens SRS-3000 conventional wavelength dispersive X-ray fluorescence spectrometer fitted with an Rh anode X-ray tube for excitation interfaced with an IBM compatible computer and controlled by Spectra-Plus software package was employed for the WD-XRF measurements (Siemens A.G., Karlsruhe, Germany).

## Reagents

### *For the ICP-OES and GF-AAS analysis:*

Concentrated Suprapur® nitric acid, 65%, Merck, Darmstadt, Germany.

Hydrogen peroxide, 30%, Merck.

Ultra pure water, was obtained from a Milli-Q™ system (Millipore, Bedford, MA, USA). Calibration solutions, multi-element working standard solutions were freshly prepared as required from individual element stock standard solutions (BDH, Poole, Dorset, UK and Aldrich, Milwaukee, WI, USA).

Standard Reference Material, NIST-2976 (Mussel tissue) supplied by the U.S. National Institute of Standards and Technology (Gaithersburg, MD, USA) with certified values for As, Cd, Cu, Fe, Pb, Se, and Zn; and reference values for Al, Cr, Ni, Ag, and Sn.

### *For the XRF analysis:*

Calibration standards, the following reference materials were employed to construct the calibrations curves: IAEA-H-4, IAEA-V-10, IAEA-MA-A-1/TM, IAEA-MA-A-2/TM, BRC-CM-060, BRC-CM-061, BRC-CM-062, BRC-CM-279, NIST-1571, NIST-1572, and NIST-1575. It should be noted that some of these reference materials have plant material matrices rather than animal tissue matrices, which can affect the accuracy of the different trace element calibration curves.

Standard Reference Materials, the same mussel tissue, NIST-2976, was also employed to estimate the accuracy of the WD-XRF determinations.

### Sampling and Sample Preservation

The locations of the sampling sites can be seen in Figure 2 and their corresponding geographical coordinates are listed in Table I.

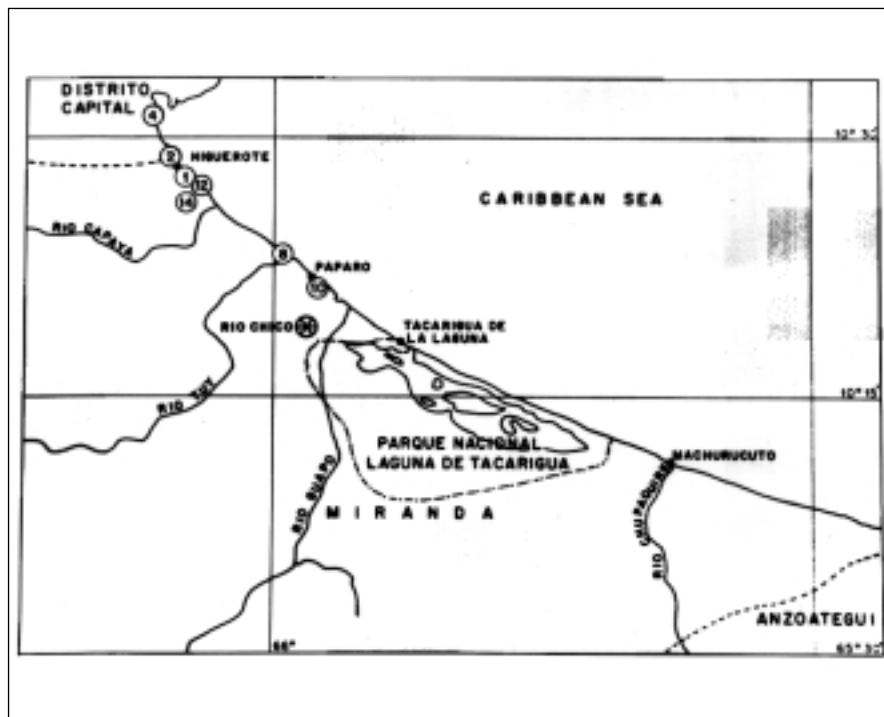


Fig. 2. A map showing the locations of the sampling and processing sites of the clam meats.

**TABLE I**  
The Geographical Coordinates of the Sampling Locations

Site No.	Geographical Coordinates	
	North	West
1	10° 27.276′	66° 04.425′
2	10° 28.326′	66° 05.392′
4	10° 31.579′	66° 06.946′
8	10° 23.321′	65° 58.842′
10	10° 21.628′	65° 57.056′
12	10° 27.671′	66° 04.841′
14	10° 31.368′	66° 04.970′

The raw clams were sampled directly from the plastic box used by the fishermen to rinse off and to separate them from marine sediments before the remaining clams were transferred to the cooking buckets or large cans to be processed as clam meat. The raw clams were then transferred to 1-L wide-mouth plastic bottles (previously cleaned in the laboratory with

dilute nitric acid and rinsed with distilled deionized water) and filled to the top. The raw clams were then rinsed twice with distilled deionized water and completely refilled with distilled deionized water before closing the bottles. Finally, the bottles were immediately placed in a cooler full of ice to be transported to the laboratory, where they were kept in a domestic refrigerator at about 2–5°C until their analysis.

#### Samples Obtained From Fishermen

One-half kilogram portions of the clam meat processed from the same batch of raw clams previously collected, were obtained directly from the fishermen. They placed them into small clean plastic bags, which were then squeezed into clean 1-L plastic wide-mouth bottles, closed, and immediately transferred to a cooler full with ice.

#### Samples Obtained at Local Fish Market

The commercial clam meats were all bought from the same fish vendor at the Rio Chico marketplace, in the State of Miranda (Venezuela), between August 2001 and October 2002. Portions of about one-half kilogram were dispatched in plastic bags (which is the normal procedure) and then transferred to a cooler containing ice for transport to the laboratory.

#### Sample Preparations

After several days of soaking in the distilled deionized water in the refrigerator, the raw clams open by themselves. The complete clam material inside the shells was removed with a pair of clean surgical gloves, washed with distilled deionized water to separate the clams from sediment and other foreign material. They were transferred to 1-L precleaned glass beakers and filled to the 200-mL mark, rinsed with distilled deionized water, discarding the excess water. The beakers were then placed in a drying oven at about 65°C until all the liquid was evaporated; then the temperature was increased to 80°C for 24 hours before cooling in a desiccator.

The dried clam material in the beaker was transferred to pre-clean 120 cc bottles. None of the clam material that was in contact with the bottom of the beaker was transferred, since it could have been affected by the evaporating liquid that concentrated in the bottom of the beaker. The dried samples were ground into a fine powder with a large agate mortar and pestle, then carefully mixed to prepare a homogeneous representative sample.

For the sample digestion for ICP-OES and GF-AAS analysis, 1.0-g portions of the clam material were dissolved in 8 mL of concentrated

super pure nitric acid with heating on a hot plate at about 70°C for about 8 hours. When the solution cooled, 2 mL of hydrogen peroxide (30%) was added and heated again at 70°C for 4 hours. Finally, the resulting digest was diluted to 50 mL with distilled deionized water. The digestions were performed in duplicate for each sample.

For the WD-XRF measurements, 4-cm diameter disks were pressed from 6-g sample portions. To eliminate contamination, both faces of the compression die were covered with thin pre-clean Teflon® disks and, as part of quality control, between two and six replicate disks were prepared for each sample.

#### ICP-OES MEASUREMENTS

In ICP-OES, the sample is subjected to temperatures high enough to cause not only dissociation into atoms but to cause a significant amount of collisional excitation (and ionization) of the sample atoms to take place. Plasmas have been used as atomization/excitation sources for OES. These are highly energetic, ionized gases, usually produced in inert gases. Once the atoms or ions are in their excited states, they can decay to lower states through thermal or radiative (emission) energy transitions. In OES, the intensity of the light emit-

ted at specific wavelengths is measured and used to determine the concentration of the elements of interest. The main advantage of ICP-OES over the AAS techniques in general are its multielemental capabilities, longer dynamic ranges, and fewer condensed phase interferences. In addition, besides the refractory compound-forming elements, elements such as I, P, and S are detected with more sensitivity by the ICP-OES technique (27).

The ICP-OES spectrometer was operated in the automatic mode with background correction employing the operating conditions stated in the Instrumentation section. The following wavelengths (nm) were employed: 259.940 for Fe, 324.754 for Cu, 231.604 for Ni, 313.856 for Zn, 226.502 for Cr, and 226.502 for Cd. The mean and standard deviation (1s) of the measured values of three independent sample digest of NIST- 2976, mussel tissue reference material are given in Table II and compared to their certified (Cu, Fe, Zn and Cd) or recommended (Cr and Ni) values. It can be clearly seen that all the trace elements had been determined very accurately. It can also be seen in Table II that the precisions are much less than 30% for all elements. Acceptable accuracy and precision for the monitoring of

trace elements in shellfish has been reported to be <30% (1).

#### GF-AAS MEASUREMENTS

The sensitivity of graphite furnace atomic absorption makes it the obvious choice for trace metal analysis applications. Routine determinations at the mg/L level for most elements make it ideal for environmental applications. Advances in instrumentation and techniques have made it possible to analyze very complex sample matrices, such as those frequently found in biological and geological samples. The microliter sample sizes used offer additional benefits where the amount of sample available for analysis is limited, as in many clinical analyses.

A graphite furnace analysis consists of measuring and dispensing a known volume of sample into the furnace. When the temperature is increased to the point where sample atomization occurs, the atomic absorption measurement is made. Variables under operator control include the volume of sample placed into the furnace and heating parameters for each step (28).

Lead and vanadium were analyzed by GF-AAS using the optimized heating program recommended by the instruction manual. Peak area was determined by the absorbance mode and deuterium background corrector was used for lead and Zeeman correction for vanadium. There was no need to use matrix modification.

#### WD-XRF Measurements

Conventional wavelength-dispersive x-ray Fluorescence (WD-XRF) involves angular dispersion of the characteristic x-rays by an analyzing crystal that were induced in the sample as a result of the interaction of electromagnetic radiation from an x-ray tube. The diffracting crystal has a high resolution but the process is very inefficient. Thus,

**TABLE II**  
**Comparison of the Determined Values of**  
**Mussel Tissue Standard Reference Material (NIST-2976)**  
**by WD-XRF and ICP-OES**  
**With the Certified (CV) and Recommended Values (RV);**  
**<dl= Below Detection Limit**

Element	Reference Material Value (µg/g)	ICP-OES Values (µg/g)	WD-XRF values (µg/g)
Cd	0.82 ± 0.16 (CV)	0.84 ± 0.02	<dl
Cr	0.50 ± 0.16 (RV)	0.53 ± 0.03	<dl
Cu	4.02 ± 0.33 (CV)	4.15 ± 0.07	<dl
Fe	171.0 ± 4.9 (CV)	175.5 ± 4.07	140 ± 1.2
Ni	1.04 ± 0.10 (RV)	0.93 ± 0.12	<dl
Zn	137 ± 13 (CV)	144.1 ± 4.4	152 ± 0.5



the detection efficiency needs to be maximized; this is accomplished by a Rowland circle geometry. Further information on WD-XRF spectrometry can be found elsewhere (29).

The sample disks were analyzed by a conventional wavelength dispersive X-ray fluorescence spectrometer (WD-XRF) with a 3KW Rh anode X-ray tube. The following elements were measured sequentially employing the parameters listed in Table III: Al, Cl, Cu, Fe, Mg, Mn, Na, P, Si, Sr and Zn.

## RESULTS AND DISCUSSION

### Investigation of the Processing of Raw Clams to Commercial Clam Meats

The following trace elements: Fe, Cu and Zn were studied by both ICP-OES and WD-XRF. The determinations of these elements in raw clams and their respective processed clam meats are presented in Table IV. While, the values for Cr, Ni, V, Cd and Pb by their respective methods are presented in Table V. For two of the five sample sets (sites 8 and 12) the iron values by ICP-OES were about

20% less in the clam meat relative to the raw clams, which is not significant considering 30% standard deviation (1s), but at site 14, the sample set showed an increase of about 150% in the clam meat. This large difference was probably due to the difference in the amount of marine sediment contamination in the clam meat or contamination during the processing from a metal screen or the cooking containers. Similarly, the values for Cu, Ni and Zn were also found to be higher, but only by about 30% for the clam meat processed at site 14. The contamination conclusion is also supported by the large enrichment of the Cr, V, and Pb concentrations in the processed clam meat at site 14 as seen in Table V. In the case of the other four sampling sites, the values for Cu, Ni, Zn, Cr, V, Cd and Pb are not significantly different considering the 30% relative variation (precision limit) suggested in the literature (1), thus no evidence was found to support contamination of the clam meats at these sites on these dates.

To check the validity of the oven-drying procedure for the clam materials, to ensure that none of

the trace element concentrations were lost in this process, we have compared this procedure with a freeze-drying procedure. The values of the freeze-dried samples (coded FD) and the oven-dried samples taken from the same lot of raw clams are shown to be similar in Tables IV and V. A similar oven-drying procedure has also been employed in the literature (1) previously, but no comparison was performed to check its validity.

The values of Fe in raw clams or clam meats have not been previously reported in Venezuela. While, Fe was determined to be between 153–441  $\mu\text{g/g}$  (1) in four different species of mussel tissue from Pina Bay (Brazil). These values are about an order less than the ICP-OES values we have determined and suspect that our values could have been high due to contamination with marine sediment.

**TABLE III**  
**WD-XRF Instrumental Parameters**  
**for the Different Elemental Determinations**

Element	X-ray Line	Voltage (Kv)	Current (mA)	Collimator (Degrees)	Crystal	Detector
Al	K $\alpha$	30	100	0.15°	PET	Proportional
Mg	K $\alpha$	30	100	0.15°	OVO-55	Proportional
Cl	K $\alpha$	30	100	0.15°	PET	Proportional
Cu	K $\alpha$	60	50	0.15°	LiF220	Proportional
Fe	K $\alpha$	60	40	0.15°	LiF220	Proportional
Mn	K $\alpha$	50	60	0.15°	LiF220	Proportional
Na	K $\alpha$	30	100	0.15°	OVO-55	Proportional
P	K $\alpha$	30	100	0.15°	PET	Proportional
Si	K $\alpha$	30	100	0.15°	PET	Proportional
Sr	K $\alpha$	60	50	0.15°	LiF220	Proportional
Zn	K $\alpha$	60	30	0.15°	LiF220	Proportional

**TABLE IV**  
**Comparison of the Fe, Cu and Zn Concentrations by the ICP-OES and WD-XRF methods in Raw Clams and Their Corresponding Clam Meats at Five Different Sampling Sites**  
**(The site locations are seen in Figure 2 and their geographical coordinates are listed in Table I. The samples coded "FD" were freeze-dried; RC=raw clams and CM=clam meat.)**

Site	Sample Code	Date Collected	Material	Fe (µg/g) ICP-OES	Fe (µg/g) WD-XRF	Cu (µg/g) ICP-OES	Cu (µg/g) WD-XRF	Zn (µg/g) ICP-OES	Zn (µg/g) WD-XRF
2	22	29/01/2002	RC	6893	5000	37	21	79	100
	35	29/01/2002	RC	7389	7190	32	21	90	110
	42-FD	29/01/2002	RC	5793	2320	36	21	72	110
	18	29/01/2002	CM	3089	4690	24	29	79	120
	34	29/01/2002	CM	3209	3500	26	28	86	110
4	24	29/01/2002	RC	1286	3040	25	20	51	45
	44-FD	29/01/2002	RC	1687	2730	23	17	58	55
	19	29/01/2002	CM	2244	3780	16	26	74	110
	33	29/01/2002	CM	2371	3600	15	19	73	92
8	28	30/01/2002	RC	3642	9086	19	39	90	92
	48-FD	30/01/2002	RC		1020		17		100
	68	01/10/2002	RC		2680		31		65
	54	01/10/2002	CM	2967	2390	13	nd	92	93
12	62	02/10/2002	RC	3807	2870	39	17	166	86
	55	02/10/2002	CM	2995	2810	24	16	110	89
14	64	02/10/2002	RC	1989	1830	25	14	98	71
	56	02/10/2002	CM	5201	3750	31	42	129	86
			mean (µg/g)	3999	3515	26	25	90	89
			sd (µg/g)	1790	2000	9	8	29	24
			rsd (%)	45	57	33	34	32	27

**TABLE V**  
**Determination of Cr, Ni, Cd, V, and Pb in Raw Clams and**  
**Their Corresponding Clam Meats at Five Different Sampling Sites**  
 (The site locations are seen in Figure 2 and their geographical coordinates are listed in Table I.  
 The samples coded "FD" were freeze-dried; RC=raw clams and CM=clam meat.)

Site	Sample Code	Date Collected	Material	Cr (µg/g) ICP-OES	Ni (µg/g) ICP-OES	Cd (µg/g) ICP-OES	V (µg/g) GFA-AAS	Pb (µg/g) GFA-AAS
2	22	29/01/2002	RC	7	14	1.4	14.3	4.1
	35	29/01/2002	RC	7	15	1.4	16	4.8
	42-FD	29/01/2002	RC	5.3	15	1.2	11.5	5.7
	18	29/01/2002	CM	1.01	9	1.3	7.54	<1.5
	34	29/01/2002	CM	1.01	10	1.3	7.66	2.29
4	24	29/01/2002	RC	1.6	10	<1	3.7	<1.5
	44-FD	29/01/2002	RC	2	12	<1	5.4	1.9
	19	29/01/2002	CM	1.45	10	<1	4.24	<1.5
	33	29/01/2002	CM	1.02	10	1.19	4.71	1.68
8	28	30/01/2002	RC	1.18	7	<1	6.78	<1.5
	54	01/10/2002	CM	1.1	6	<1	5.57	<1.5
12	62	02/10/2002	RC	1.57	15	<1	3.13	<1.5
	55	02/10/2002	CM	<1	9	<1	3.68	<1.5
14	64	02/10/2002	RC	<1	10	<1	2.38	<1.5
	56	02/10/2002	CM	1.96	12	<1	5.14	1.62
mean (µg/g)				2.2	10.6	1.0	6.1	2.9
sd (µg/g)				1.9	2.7	0.4	3.3	1.7
rsd (%)				87.9	25.4	39.0	54.1	57.6

### Monitoring of Commercial Clam Meats for Health Risk Assessment

The values of Fe, Cu and Zn were determined by both ICP-OES and WD-XRF for commercial clam meats bought at the Rio Chico marketplace between August 2001 and October 2002 and presented in Table VI; the concentrations of the other trace elements (Cr, Ni, Cd, V and Pb) determined by ICP-OES and GF-AAS are listed in Table VII. It should be mentioned that their supplies did not always come from the same site, but rather than from different area between Higuero and Taraguia de La Laguna. Thus, one would expect some minor compositional deviations. Besides, the much better detection limits for the determinations of Fe, Cu and Zn as shown in Table VIII, the ICP-OES method was much more sensitive and selective for the analysis of clam material in respect to the general conventional WD-XRF method employed. The detection limits could have been lower by maximizing the counting times of the different characteristic x-rays and their corresponding backgrounds but not significantly.

There were some very large differences in Table VI between some of the ICP-OES and WD-XRF values for Fe, for example sample 7 and 48 which had 37% and 55% differences respectively; again this was most probably due to the difference quantities of marine sediments in the different sample portions employed for the determinations.

The Cu mean value for the WD-XRF determinations was 50% higher than the mean value of the ICP-OES method. It can be concluded that the ICP-OES values were more accurate, because of the results of the accuracy study with the mussel tissue reference material as seen in Table II and the proximity of the determined values to the

detection limit of Cu in biological materials by WD-XRF. It can also readily be seen in Table VIII that the detection limits for Fe, Cu and Zn by the ICP-OES method were many factors lower than the WD-XRF method. In a preliminary study (4) of raw clams from the same area in Venezuela in 1990, the reported values ranged from 59–152 µg/g. But, the range of values of four different mussel species from the Pina Bay, Brazil was reported to be 5–17 µg/g (1).

The previously reported values of Ni (4) for raw clams from this same area were between 16–31 µg/g about four times higher than our determined values; while the reported range of values for the four species of mussel from Brazil was 0.7–1.8 µg/g (1).

The mean value of Zn was about 21% less by ICP-OES method than the mean value determined by the WD-XRF method, which is less than the 30% precision limit suggested by Santos de Lima et al. (1), therefore, again we support the ICP-OES values as more correct because of the accuracy study and its inherent advantage over WD-XRF for trace element analysis in biological materials. The reported values of Zn in raw clams in 1990 (4) from the same zone were between 227–266 µg/g, again much higher than our results which were in the range of 61–104 µg/g and the reported values for four different species of mussels from Brazil were from 62 to 159 µg/g (1).

The values of Cr in the clam meats were determined only by ICP-OES, since the concentrations were below the detection limit for WD-XRF; the values were between 0.7–1.9 µg/g with a relative standard deviation ( $1\sigma$ ) of 30% over more than a one year period of time. The previously reported values (4) of Cr in 1990 for raw clams from the same area were between

2.9–4.3 µg/g. While, the reported values of Cr for the four different species of mussel from Brazil ranged from 0.7–1.1 µg/g (1).

The determined values of the common toxic elements, Cd and Pb were all below their measured detection limits in the monitored clam meats, which were <1 µg/g for Cd and < 1.5 µg/g for Pb. This was surprising, since we have measured levels up to 1.3 µg/g for Cd and 2.3 µg/g for Pb in clam meats (see Table III) that were collected directly from the fisherman on the beach immediately after processing at other sites.

Finally, the V values for the commercial clam meats were between 2.5–6.0 µg/g with a relative standard deviation ( $1\sigma$ ) of 26%. The determination of Vanadium was not performed previously in raw clams or their meats in Venezuela. While the values of V in four different species of mussels in Brazil were between 0.05 and 1.0 µg/g, but a study of marine mussels from the German Bright (5) had shown similarly high values for V. The health risk level for V is less than one µg/g according to the EPA standards (2), thus our values and the levels at the German Bright are many factors above the risk level. They have explained the higher levels of V to be a result of fossil oils and fuels near the shipyards and shipping routes. In our case, not only are oil and other petroleum products shipped along this coast, but also there is a large petroleum terminal near Higuero, thus, an explanation for these high V values in the clam meats. A study of the marine sediments, along the coast between Higuero and Tacarigua de la Laguna at the same sampling sites as the clams also showed high levels of V, in the range of 60–120 µg/g (see Table IX).

### The Effect of Marine Sediment Contamination on the Determination of the Selected Trace Elements in Raw Clams and Their Meats

Since the sample digests, all resulted with some form of residue, that resembled marine sediment and degree of cloudiness on the bottom of digest tubes before the final dilution, it was decided to further investigate this, specially since the our determined values for Fe in the clams and their meats were very high. Residues in the digest of bivalve materials have been previously reported (2,7) and were allowed to settle to the bottom or be filtered, but they were not further studied.

First, we filtered five sample digests with 45  $\mu\text{m}$  micro pore papers to obtain sufficient material to perform conventional powder X-ray diffraction. The results showed that there were two phases, one was a clear fine powder, which was determined to be quartz, a major component of marine sediment. And the other phase was a brown sticky substance, which was identified to be an unknown organic compound or mixture. Therefore, we concluded that the samples did contain some marine sediment. This contamination could possibly have been eliminated in the raw clam samples by only analyzing the clam tissue rather than the whole clam, but the whole clam is digested with the marine sediment contamination when consumed by humans. In the case of the clam meat, it would be difficult if possible to separate the clam tissue from the other parts.

An experiment to determine how much of the sediment would be extracted into the digest was performed on marine sediments taken at three of the sampling sites at the same time the clams were collected. This was done by treating one gram of marine sediment

by the same sample dissolution method as the clams and determining how much was extracted into the digests by filtering the residue. The results showed that 5.9%, 13.5% and 2.6% by weight of the marine sediment was extracted into the sample digest from the sediment samples taken at site 2, 4 and 10, respectively. But, since different elements could be extracted differently, the total composition of the marine sediments was determined by conventional WD-XRF and the trace element content of the digests by ICP-OES, to determine the extraction recoveries. The results of these experiments are shown in Table IX. In general, the extraction recoveries are similar for the different sites; about 40% for Fe, 10% for V and about 5% for Cu and Cr. Thus, the contamination of the clams and their meats by marine sediments affect the determination of Fe greatly and somewhat for the other trace elements. Finally, it should be noted that the marine sediments in study area all have a very fine particle component and is always suspended in waters were the clams live.

### CONCLUSION

It was shown that both the ICP-OES and WD-XRF methods could both produce results for the nutritional elements: Fe, Cu and Zn, but the ICP-OES method was shown to be much more accurate. The percent difference for the ICP-OES method for the determination of Fe in the mussel tissue standard reference material was less than 3% in respect to more than 20% by the WD-XRF method. In the case of the Zn determination, the percent difference was about 5% for the ICP-OES method versus more than 10% by the WD-XRF method. The Cu concentration (4.02  $\mu\text{g/g}$ ) in the reference was below the detection limit of the WD-XRF method, but not for our clam materials. The WD-XRF method could not detect Ni,

Cr, Cd, V and Pb at the concentration levels in the clam materials. Thus, we employed the ICP-OES method to determine Ni, Cr and Cd and the GF-AAS method to determine the V and Pb in the clams and their processed meats because they exhibited better precision and accuracy for the respective determinations. In conclusion, we prefer to employ only the ICP-OES and GF-AAS methods for the respective trace element determinations, even though the WD-XRF method does not require a costly and time-consuming dissolution procedure. But, the WD-XRF method can be employed when only Fe, Cu and Ni are required and the accuracy does not need to be less than 30%.

In general, there were no significant differences for the concentration values of trace elements, between the oven-drying procedure and the freeze-drying method for the same samples, except for Fe which can be contributed to the sediment contamination. Most of the percent differences between the portions of the oven-dried clam material and the freeze-dried portions were less than 20%, even those from the WD-XRF method.

The study of the residue in the sample digest was shown to be quartz, a major component of marine sediment in part and an unknown organic compound or mixture. An extraction recovery study showed large percentages of Fe, about 40% and minor percentages of about 10% of V would be extracted from typical marine sediment at these sites. Thus, these effects need to be taken into account.

It was seen that the measured concentration values of the raw clams for Cd, Cr, Cu, Ni, Pb and Zn were all lower than a previous study in the same area in 1990 (4), which tend to suggest that the marine environment is of better

**TABLE VI**  
**Comparison of Fe Cu and Zn Values Determined by the WD-XRF and ICP-OES Methods in**  
**Commercial Clam Meats Bought at the Rio Chico Marketplace Over a 14-months' Period**

Sample Code	Date	Fe (µg/g) ICP-OES	Fe (µg/g) WD-XRF	Cu (µg/g) ICP-OES	Cu (µg/g) WD-XRF	Zn (µg/g) ICP-OES	Zn (µg/g) WD-XRF
5	09/08/2001		1350		27		125
6	09/08/2001		1500		28		140
7	17/08/2001	2973	2170	14	26	94	135
8	20/08/2001		2300		30		151
9	23/08/2001		2520		22		132
10	30/09/2001		1170		22		136
11	12/10/2001		1630		36		130
12	26/10/2001	920	1050	7	18	72	99
13	16/11/2001		1460		18		117
14	17/12/2001		1810		26	61	120
16	22/12/2001		2100		25		101
17	03/01/2002		2090		25	92	100
31	15/02/2002		1750		17	85	99
32	08/03/2002		1670		18		100
36	22/03/2002	2238	2680	17	21	90	110
38	18/04/2002		2100		18		100
40	10/05/2002	2102	2300	13	33	79	110
41	09/06/2002		2250	12	18	78	100
42	21/06/2002		2320		20		115
44	12/07/2002	1599	1620	12	17	82	101
45	17/07/2002		2170				81
46	25/07/2002	2413	3070	13		88	130
47	31/07/2002		3190		14		96
48	21/08/2002	656	1020	10	17	86	100
49	26/08/2002		1010		16		110
50	29/08/2002		1580		16		67
51	04/09/2002	1105	1200	20	15	86	66
52	13/09/2002	2143	2370	18	19	101	100
53	02/10/2002	2015	2050	20	16	104	100
	mean (µg/g)	1816	1914	14	21	86	109
	sd (µg/g)	730	581	4	6	11	20
	rsd (µg/g)	40	30	29	27	13	19

**TABLE VII**  
**The Determination of Cr, Ni, Cd, V and Pb in Commercial Clam Meats Bought at the Rio Chico Marketplace Over a 14-month's Period**

Sample Code	Date	Cr (µg/g)	Ni (µg/g)	Cd (µg/g)	V (µg/g)	Pb (µg/g)
		ICP-OES	ICP-OES	ICP-OES	GFA-AAS	GFA-AAS
7	17/08/2001	1.9	7.7	<1	2.4	
12	26/10/2001	0.8	5.8	<1	2.4	
36	22/03/2002	1.7	6.4	<1	4.5	<1.5
40	10/05/2002	1.4	5.7	<1	3.9	
41	09/06/2002	1.4	6.5	<1	4.5	
44	12/07/2002	0.9	5.2	<1	3.9	<1.5
46	25/07/2002	1.3	6.5	<1	4.6	<1.5
48	21/08/2002	0.7	4.4	<1	2.5	<1.5
51	04/09/2002	1.2	4.7	<1	3.4	<1.5
52	13/09/2002	1.8	4.8	<1	5.2	
53	02/10/2002	1.4	5	<1	4.3	
Mean (ug/g)		1.3	5.7	<1	3.8	<1.5
sd (ug/g)		0.4	1.0		1.0	
rsd (%)		30.1	17.6		25.9	

**TABLE VIII**  
**Comparison of the Detection Limits for Fe, Cu, and Zn in Clam Material by the ICP-OES and WD-XRF Methods**

Element	Detection Limit (µg/g)	
	ICP-OES Method	WD-XRF Method
Fe	0.26	9
Cu	0.12	5
Zn	0.08	12

**TABLE IX**  
**Determination of Selected Elements in Marine Sediments From Three Sampling Sites by WD-XRF and the Amount Extracted Into the Sample Digest Employing the Same Method Used for the Clam Materials by ICP-OES (nd= not detected)**

Element	Sediment	Extraction	Sediment	Extraction	Sediment	Extraction
	Site #1 (µg/g)	#1 (µg/g)	Site #4 (µg/g)	#4 (µg/g)	Site #10 (µg/g)	#10 (µg/g)
Cd	nd	<1	nd	<1	nd	<1
Cr	87	5.09	70	5.03	nd	2.56
Cu	25	4.88	26	3.16	nd	<1
Fe	21.470	8.363	19.320	7.943	8.840	3.300
Ni	nd	11.70	nd	9.74	nd	4.54
V	100	10.61	120	11.91	64	6.4
Zn	nd	28.81	nd	22.23	nd	13.0

quality presently, but this conclusion would be affected by the amount of the contamination of the clams by the marine sediments in both of these studies. In the previous study, no precaution was taken to eliminate the marine sediment that was in the bivalves and the samples were prepared from homogenized tissue, since the principal objective of that study was to determine organic compounds by gas chromatography (4).

The measured concentrations of the trace elements in the commercial clam meats sold at the Rio Chico marketplace, except V are all below the health risks for human consumption according to the guidelines of the US EPA (2). The mean vanadium value was about a factor of four above the one µg/g level, thus it is most likely that levels in the clam tissue itself are above the risk level for human consumption and not just from the marine sediment contamination. As a food (diet) source, clams and their processed meats are rich in Cu and Zn, thus are very nutritional; their content of the toxic elements Pb and Cd are below their respective detection limits of 1.5 µg/g and 1 µg/g, but the high levels of V, much greater than 1 µg/g classify them as health risk according to the US EPA guidelines (2).

Finally, there were no significant differences between the trace element content of the raw clams and their respective processed meat for four of the five sample sites studied, but it was clearly seen that the processed meat at site 14 was contaminated. In general, the trace element concentrations levels in the processed meat at site 14 were much higher than the raw clams, this was probably due to the marine sediment in general, but Pb contamination probably had an additional source.

*Received October 13, 2003.*

## REFERENCES

1. E. Santos de Lima, M.F. Costa, A. Pastor and M. de la Guardia, *Atomic Spectroscopy*, 22, 405 (2001).
2. I. Chamberlain, K. Adams and S. Le, *Atomic Spectroscopy*, 21, 118 (2000).
3. W.E.P. Avelar, F.L.M. Mantelatto, A.C. Tomazelli, D.M.L. Silva, T. Shuhama and L.C. Lopes, *Water, Air and Soil Pollution*, 118, 65 (2000).
4. R. Jaffe, I. Leal, J. Alvarado, P. Gardinal and J. Sericano, *Marine Pollution Bulletin*, 30, 820 (1995).
5. K-R Sperling, B. Bahr and J. Ott, *Fresenius Journal of Analytical Chemistry*, 366, 132 (2000).
6. F.J. Copa-Rodriguez and M.I. Basadre-Pampin, *Fresenius Journal of Analytical Chemistry* 348, 390 (1994).
7. W.A. Grant and P.C. Ellis, *Journal of Analytical Atomic Spectroscopy* 3, 815 (1988).
8. J.L. Sericano, *International Journal of Environmental Pollution* 13, 340 (2000).
9. A. Talyor, S. Branch, A. Fisher, D. Halls and M. White, *Journal of Analytical Atomic Spectrometry* 16, 421 (2001).
10. A.K. Das, *International Journal of Environmental Pollution* 13, 208 (2000).
11. M.R. Cave, O. Bulter, S.R.N. Chenery, J.M. Cook, M.S. Cresser and D.L. Miles, *Journal of Analytical Atomic Spectrometry* 16, 194 (2001).
12. R.E. Clement, P.W. Yang and C.J. Koester, *Analytical Chemistry*, 71, 257R (1999).
13. R.E. Clement, P.W. Yang, *Analytical Chemistry*, 73, 2761 (2001).
14. E.H. Evans, J.B. Dawson, A. Fisher, S.J. Hill, W. J. Price, C.M.M. Smith, K.L. Sutton and J.F. Tyson, *Journal of Analytical Atomic Spectrometry*, 16, 672 (2001).
15. R.E. Van Grieken and J. J. LaBrecque, *Trace Analysis*, vol. 4, J.F. Lawrence (ed.), Academic Press, Inc., Orlando, Fl., 102-183 (1986).
16. P.J. Potts, A.T. Ellis, M. Holmes, P. Kregsamer, J. Marshall, C. Strel, M. West and P. Wobrauschek, *Journal of Analytical Atomic Spectrometry*, 17, 1439 (2002).
17. P.J. Potts, A.T. Ellis, M. Holmes, P. Kregsamer, C. Strel, M. West and P. Wobrauschek, *Journal of Analytical Atomic Spectrometry*, 15, 1417 (2000).
18. D.T. Takuwa, G. Sawula, G. Wibetoe and W. Lund, *Journal of Analytical Atomic Spectrometry*, 12, 849 (1997).
19. J.H. Brown, J.E. Vaz, Z. Benzo and M. Velosa, *Analyst*, 120, 1215, (1995).
20. Z.A. de Benzo, M. Velosa, C. Ceccarelli, M. de la Guardia and A. Salvador, *Fresenius' J. Anal. Chem.*, 339, 235 (1991).
21. Z.A. de Benzo, R. Fernández, N. Carrion and E. Eljuri, *Atomic Spectroscopy* 9, 87 (1988).
22. N. Carrion, Z.A. de Benzo, B. Moreno, A. Fernández, E. Eljuri and D. Flores, *Journal of Analytical Atomic Spectrometry* 3, 479, 1988.
23. N. Carrion, Z.A. de Benzo, E. Eljuri, F. Ipoliti and D. Flores, *Journal of Analytical Atomic Spectrometry* 2, 813, (1987).
24. M. Murillo, Z. Benzo, E. Marcano, C. Gómez, A. Garaboto and C. Marin, *Journal of Analytical Atomic Spectrometry* 14, 815 (1999).
25. Z. Benzo, E. Marcano, C. Gómez, F. Ruiz, J. Salas, M. Quintal, A. Garaboto and M. Murillo, *Journal of AOAC International* 85, 967 (2002).
26. Z. Benzo, M. Murillo, E. Marcano, C. Gómez, A. Garaboto, and A. Espinoza, *Journal Analytical of Oil Chemical Society* 77, 997 (2000).
27. R.D. Beaty and J.D. Kerber, "Concepts, Instrumentation and Techniques in Atomic Absorption Spectrophotometry", PerkinElmer Life and Analytical Sciences, Shelton, Connecticut, USA (1993).
28. C.B. Boss and K.J. Fredeen, "Concepts, Instrumentation and Techniques I Inductively Coupled Plasma Optical Emission Spectrometry", 2nd edition, PerkinElmer Life and Analytical Sciences, Shelton, Connecticut, USA (1999).
29. E.P. Bertin, "Introduction to X-Ray Spectrometric Analysis", Plenum Press, New York (1978).



# Characterization of Hyphenated HPIC/ICP-OES System Response for Iron Speciation in Natural Waters

\*Sanda Roncevic<sup>a</sup> and Ilse Steffan<sup>b</sup>

<sup>a</sup> Laboratory of Analytical Chemistry, Faculty of Science, University of Zagreb, Strossmayerov trg 14, Zagreb, Croatia

<sup>b</sup> Institute of Analytical Chemistry, University of Vienna, Waehringerstrasse 38, Vienna, Austria

## INTRODUCTION

Determination of iron species present in the environment is a task of growing interest to scientific fields such as geochemistry, atmospheric chemistry, and oceanography research. The redox reactions, which occur in the chemical weathering of rocks, involve iron from different minerals, and consequently, the oxidation state of the Fe ions depends on the reducing or oxidizing conditions (1). The appearance of Fe(II) is expected in reducing environmental conditions which can occur in groundwater systems [i.e., lower, more saline levels of stratified lakes, as well as in clouds, fogs, and rain water due to the photo reduction of Fe(III) (2-4)]. Investigations of organic complexation of iron in seawater and the open oceans show that prokaryotic cells excrete specific organic ligands, known as siderophores, in response to low levels of iron (5-9). It is assumed that the bioavailability of iron species has an effect on the phytoplankton population. However, the redox cycling between Fe(II) and Fe(III) also has a significant effect on other redox processes in many natural water systems. Therefore, speciation of iron is one of the most important considerations for a better understanding of these natural processes.

However, iron speciation has not yet found its way to standardized procedures. For example, in drinking and wastewater

## ABSTRACT

The capability of hyphenated high performance ion chromatography coupled with inductively coupled plasma optical emission spectrometry (HPIC/ICP-OES) was investigated for iron speciation in natural water samples. A discrete sample introduction system produced transient signals to the ICP-OES detector. These signals were characterized through peak asymmetry factors. The reproducibility of the signal using peak height and peak area values was found to be good. The elution of Fe(II) and Fe(III) from chromatographic columns using pyridine-2,6-dicarboxylic acid was measured, and the results were satisfactory for most of the prominent iron emission line at 259.925 nm; two resolved chromatographic peaks were detected by ICP-OES.

The iron standard solution stability was studied and found to be sufficient to allow the determination of total iron at very low concentration ranges. Speciation of iron in natural water samples was achieved with on-line preconcentration, and the measured concentrations of Fe(III) and Fe(II) were 7.5 and 1.2 ng mL<sup>-1</sup>, respectively. The appearance of another iron species overlapping the peak of Fe(III) can probably be attributed to the bonding of Fe(III) with the organic compounds in the water samples.

legislation, the total iron value is all that is measured. Many instrumental methods and ways of determining total iron have been proposed such as spectrophotometry, amperometry, atomic absorption spectrometry (AAS), and inductively

coupled plasma optical emission spectrometry (ICP-OES). Most of these methods are quick and selective but lack the sensitivity for element determination at low concentration levels. Preconcentration and separation techniques are usually required prior to analysis. The determination of oxidation states of iron in natural waters has generally been achieved by complexation with specific chelating reagents such as 1,10-phenanthroline and ferrozine, followed by spectrophotometric or voltammetric measurement (10-14). Several flow injection analysis (FIA) methods have also been applied for the simultaneous determination of Fe(II) and Fe(III) (15-17). Some voltammetric techniques take advantage of complexation with organic chelators as a preconcentration step, and they assume that there is no strong natural organic chelator that can cause interferences, but this is not always the right assumption. Determination of iron species can also be complicated by the presence of a variety of iron oxides with a range of reduction potentials with respect to Fe(III). Spectrophotometric methods also suffer from interferences caused by complexation of iron by ligands present in real samples.

Iron species in natural waters can be preconcentrated and separated on an ion chromatographic column. Excellent separation of transition and rare earth metals is achieved by using pyridine-2,6-dicarboxylic acid (PDCA) as the eluent, or by forming chelating surfaces with impregnation of the resins (18,19). Significant improvements in speciation detection have

\*Corresponding author.  
E-mail: roncevic@chem.pmf.hr  
Tel: +385-1-48 19 283  
Fax: +385-1-48 18 458

been realized by coupling chromatography with an element-specific detection technique such ICP-OES. The first investigation of this hyphenated system involved the formation of iron-PDCA complexes and the results showed that preparation and preservation of the samples has a considerable effect on the results (20).

There are other problems associated with the coupling of two instruments. The conventional concept of a steady state signal measurement has to be abandoned when the ICP-OES spectrometer serves as the detector for chromatographic separation. This is because the chromatographic peak is transient and must be measured using peak area. In order to evaluate ICP-OES as the detector in ion chromatography, it is crucial to examine important parameters such as the influence of mobile phase on signal measurement, the contribution of the detector to peak broadening, and the detection power. Since PDCA effects in the plasma have already been reported (21), the focus of our study was to observe the detector performance in this tandem system. Therefore, the purpose of this study was to demonstrate the applicability of high performance ion chromatography (HPIC) coupled with ICP-OES in the complex analytical task of iron speciation.

## EXPERIMENTAL

### Instrumentation

The instruments used were a Model Dionex 2000 ion chromatograph (Dionex Corporation, Sunnydale, CA, USA) and a PerkinElmer Plasma 40 inductively coupled plasma optical emission spectrometer (PerkinElmer Life and Analytical Sciences, Shelton, CT, USA). The instrumental parameters and operating conditions are given in Table I.

### Signal Reading

The emission signal from the photomultiplier tube of the ICP-OES was measured directly as a voltage using a Digital-Multimeter DMM M 4560CR, which was connected to the detector output from the spectrometer box. The voltmeter was connected to a

computer through an MT/RS232 interface connection. The signal was read out every 500 ms and collected by Digiscope (Digital, Maynard, MA, USA) software, which enabled instantaneous monitoring of the signal and transference of the collected data to any other data handling software.

**TABLE I**  
**Instrumental Parameters and Operation Conditions**

<b>ICP-OES</b>	
Spectrometer	Czerny-Turner, 408 mm
Gratings	Holographic blazed UV: 4200 lines/mm Visible: 1800 lines/mm
Spectral bandwidth	UV: 0.019 nm Visible 0.10 nm
Slit widths	Both entrance and exit slits fixed at 25 mm
R.F. Power supply	Free-running ICP generator, 40 MHz, nominal output power 1000 W
Torch	Fassel type, piezo-electric ignitor
RF induction coil	4 turns of copper wire
Ar flows	Outer: 12.0 L min <sup>-1</sup> Intermediate: 0.8 L min <sup>-1</sup> Carrier: 1.0 L min <sup>-1</sup>
Observation height	15 mm above coil
Spray chamber	Scott type
Nebulizers	Cross-flow, transversely mounted Meinhard concentric, type TR-30-A3
Sample uptake rate	1.0 L min <sup>-1</sup>
<b>HPIC</b>	
Sample loop	50 mL
Rheodyne six-port rotary valve	
Chromatographic pump	
Analytical column	(Dionex) HPIC-CS5 Cation (mixed anion and cation exchange) Core size: 13 mm Latex size: 100 nm Latex cross-linking: 2.0% Functional group: SO <sub>3</sub> <sup>-</sup> and N <sup>+</sup> R <sub>2</sub> (R''OH)
Guard Column	(Dionex) HPIC-CG5
Recommended flow rate	1 mL min <sup>-1</sup>
UV detector wavelength	520 nm
Postcolumn reagent flow rate	0.7 mL min <sup>-1</sup>

### HPIC/ICP-OES Connection

The outlet of the analytical column of the ion chromatograph was connected through Teflon® tubing (20 cm length, 0.3 mm i.d.) to the cross-flow nebulizer mounted to the sample introduction system of the ICP-OES. The tube length was as short as possible to prevent additional dispersion of the eluted analyte and broadening of the chromatographic peaks.

### Reagents and Solutions

A 1.0-g amount of pyridine-2,6-dicarboxylic acid [PDCA, Mr-167.12 (g/mol)] was placed into a 1-L flask. A volume of 0.7 L ultrapure water (18M $\Omega$ ), purified with the Milli-Q™ (Millipore, Bedford, MA, USA) deionizing system, was added and the dissolution performed using an ultrasonic bath. Acetate buffer was added to the prepared solution, and the pH of the solution adjusted to 4.8. The flask was filled with ultrapure water and the final concentration of the PDCA solution was 6 mmol L<sup>-1</sup>. Several solutions of equal concentrations of PDCA were prepared in the pH range from 3.0–8.0. These solutions were used for testing the effects of different pHs on Fe(II) and Fe(III) separation.

The standard solutions of iron were prepared by dilution of the appropriate volume of FeCl<sub>3</sub> stock solution [Titrisol® Fe standard (1 g L<sup>-1</sup>), Merck, Darmstadt, Germany] with ultrapure water. A solution of 1000 mg mL<sup>-1</sup> Fe(II) was prepared by dissolving the appropriate amount of (NH<sub>4</sub>)<sub>2</sub>Fe(SO<sub>4</sub>)<sub>2</sub> × 6 H<sub>2</sub>O in water, followed by addition of 1 mL concentrated H<sub>2</sub>SO<sub>4</sub> and dilution with water to 100-mL volume. The final concentration of this solution was determined by titration with KMnO<sub>4</sub> standard solution. A solution of Fe(II) must be freshly prepared before each set of measurements. Solutions of lower concentrations were prepared

by dilution with an appropriate volume of ultrapure water.

Detection of iron species by means of a UV/VIS detector included the formation of colored complexes with 4-(2-pyridilazo) resorcinol (PAR) post-column reagent. A 0.05-g amount of PAR was weighed and dissolved in 1:1 ammonia solution. After dissolution of PAR, 57 mL of glacial acetic acid was added, and the flask filled with water to 1-L volume.

Ascorbic acid used as a reducing agent was prepared by dissolution in ultrapure water. The final concentration was 3% (m/v).

A solution of 1% (m/v) Na<sub>2</sub>SO<sub>3</sub> was prepared by dissolution of salt in ultrapure water. It was used to flush the column in order to prevent oxygen buildup inside the column.

All solutions were degassed before entering into the ion chromatograph. The rapidly oxidizing solutions were stored under nitrogen.

### Measuring Procedure

The appearance of the transient signal on the detector was first tested without ion chromatography separation in the column. The outlet of the rotary valve from the chromatograph was connected with 30-cm long Teflon tubing (0.3 mm i.d.) to a cross-flow nebulizer on the ICP-OES spectrometer. The blank and standard solutions of iron were injected by means of a syringe into a sample loop of the ion chromatograph. Injection of 50  $\mu$ L of a fresh portion of standard solution was repeated several times. The time period between two injections was kept constant at 20 seconds. A solution of PDCA was used for elution of the standard from the sample loop. The pumping rate in the ion chromatograph was held at 1 mL min<sup>-1</sup> to match the sample uptake rate on the ICP-OES. The emission intensity was measured by ICP-OES using the most prominent Fe(II) line at 259.925 nm.

The separation of mixtures of Fe(II) and Fe(III) standard solution on the chromatographic column was tested with the chromatograph connected to the ICP-OES. Standard solutions in the 1–10  $\mu$ g mL<sup>-1</sup> range were injected into a sample loop. The detected emission signals obtained after elution of iron-PDCA species from the analytical column were stored in the computer program. Replicate intensity measurements from a single run of solutions as performed in the ICP-OES in a continuous-flow operation mode were not feasible in the coupled system. Therefore, three chromatographic runs of each prepared standard solution were performed to determine precision (%RSD).

### Sample Handling and Analysis

The polyethylene containers used to collect the natural water samples were cleaned by soaking in 10% nitric acid and rinsing with ultrapure water. They were then left soaking in ultrapure water until use. Samples of spring and pond water were collected in containers. The containers were filled to volume and sealed hermetically to prevent influence from atmospheric oxygen. In the laboratory, the samples were immediately filtered and stored at 4°C. There was no additional acidification of the samples, and the period between collection and analysis was shortened as much as possible.

The guard column was connected to the analytical column, and the flow rate during preconcentration was adjusted to 2.0 mL min<sup>-1</sup>. After preconcentration of a 1000-mL sample, the elution with 6 mmol L<sup>-1</sup> PDCA was started. The flow rate was adjusted to 1.0 mL min<sup>-1</sup> and the iron elution from the column was observed as an emission signal at 259.925 nm.

## RESULTS AND DISCUSSION

Element-specific detection by an ICP-OES spectrometer with chromatography does not allow measurements on the signal plateau (steady-state) because ICP-OES becomes a sort of flow-through detector. Discrete repetitive introduction of iron standard solutions into the HPIC/ICP-OES system, where the separation column was not connected, produced an asymmetrical transient signal (see Figure 1).

Peak height varied slightly between two points in the maximum due to a readout frequency of 2 digits per second. It is obvious that the basic shape of the signal was not affected by changes in iron concentration. It was also found that the signal remained the same with injection of Fe(II) or Fe(III). The observed peak asymmetry can be explained in light of the basic principles of flow injection analysis (FIA) (22). According to FIA theory, symmetrical gradient profiles will be obtained in a long narrow tube, which accommodates a large number of identical mixing stages, while shorter or wider tubes of a lower tank system will yield more asymmetrical peaks. In a one-tank system, an asymmetrical peak with an exponential rise and fall will be obtained. This fact must be taken into consideration when using ICP-OES as the detector in the flow injection mode, as presented in this work. The peak asymmetry factors (PAF) were calculated in the standard way as being the ratio of the distance from peak center to the lagging edge and the distance from the peak leading edge to the peak center (23), both at 10% of peak height. The results are given in the Table II.

The calculated PAF values describe the shape of the transient signal. When the PAF value is 1.00, the shape of the signal is an ideal Gaussian curve; if it is less than unity, the peak tailing is pronounced; if it is greater, a lagging of the peak occurs. From the results shown in Table II, it

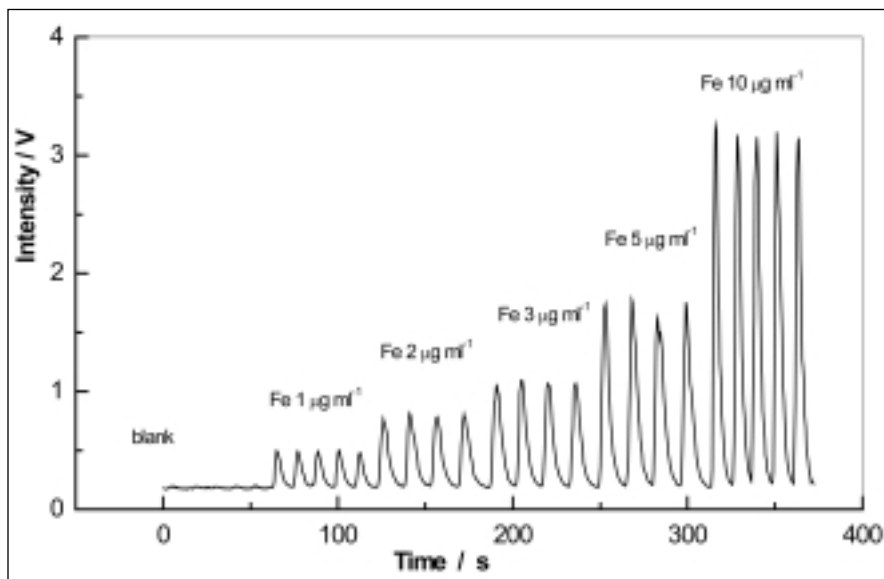


Fig. 1. Transition signals after repetitive injection of iron standard solutions.

**TABLE II**  
Peak Asymmetry Factors (PAF) From ICP-OES Transient Signals

Standard Solution Injected						
c (Fe) ( $\mu\text{g mL}^{-1}$ )	0	1	2	3	5	10
PAF	0.25	0.44	0.40	0.40	0.40	0.36

**TABLE III**  
Peak Variances From ICP-OES Transient Signals

Standard Solution Injected						
c (Fe) ( $\mu\text{g mL}^{-1}$ )	0	1	2	3	5	10
$\sigma_2$ / mL	2.78	6.25	6.25	7.0	6.48	6.25

is obvious that tailing of the signal prevails in the discrete sample introduction into the ICP-OES detector.

The variances of peaks in FIA are additive and similar to chromatography. From the different variances of the FIA peaks with or without a particular component included in the measuring system, it can be established that the contribution is from a certain part of the system to the peak broadening. Variances of measured transient signals were calculated at 2/3 of the peak height and are listed in Table III.

The values in Table III show the contribution of the detector and the connections (tubing) between HPIC and ICP-OES to the non-chromatographic peak broadening. Precision of detection using the discrete sample introduction mode was determined as the relative standard deviation of peak height, as in routine FIA analysis. The measured relative standard deviation was 3% for each measured solution and showed good stability and repeatability of signal detection for maximum transient signal height. Another approach must

consider peak area calculations attributed to routine chromatographic analytical work. The peak area of transient signals was integrated as in routine chromatography using a range of 4s on the time axis. The RSD of peak area was 6.3% for the blank, 5.4% for the solution of  $1 \mu\text{g mL}^{-1}$ , 4.1% for the solution of  $2 \mu\text{g mL}^{-1}$ , 2.8% for the solution of  $3 \mu\text{g mL}^{-1}$ , 1.9% for the solution of  $5 \mu\text{g mL}^{-1}$ , and 1.7% for the solution of  $10 \mu\text{g mL}^{-1}$  of iron injected. The stability of the signal area measurements was not as good as the stability of the signal height measurements. Generally, this was influenced by the components of the chromatograph (i.e., the rotary valve, sample loop, tubing, and pumping rate), and the effects were more pronounced at lower concentrations.

The elution order of two iron-PDCA complexes was tested by means of a UV/VIS detector after post-column reaction with the PAR reagent. Two resolved peaks appeared in the chromatogram: the first peak of Fe(III) at 3.93 min, and the second peak of Fe(II) at 8.61 min. Conventional UV detection in HPIC was performed to test the effects of PDCA concentration on retention time of the iron species and on using a different pH for the mobile phase. There were no significant changes in retention time in the pH range of 4–6. Retention time started to rise at a higher pH, probably due to the formation of stable hydroxide compounds. Elution of iron with  $3 \text{ mmol L}^{-1}$  PDCA was slow and took 30 minutes for complete removal of the iron species from the column. This was found to be time-consuming and therefore inadequate for speciation by hyphenated ICP-OES. A more concentrated mobile phase (i.e.,  $6 \text{ mmol L}^{-1}$  PDCA) led to faster elution, but the higher organic matter content introduced into the plasma caused remarkable changes in excitation conditions and consequently the questionable detection of iron emission intensity (21).

Two species of iron, eluted after injection of a mixture of standard solutions, were detected by ICP-OES in this hyphenated system as two resolved peaks: the first of Fe(III)-PDCA complex at 140 s (2.3 min) and the second of Fe(II)-PDCA complex at 320 s (5.3 min). The resulting chromatograms are shown in Figure 2. The shorter retention compared to standard UV detection is mainly due to a shorter connection between the HPIC and the ICP-OES than between the HPIC and the UV detector, where a long reaction coil for mixing with the PAR reagent is needed.

There were no measurable effects on the baseline intensity magnitude

in the order of rising iron concentration which implied that there was no residual iron on the chromatographic column that might affect the separation of the next sample injected. It clearly demonstrates that iron species were eluted from the column in a single chromatographic run.

Peak asymmetry factors (PAF) were calculated in the same manner as PAF of transient signals, and the results are shown in Table IV.

PAF values showed that peak tailing occurred during the elution of both iron species, and it was more pronounced for the Fe(III) peak. Chromatographic variances ( $\sigma^2$ ) were calculated at 2/3 of the peak

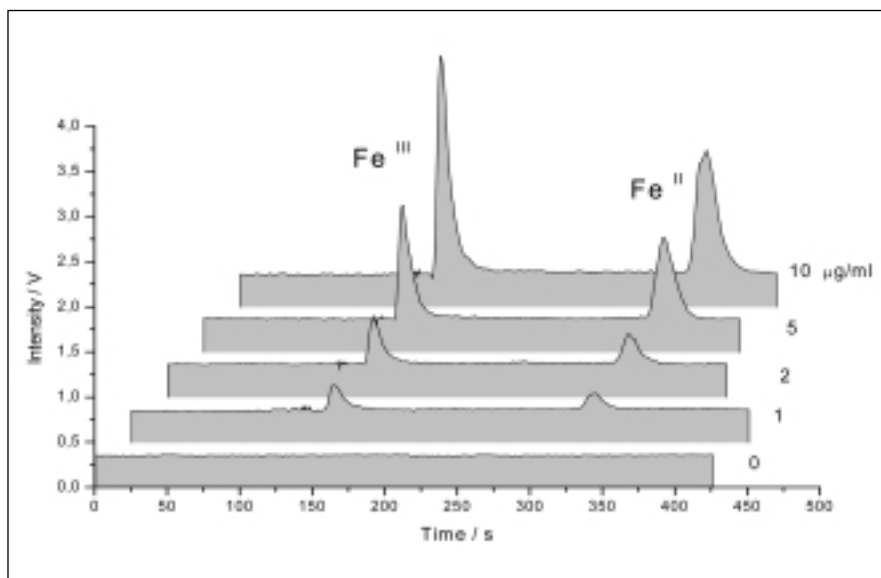


Fig. 2. Chromatograms of Fe(III) and Fe(II) standard solutions detected by ICP-OES.

**TABLE IV**  
**Peak Asymmetry Factors (PAF) for Chromatographic Peaks**

Standard Solution Injected c ( $\mu\text{g mL}^{-1}$ )	PAF-Fe(III)	PAF-Fe(II)
1	0.30	0.75
2	0.33	0.54
5	0.36	0.66
10	0.42	0.43

height and when expressed in volume units, they were 44 mL and 69 mL for Fe(III) and Fe(II), respectively. Comparing these values to a 6.25 mL variance of the transition signal of iron in ICP-AES, it can be assumed that the detector contribution to the peak broadening was much smaller than the contribution of the chromatographic system.

The calibration curves for a set of injected standard iron solutions (see Figure 3) represent measured peak area versus concentration. In the observed concentration range, dependence was linear with slightly poorer linearity for Fe(II) than for Fe(III).

It was assumed that the slightly different slopes of the curves were not caused by the ICP-OES detection because monitoring of the emission intensity was fixed on one and the same iron emission line during complete elution of both species. This is probably due to the oxidative conversion of the solution on its way from injection, passing through sample loop and chromatographic column. Therefore, the column needs refushing with a sodium sulphite solution before another set of injections in order to minimize oxidation.

The problem of detection limit determination in hyphenated systems has already been described in an earlier work (24). It was, therefore, concluded that a conventional approach based on  $3\sigma$  of blank intensity measurements, as performed in atomic spectrometry methods, is of no use in hyphenated systems (24). The best term to describe the detection power of hyphenated systems is "minimum detectable concentration" (MDC), which expresses extrapolation of detector sensitivity to a value twice that of the noise signal. Following this principle, the calculated MDC for Fe(III) and Fe(II) measured by hyphenated HPIC/ICP-OES was 0.147 and 0.150  $\mu\text{g mL}^{-1}$ , respectively. The relatively poor detection power in comparison to ICP-OES detection in

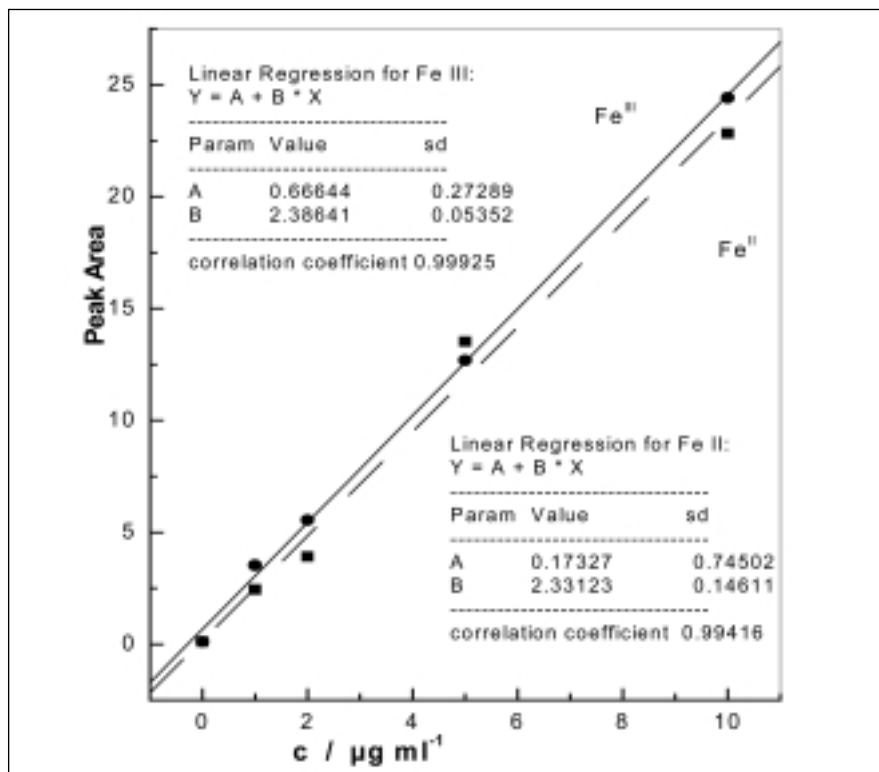


Fig. 3. Calibration curves from HPIC/ICP-OES measurements of iron standard solutions.

the continuous mode of sample introduction is caused by additional dilution during the chromatographic run. The excellent capability of on-line preconcentration by HPIC overwhelms the power of ICP-OES detection and is of no significance. In the analysis of natural water samples, where iron concentrations are very low, preconcentration of the samples is required before analysis.

A mixture of iron standard solutions was analyzed by HPIC/ICP-OES after 24 and 48 hours of initial preparation in order to examine the stability of the Fe(II) standard solution. Another experiment involved the same solutions with ascorbic acid addition and measurement in the same time span. The obtained chromatograms are given in Figure 4.

It was found that the peak area of Fe(II) in aqueous solution was lower by 2% in the first 24 hours, and by 20% after a 48-hr sample preparation.

The peak area of Fe(III) did not show a significant difference in the first 24 hours, but it was raised up to 18% after 48 hours from preparation. This confirmed the oxidative conversion of Fe(II) to Fe(III), which is also present in natural water systems, and most often is the main source of error in speciation analysis. This problem indicates the necessity of increasing the speed of speciation analysis starting from sample collection, transfer to the laboratory, preconcentration procedure, and measurement with adequate equipment. Reduction with ascorbic acid converted Fe(III) to Fe(II), as shown in Figure 4b. Changes in peak area were negligible in the observed period of measurements. Extrapolating of peak area to calibration curves gave two times greater concentration, which confirmed the total conversion of iron into the reduced form. It can be demonstrated that addition of ascorbic acid allows the

determination of total iron content by hyphenated HPIC/ICP-OES, and the results are equivalent to sample analysis by standard analytical techniques.

The applicability of this hyphenated system in real sample analysis was examined using several natural water samples. A volume of 1 L of each sample was pre-concentrated through a guard column where iron species were retained. The ICP-OES detector was switched on during the pre-concentration step to measure the changes in iron emission which might indicate a breakthrough of the column. The stable baseline signal did not show any increase in intensity. After this step, the elution step was started with the PDCA mobile phase; the resulting chromatograms are shown in Figure 5.

Peak area values were extrapolated on calibration curves and divided by pre-concentration factors to calculate the iron species concentration in samples. The resulting concentrations are given in Table V.

By hyphenated HPIC/ICP-OES with on-line pre-concentration, it was found that iron was present in very low concentration levels in both samples. The existence of different iron species was confirmed. It was also found that a new iron peak occurred, which overlapped that of Fe(III). The appearance of different iron species when natural waters were acidified with hydrochloric acid has already been discussed in the literature (20). The dynamic equilibrium between the iron species in water samples, used in this work, was not disturbed by acid. Therefore, the origin of another peak might be attributed to another chemical process. It is already known that the higher oxidation state of iron has a relatively low solubility product in the form of ferric hydroxide. However, in aquatic samples, Fe(III) is present as colloidal amorphous Fe(OH)<sub>3</sub>, which may dissolve and bind with organics such as humic

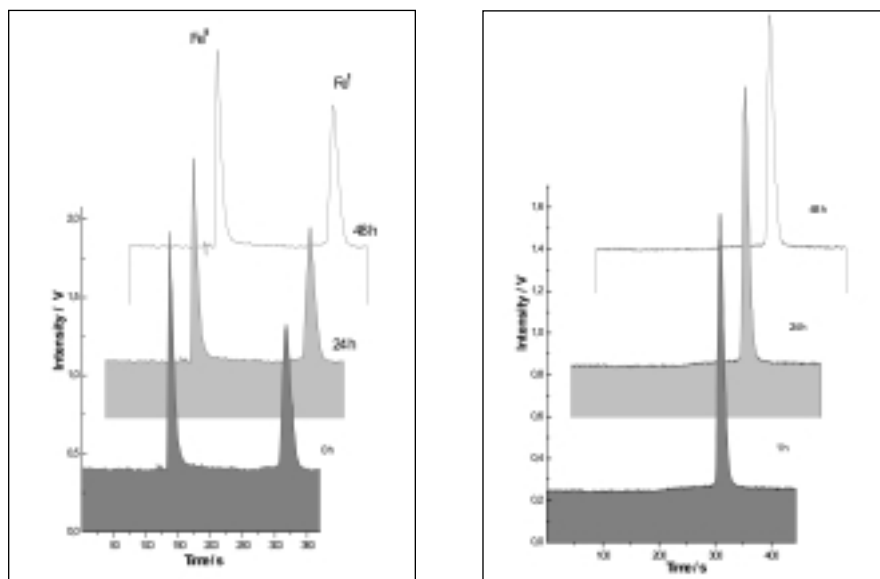


Fig. 4 (a and b). HPIC/ICP-OES chromatograms of iron standard solutions obtained immediately after preparation, at 24 and 48 hours intervals: (a) without ascorbic acid, (b) with ascorbic acid.

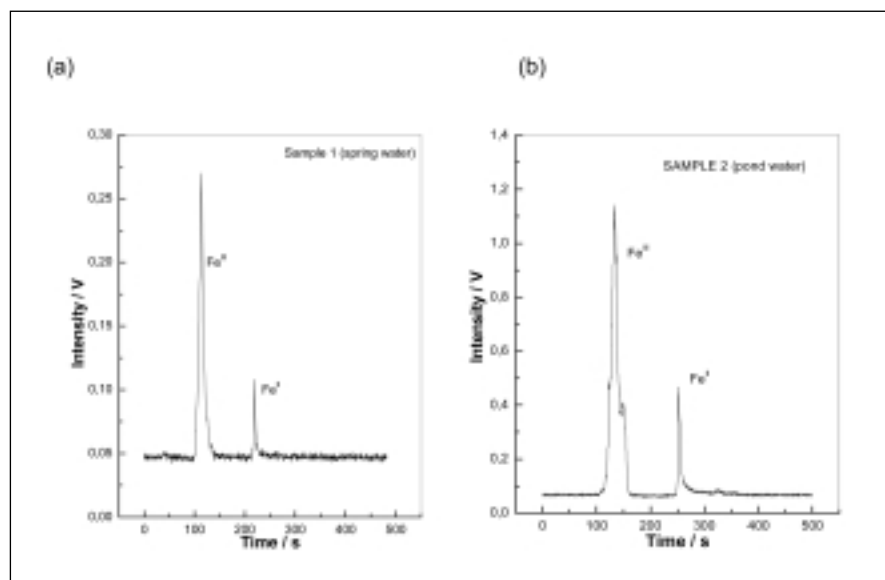


Fig. 5 (a and b). HPIC/ICP-OES chromatograms of natural waters: (a) spring water, (b) pond water.

**TABLE V**  
**Iron Species Concentration in Natural Water Samples**

Sample	c [Fe(III)] (ng mL <sup>-1</sup> )	c [Fe(II)] (ng mL <sup>-1</sup> )
(a) Spring Water	7.55	0.74
(b) Pond Water	7.27	1.19

substances. The acidity of the sample may change owing to the binding of iron by organic acid anions, which are present as protonated species. Any increase in sample pH can cause formation of colloidal Fe(III) hydroxides and interfere with iron speciation. In contrast, Fe(II) compounds are soluble over a wide pH range and do not form colloids or precipitates. There are also strong oxalate complexes with iron present in many aquatic systems. They are not included in equilibrium calculations even though they dominate the speciation of Fe(III). The main reason is that the concentrations are too low to be detected by means of ion chromatography involving specific chelating agents to form iron ligand complexes.

## CONCLUSION

Although different analytical techniques were suggested in solving the iron speciation problem, best performance is obtained by using an excellent separation method and specific detection of the different species. Element-specific detection capabilities of hyphenated ICP-OES with high performance ion chromatography (HPIC) were examined in this work. The study of detector response in the repetitive discrete sample introduction mode showed that a transient signal with a characteristic shape occurred. The peak asymmetry calculations described a characteristic ICP-OES signal similar to that obtained in flow injection analysis. The contribution of the detector to the broadening of the chromatographic peaks was expressed as the variance of the transient signal, and it was found to be negligible compared to the broadening due to the chromatographic system components.

Separation of two iron species, Fe(II) and Fe(III), from a mixture of standard solutions was achieved using a 6 mmol L<sup>-1</sup> PDCA solution on a chromatographic column; it was detected as the emission intensity by

ICP-OES at the most prominent iron line. The unique measuring conditions for an analyte eluted from the column showed that all iron species present in the sample can be measured with equal efficiency.

Analysis of natural water samples by HPIC/ICP-OES was achieved with on-line preconcentration and thus eliminated the time-consuming sample preparation steps. The somewhat poorer detection limits of ICP-OES in discrete sample introduction were overcome by the excellent preconcentration capability of using the hyphenated ICP-OES/chromatography technique.

The problem of sample stability and iron oxidative conversion was studied and showed that HPIC/ICP-OES is an excellent tool to determine the total iron content at low concentration ranges. Using the technique described showed that Fe(II) and Fe(III) determination in natural water samples resulted in the appearance of other PDCA complexes. However, the capability of HPIC/ICP-OES alone is not enough to determine the origin of a new iron species in the samples. Further multidimensional techniques will need to be developed to achieve the complex and demanding tasks of speciation analysis.

*Received October 18, 2003.*

## REFERENCES

1. P. Henderson, *Inorganic Geochemistry*, Pergamon Press, Oxford (1986).
2. D.W. King, J. Lin, and D.R. Kester, *Anal. Chim. Acta* 247, 125 (1991).
3. F. Van Lente, *Anal. Chem.* 65, 374R (1993).
4. I. Kolotyrykina, L.K. Shpigun, Y.A. Zolotov, and A. Malahoff, *Analyst* 120, 201 (1995).
5. W.G. Sunda and S.A. Huntsman, *Mar. Chem.* 50, 189 (1995).
6. C.M.G. Van der Berg, *Mar. Chem.* 50, 139 (1995).
7. J. Wu, and G.W. Luther, *Mar. Chem.* 50, 159 (1995).
8. S. Takeda, and H. Obata, *Mar. Chem.* 50, 219 (1995).
9. L.J.A. Gerring, H.J.W. de Baar, and K.R. Timmermans, *Mar. Chem.* 68, 335 (2000).
10. K. Hirayama and N. Unohara, *Anal. Chem.* 60, 2573 (1988).
11. S. Krekler, W. Frenzel, and G. Shulze, *Anal. Chim. Acta* 296, 115 (1994).
12. U. Hase and K. Yoshimura, *Analyst* 117, 1501 (1992).
13. L. Battistini and J. Lopez-Palacios, *Anal. Chem.* 66, 2005 (1994).
14. A.K. Shrivastava, *Rev. Anal. Chem.* 14, 142 (1995).
15. L. Campanella, K. Pyrzynska, and M. Trojanowicz, *Talanta* 43, 825 (1996).
16. M. Kabacinski, S.J. Zerbe, and J. Baralkiewicz, *Chem. Anal.* 41, 55 (1996).
17. S. Blain and P. Treguer, *Anal. Chim. Acta* 308, 425 (1995).
18. A.I. Elfeterov, S.N. Nosal, P.N. Nestrenko, and O.A. Shpigun, *Analyst* 119, 1329 (1994).
19. R.M.C. Sutton, S.J. Hill, P. Jones, A. Sanzmenel, J.I. Graciaalonso, *J. Chromatogr.* 816, 286 (1998).
20. I.T. Urasa and W.J. Mavura, *Intern. J. Environ. Anal. Chem.* 48, 229 (1992).
21. S. Roncevic and I. Steffan, *At. Spectrosc.* 23, 24 (2002).
22. J. Ruzicka and E.H. Hansen, *Anal. Chim. Acta* 99, 37 (1978).
23. C. B'Hymer, K.L. Sutton, and J.A. Caruso, *J. Anal. At. Spectrom.* 13, 855 (1998).
24. D.M. Fraley, D. Yates and S.E. Manahan, *Anal. Chem.* 51, 2225 (1979).



# Evaluation of Sample Treatment for the Simultaneous Flow Injection Hydride Generation and Determination of As, Bi, Sb and Se by GFAAS

Carolina D. Freschi, Gian Paulo G. Freschi, and José A. Gomes Neto\*  
Instituto de Química, Universidade Estadual Paulista, PO Box 355,  
14801-970 Araraquara-SP, Brazil

## INTRODUCTION

Hydride generation (HG) coupled to atomic and mass spectrometric techniques has become a powerful analytical tool (1–6). Since the first proposal of in situ trapping of hydride-forming elements in a graphite atomizer by Drasch et al. (7), several works have been published on the coupling of HG-GFAAS (8–12). Among the main advantages of the hydride-based techniques are analyte separation from the matrix solution, high relative sensitivity, low detection limits, automation possibility, and speciation potential (1). Besides these useful characteristics, the "Achilles heel" of the technique is related to the different efficiency of the HG from the different oxidation states of the same element. As a consequence, most workable samples require treatment before analysis. This is more critical when simultaneous hydride generation is involved. Various studies on the simultaneous determination of total inorganic As and Se(IV) (13), Bi(III) and Se(IV) (14), total inorganic As, total inorganic Sb and Bi(III), total inorganic Se and Bi(III) (15), total inorganic As, Bi(III), Sb(V), and Se(IV) (16) by hydride generation coupled to electrothermal atomic absorption spectrometry can be found in the literature. However, little attention has been given to the simultaneous reduction of As, Bi, Sb, and Se because this is a laborious sample pre-treatment process.

Garbós et al. (13) described a method for total inorganic As, and

## ABSTRACT

A new method was developed for the simultaneous determination of As, Bi, Sb, and Se by flow injection hydride generation graphite furnace atomic absorption spectrometry. An alternative two-step sample treatment procedure was used. The sample was heated (80°C) for 10 min in 6 M HCl to reduce Se(VI) to Se(IV), followed by the addition of 1% (m/v) thiourea solution to reduce arsenic and antimony from the pentavalent to the trivalent states.

With this procedure, all analytes were converted to their most favorable and sensitive oxidation states to generate the corresponding hydrides. The pre-treated sample solution was then processed in the flow system for in situ trapping and atomization in a graphite tube coated with iridium. The Ir permanent modifier remained stable up to 300 firings and new coatings were possible without significant changes in the analytical performance.

The accuracy was checked for As, Bi, Sb, and Se determination in water standard reference materials NIST 1640 and 1643d and the results were in agreement with the certified values at a 95% confidence level. Good recoveries (94–104%) of spiked mineral waters and synthetic mixtures of As(III), As(V), Sb(III), Sb(V), Se(VI), and Se(IV) were also found. Calculated characteristic masses were 32 pg As, 79 pg Bi, 35 pg Sb, and 130 pg Se, and the corresponding limits of detection were 0.06, 0.16, 0.19, and 0.59  $\mu\text{g L}^{-1}$ , respectively. The repeatability for a typical solution containing 5  $\mu\text{g L}^{-1}$  As, Bi, Sb, and Se was in the 1–3% range.

only Se(IV) with in situ trapping and atomization in a graphite tube coated with zirconium. Murphy et al. (14) investigated the simultaneous determination of Bi and Se after trapping in Ir-coated platform. The authors also published a paper (15) on the use of L-cysteine or hydrochloric acid for the determination of As, Bi, and Sb or Bi and Se, respectively. The performance of the Ir-coated platform was compared with the Zr-coated platform.

The operating parameters for the simultaneous determination of As, Bi, Sb, and Se were optimized by employing a multivariate approach based on the concepts of experimental design and empirical modeling by HG-GFAAS using W-coated tubes co-injected with a Pd-Mg modifier solution (16). As only Se(IV) was tested, the conditions of pre-reduction of Se(VI) to Se(IV) were not studied.

The pronounced effect of the oxidation states of analytes to generate the respective gaseous hydrides needs to be considered. The reduction of Sb(V) to the Sb(III) species described in the literature is similar to those for arsenic species and it can use iodide, ascorbic acid, or thiourea. On the other hand, some reducing agents can lead Se(VI) to elemental Se, which is unable to form  $\text{SeH}_2$ . Boiling HCl is usually used to reduce selenium to the Se(IV) form prior to the formation of the hydride (1,17–19).

Based on the above considerations, the objective of this study was to develop a simple and efficient sample treatment strategy for the simultaneous determination of As, Bi, Sb, and Se. Pretreatment of

\*Corresponding author.  
E-mail address: [anchieta@iq.unesp.br](mailto:anchieta@iq.unesp.br)  
Fax: + 55 16 2227932

the sample with heated hydrochloric acid followed by thiourea guaranteed the reduction of analytes to the most favorable species to form hydrides. The proposed procedure was applied to the As, Bi, Sb, and Se determination in water samples by flow injection hydride generation graphite furnace AAS.

## EXPERIMENTAL

### Instrumentation

A PerkinElmer SIMAA<sup>TM</sup> 6000 (PerkinElmer Life and Analytical Sciences, Shelton, CT, USA) simultaneous graphite furnace atomic absorption spectrometer with a THGA<sup>TM</sup> transversely heated graphite atomizer and longitudinal Zeeman-effect background corrector was used. End cap THGA tubes with integrated platforms and "System 2" electrodeless discharge lamps operated at the manufacturer's recommended conditions were used for this study. Argon (99.999%, White Martins) was employed with a gas flow rate of 250 mL min<sup>-1</sup>. The furnace program used is shown in Table I. It should be stressed that a temperature higher than 2300°C should not be used at the cleanout stage in order to avoid Ir losses. The platform of the graphite tube of the spectrometer was pre-treated with 120 µg Ir after a new tube had first been thermally conditioned. A volume of 120 µL IrCl<sub>3</sub> solution was injected onto the platform in three successive aliquots of 40 µL. The heating program (temperature, ramp time, hold time) comprising four steps for Ir deposition was run using the following program described elsewhere (20): (a) 110°C, 1 s, 50 s; (b) 130°C, 30 s, 50 s; (c) 1200°C, 20 s, 30 s; (d) 2000°C, 1 s, 5 s. After the last step, the tube can be used for measurements.

A PerkinElmer FIAS<sup>TM</sup>-400 flow system, equipped with an AS-90 autosampler, was used. A quartz

capillary (i.d. 1.0 mm) was employed replacing the PTFE capillary of the autosampler by a PTFE transfer line (i.d. 2.0 mm) to transport the hydrides from the gas-liquid separator to the atomizer. The quartz capillary (QC) was adjusted for a distance of about 1.5 mm between the tip and platform surface. Tygon<sup>®</sup> tubes were used to pump the reagent R, the sample S, and the carrier stream C (Figure 1). PTFE tubing (i.d. 0.7 mm) was employed for loop L, coiled reactor B, and the transmission lines. The operation of the flow system shown in Figure 1 (A and B) comprises two steps: sampling (Figure 1A); and injection, hydride generation, and trapping (Figure 1B). In

the position specified in the figure, a sample volume of 500 µL was selected by the sampling loop. After loop-based injection, the analyte zone merges at the confluent point x with an alkaline NaBH<sub>4</sub> solution. The As, Bi, Sb, and Se hydrides are formed inside the reactor (300 mm length). The established analyte zone merges with an argon flow (Ar) that carries hydrides into the gas-liquid separator chamber (GLS) containing a 0.2-µm PTFE membrane. Gaseous hydrides are directed to the graphite tube where they are trapped, while the remaining solution inside the chamber is discharged (W2). After the valve is switched back to the position spec-

**TABLE I**  
**Heating Program of the THGA of the Spectrometer**

Step	Temperature (°C)	Ramp Time (s)	Hold Time (s)	Gas Flow (mL min <sup>-1</sup> )
1	400	1	40	0
2	400	1	20	250
3	2200	0	5	0
4	2300	1	3	250

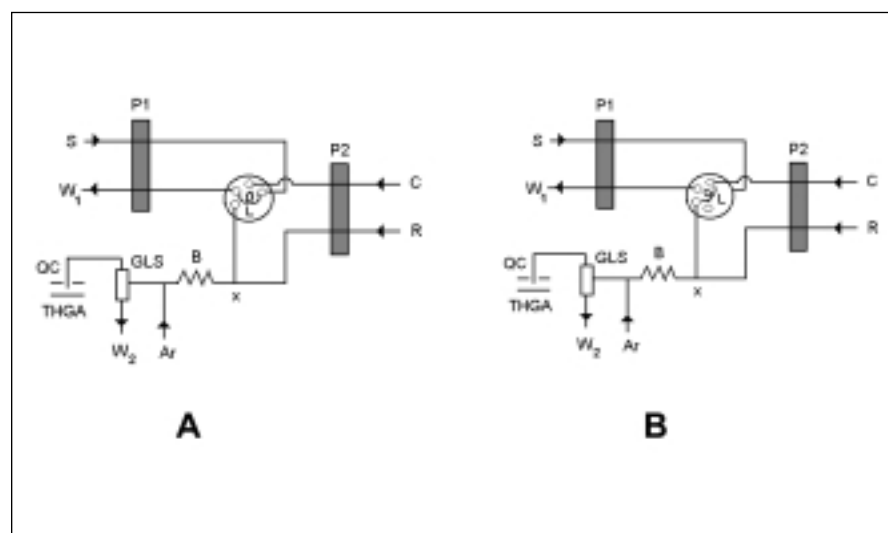


**Fig. 1.** Schematic diagram of the flow system used for the simultaneous determination of As, Bi, Sb and Se. S: sample or analytical solution (7.8 mL min<sup>-1</sup>); R: 0.5% (m/v) NaBH<sub>4</sub> + 0.5% (m/v) NaOH (4.8 mL min<sup>-1</sup>); C: 2M HCl (7.4 mL min<sup>-1</sup>); Ar: argon at 125 mL min<sup>-1</sup>; W<sub>1</sub>: wastes; P1, P2: peristaltic pumps; L: sampling loop (500 µL); B: coiled reactor (30 cm); GLS: gas-liquid separator; QC: quartz capillary; THGA: graphite tube.

ified in Figure 1A, another cycle can be started. Details of time/pumping program of the flow system and the sequence of the THGA program used are shown in Table II and I, respectively. Atomic signals were measured in integrated absorbance mode.

### Reagents, Analytical Solutions, and Samples

All solutions were prepared with high-purity chemicals and distilled deionized water (Milli-Q™ system, Millipore, Bedford, MA, USA). Suprapur® hydrochloric acid (Merck, Darmstadt, Germany) was used to prepare the standard solutions.

Arsenic(III) stock standard solution (1000 mg L<sup>-1</sup>) was prepared by dissolving 1.320 g As<sub>2</sub>O<sub>3</sub> (Aldrich, St. Louis, MO, USA) in about 20 mL 1.0 M NaOH. To this solution, 50 mL of 0.5 M HCl was added and the volume brought to 1000-mL volume with water. Arsenic(V) stock standard solution (1000 mg L<sup>-1</sup>) was prepared by dissolving 4.1656 g Na<sub>2</sub>HAsO<sub>4</sub>·7H<sub>2</sub>O (Aldrich, St. Louis, MO, USA) in 1000 mL of 0.1 M HCl.

Selenium(IV) stock standard solution (1000 mg L<sup>-1</sup>) was prepared by dissolving 1.405 g SeO<sub>2</sub> (Aldrich, St. Louis, MO, USA) in 1000 mL of 1.0 M HCl. Selenium(VI) stock standard solution (1000 mg L<sup>-1</sup>) was prepared by dissolving 2.3925 g Na<sub>2</sub>SeO<sub>4</sub> (Aldrich, St. Louis, MO, USA) in 1000 mL of 0.1 M HCl.

Antimony(III) stock standard solution (1000 mg L<sup>-1</sup>) was prepared by dissolving 2.7385 g K(SbO)C<sub>4</sub>H<sub>4</sub>O<sub>6</sub>·1/2H<sub>2</sub>O (Aldrich, St. Louis, MO, USA) in 1.0 M HCl. Antimony(V) stock standard solution (1000 mg L<sup>-1</sup>) was prepared by diluting 10 mL SbCl<sub>5</sub> solution (Aldrich, St. Louis, MO, USA) in 1000 mL of 6.0 M HCl.

Bismuth stock solution (1000 mg L<sup>-1</sup>) was prepared by diluting the Normex™ standard solution of Bi(NO<sub>3</sub>)<sub>2</sub>·5H<sub>2</sub>O (Carlo Erba, Milan, Italy) in 1000 mL of water.

**TABLE II**  
**Sequence Control and Optimized Program for the Flow System**

FIAS Step	Time (s)	Pump 1 (rpm)	Pump 2 (rpm)	Valve Position	Comments
Prefill	15	100	0	Fill	For the first replicate, FIAS 400 autosampler sampling tube is rinsed with sample solution
1	10	100	0	Fill	The sample loop is filled
2	5	100	80	Fill	Carrier, reducing agent and sample flow stabilize. At the same time, the furnace is pre heated
3	20	0	80	Inject	The reaction takes place. The pipet moves into the graphite furnace and at the same time sample is injected into the carrier stream. The hydrides are trapped.

While FIA pumps stop to save reagents, furnace run the steps 2–4, to dry, atomization, measurements and clean out for a new sample analysis.

Sodium borohydride solution (0.5% m/v) was prepared daily by dissolving 0.5 g NaBH<sub>4</sub> (Merck, Darmstadt, Germany) in 100 mL of 0.5% (m/v) NaOH (Merck, Darmstadt, Germany) solution. A 10% (m/v) thiourea solution was prepared by dissolving 5 g H<sub>4</sub>N<sub>2</sub>CS (Aldrich, Milwaukee, WI, USA) in 50 mL of 2 M HCl. This solution was prepared weekly and stored in the refrigerator.

Iridium (IrCl<sub>3</sub>·3H<sub>2</sub>O) modifier solution (1000 mg L<sup>-1</sup>) was a stock solution (Part No. B3140391, PerkinElmer Life and Analytical Sciences, Shelton, CT, USA) used without dilution.

A 10-mL mineral water sample (purchased at a local supermarket, Araraquara City, Brazil) or standard reference material (NIST 1643d and NIST 1640 - National Institute of Standards and Technology, Gaithersburg, MD, USA) and 10 mL concentrated hydrochloric acid were added into 100-mL digestion tubes, then placed on a digestion block at 80°C for 10 min. Then,

5 mL of the cooled digestion solution was added to a 15-mL flask, followed by addition of 1.5 mL of 10% (m/v) thiourea solution. The resulting solution was diluted to 15 mL with water. The flasks were then adjusted to the AS-90 autosampler and their solutions were controlled through the flow system (Figure 1) using the program as specified in Table II.

For comparison purposes, the samples were also prepared in a Multiwave® microwave oven (Anton Paar, Graz, Austria), equipped with high-pressure TFM vessels. A program comprising four steps was used. The total time was 20 min, of which 3 min at 600 W power were necessary to complete the reduction step. The remaining time was used to cool the system.

Working standard solutions of As, Bi, Sb, and Se were similarly pretreated in order to obtain solutions in the 2.00–10.0 µg L<sup>-1</sup> concentration range.

## RESULTS AND DISCUSSION

### Optimization of the First Pre-reduction Stage

Sample treatment is of utmost relevance for the HG techniques, mainly for simultaneous detection purposes. The oxidation and binding state of the analytes strongly affects the HG reaction rate for elements such as As, Sb, and Se, which exhibit pronounced differences in their analytical behavior. For this

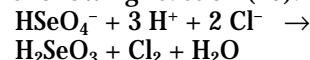
reason, in most procedures a pre-reduction stage is required.

Regarding the first pre-reduction step of the proposed procedure, the influence of HCl concentration was not investigated because it is known from the literature that selenium can be reduced to the tetravalent state by boiling 4–6 M HCl (1).

The influence of time on the reduction of the analytes in 6 M HCl was investigated in the 0–45 minute range using a block digester

at 80°C. Bismuth is present in the medium as trivalent species and was not affected by time (Figure 2).

Integrated absorbance for As(V) and Sb(V) did not alter significantly with an increase in time up to 45 min. The integrated absorbance for Se(VI) increased steeply with a reduction in time up to 5 minutes, above which it became nearly constant (Figure 2A). On the other hand, the ability of As(III) and Sb(III) to generate arsine and stibine, respectively, was affected by time (Figure 2B). This may be attributed to the possible formation of As(V) and Sb(V) caused in the presence of the oxidizing agent chlorine which is formed during the Se(VI) reduction according to the following reaction (19):



For a total determination of inorganic As and Sb, a second reduction step is necessary involving the addition of other reducing agents to convert pentavalent As and Sb species to the trivalent state. As a similar integrated absorbance for 5.0  $\mu\text{g L}^{-1}$  Se(VI) or Se(IV) solutions was obtained after a 5 minute reduction time, this time was then also selected for the first step of the sample pretreatment procedure.

Taking this fact into account and in order to establish an alternative heating source to speed up the reduction, a microwave-assisted closed system was studied. In this system, the eventual loss of analytes was minimized and the time was reduced to 3 minutes at 600 W. The results of the performance of the closed system are depicted in Figure 3. An analysis of this figure reveals that there is no difference between the closed or the open system.

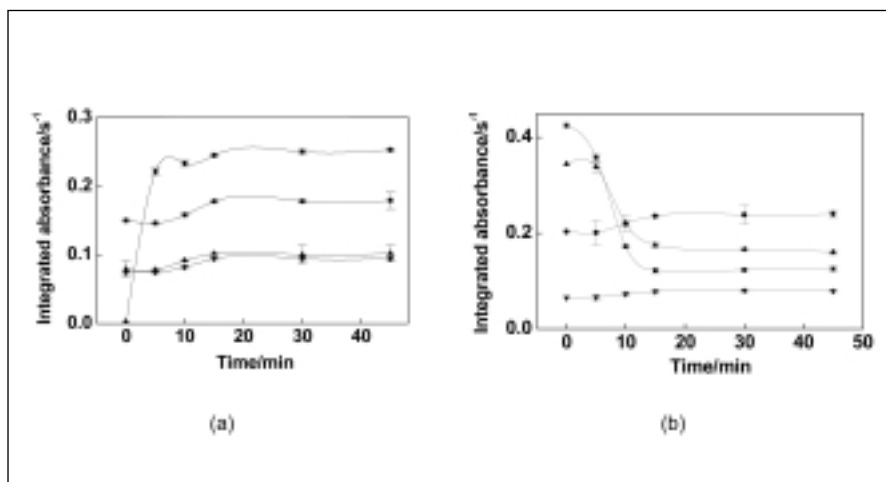


Fig. 2. Influence of the heating time on reduction of (a) (●) Se(VI), (■) As(V), (▲) Sb(V), (▼) Bi(III) and (b) (●) Se(IV), (■) As(III), (▲) Sb(III), (▼) Bi(III). Conditions: 6M HCl and open system.

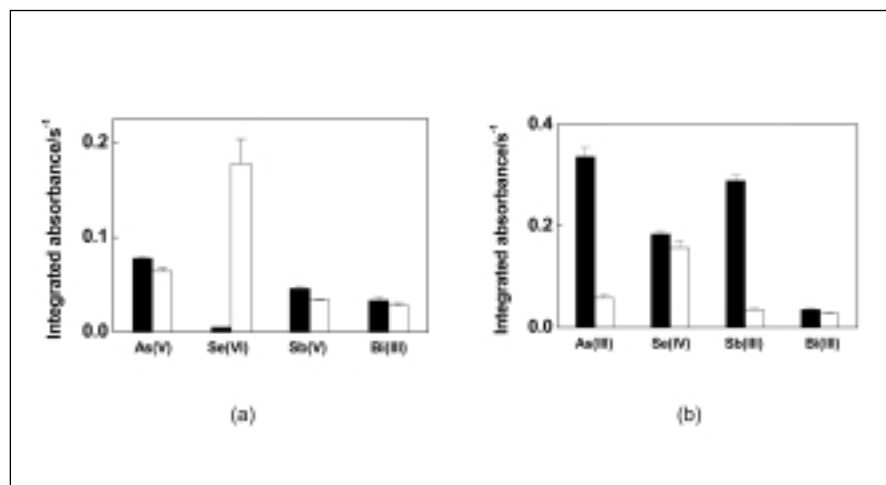


Fig. 3. Comparative results of the simultaneous measurements of (a) 5.0  $\mu\text{g L}^{-1}$  Se(VI), As(V), Sb(V), Bi(III) and (b) 5.0  $\mu\text{g L}^{-1}$  Se(IV), As(III), Sb(III), Bi(III) obtained before (black columns) and after (white columns) reduction pretreatment in a closed system.

## Optimization of the Second Pre-reduction Stage

With regard to the second pre-reduction step, which involves reduction of pentavalent As and Sb to the trivalent states, potassium iodide and ascorbic acid could not be tested since these reagents rapidly reduce selenium to the elemental state, impairing the detection of Se. Thiourea and L-cysteine were investigated as possible reducing agents for As(V) and Sb(V). When a multielement solution containing  $5 \mu\text{g L}^{-1}$  As(V), Sb(V), Se(IV), and Bi(III) was pretreated with 1% (m/v) of L-cysteine and processed in the flow system, no measurable absorbance for atomic Se was observed. This was attributed to the capability of L-cysteine to reduce Se(IV) to the elemental state (21). Indeed, absorbance values for As and Bi were 50% lower than those obtained with the thiourea medium. Besides, similar signals were obtained for Sb using L-cysteine or thiourea as the reducing agent. Thiourea was selected for further experiments since the main objective of this work deals with the simultaneous generation of As, Bi, Sb and Se hydrides.

The influence of thiourea amount on analyte signal was investigated within a 0–1% (m/v) concentration range (Figure 4). Different multielement solutions containing  $5 \text{ mg L}^{-1}$  As(V), Sb(V), Se(VI), and Bi(III) plus 6 M HCl were pre-heated ( $80^\circ\text{C}$ ) for 10 min, thereafter the cooled solutions were pre-treated with different amounts of reducing agent and the final solutions containing 0, 0.2, 0.4, 0.6, 0.8 and 1% (m/v) of thiourea were positioned in the autosampler of the flow system depicted in Figure 1. The measured maximum integrated absorbance of As, Sb, and Bi increased with thiourea amounts up to 0.4% (m/v). Higher concentrations did not alter the absorbance significantly. On the other hand, poor precision of measurements for As was obtained for thiourea amounts  $< 0.6\%$  (m/v). Atomic signals for Se decreased steeply by approximately 50% when the thiourea concentration was varied from 0 to 0.8% (m/v), above which they became constant. Despite the Se losses, the 1% (m/v) concentration of this reducing agent was selected for further experiments as a compromise

for achieving maximum sensitivity for As, Bi, and Sb and suitable precision of As measurements.

## Influence of Foreign Ions

Metals that usually inhibit arsine, bismuthine, stibine, and  $\text{SeH}_2$  generation and are generally present in water samples (1,22) were tested as potential interferents. For the interference studies, a multielement solution containing  $5 \mu\text{g L}^{-1}$  As, Bi, Sb, and Se in 2 M HCl was processed ( $n=3$ ) in the flow system (see Figure 1) in the absence and presence of different concentrations of the interferents ( $0.05, 0.5, 5.0, \text{ or } 50 \text{ mg L}^{-1}$ ) in order to evaluate the influence of Cu, Co, Fe, Ni, and Pb over analyte determination. The transition metals were selected due to their serious effects in most workable samples. Interferences were quantified by a tolerance limit which is the interferent concentration leading to a 10% signal depression. The experimental results showed that interferences obtained in the presence of thiourea were lower than those observed without the reducing agent. Bismuth and selenium were more affected; in particular, in the presence of  $5 \text{ mg L}^{-1}$  Fe(III) and  $50 \text{ mg L}^{-1}$  Ni(II). Arsenic and antimony were only affected by Ni(II) at concentrations above  $50 \text{ mg L}^{-1}$ . For the selected application in this work, arsine, bismuthine, stibine, and  $\text{SeH}_2$  occur usually in the presence of nearly negligible amounts of these potential interfering species.

## Long-term Stability of the Ir-coated Platform

The stability of the Ir-coated platform was investigated by checking the repeatability of the integrated absorbance measurements after successive firings of a  $5.0 \mu\text{g L}^{-1}$  As, Bi, Sb, and Se multielement solution. An average of 15 measurements and the respective RSD values were obtained. Under these conditions,

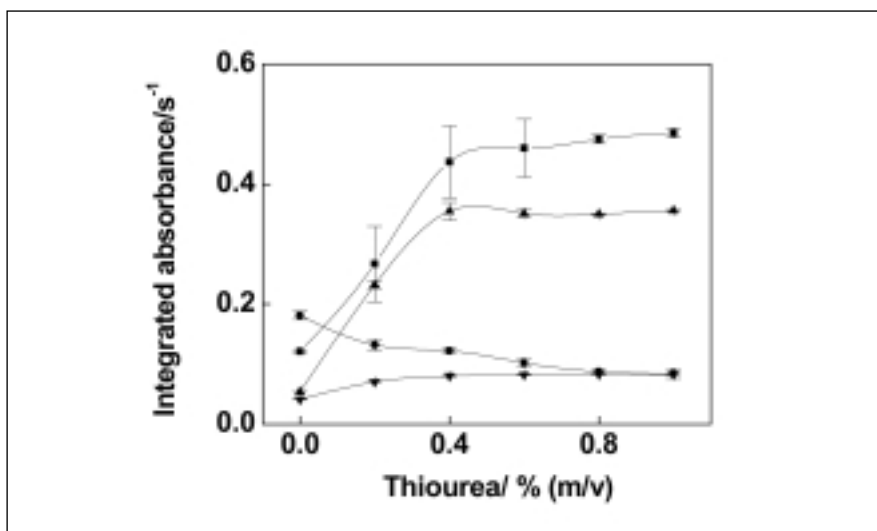


Fig. 4. Influence of thiourea concentration on analyte reduction. Curves correspond to a solution containing  $5.0 \mu\text{g L}^{-1}$  (■) As(V), (▼) Bi(III), (▲) Sb(V), and Se(VI) (●) in 2% (v/v) HCl after reduction pretreatment step.

the coating lifetime was equivalent to about 300 firings. After these, two re-coatings were performed without experiencing any loss in sensitivity and repeatability. Shown in Figure 5 are long term-stability curves of Ir indicated by integrated absorbance and precision for all analytes. The Ir-permanent modifier allows the use of the graphite tube up to about 800 firings. It is important to point out that the atomizer lifetime was limited to tube wall durability. When the upper surface of the atomizer was destroyed after  $\approx 800$  firings, the Ir-treated platform remained intact. The lifetime of a THGA atomizer could be significantly increased if the use of permanent modifiers in ETAAS analysis were used in a laboratory.

### Analytical Performance

Two water standard reference materials, NIST 1640 and NIST 1643d, were analyzed to investigate the feasibility of the sample pretreatment method using the open system. It should be noted that the hydride generation efficiency for Se was affected when microwave-assisted pretreatment of the SRMs was performed. This problem was attributed to the NO<sub>x</sub> interference in the high-pressure closed system. It is good practice to heat the samples containing high amounts of nitric acid in the open system in order to minimize the effects of this oxidizing agent on Se determination. The results of the determination of analytes were compared with the certified values

of SRMs (Table III). According to a paired *t*-test, all results were in agreement at the 95% confidence level, which is a good indication of the robustness of the proposed method. Calibration curves with good linear correlation coefficients ( $r > 0.999$ ) were obtained within the 2.0–10  $\mu\text{g L}^{-1}$  concentration range. The relative standard deviations ( $n = 12$ ) were  $\leq 1.1\%$ ,  $\leq 2.9\%$ ,  $\leq 0.9\%$ , and  $\leq 1.4\%$  for 5  $\mu\text{g L}^{-1}$  As, Bi, Sb, and Se, respectively, indicating good repeatability of the proposed method. Good recoveries (within the 94–104% range) of the spiked (1.0–2.0  $\text{mg L}^{-1}$ ) mineral waters and synthetic mixtures of As(III), As(V), Sb(III), Sb(V), Se(VI), and Se(IV) were also obtained. For a 500- $\mu\text{L}$  injected sample volume,

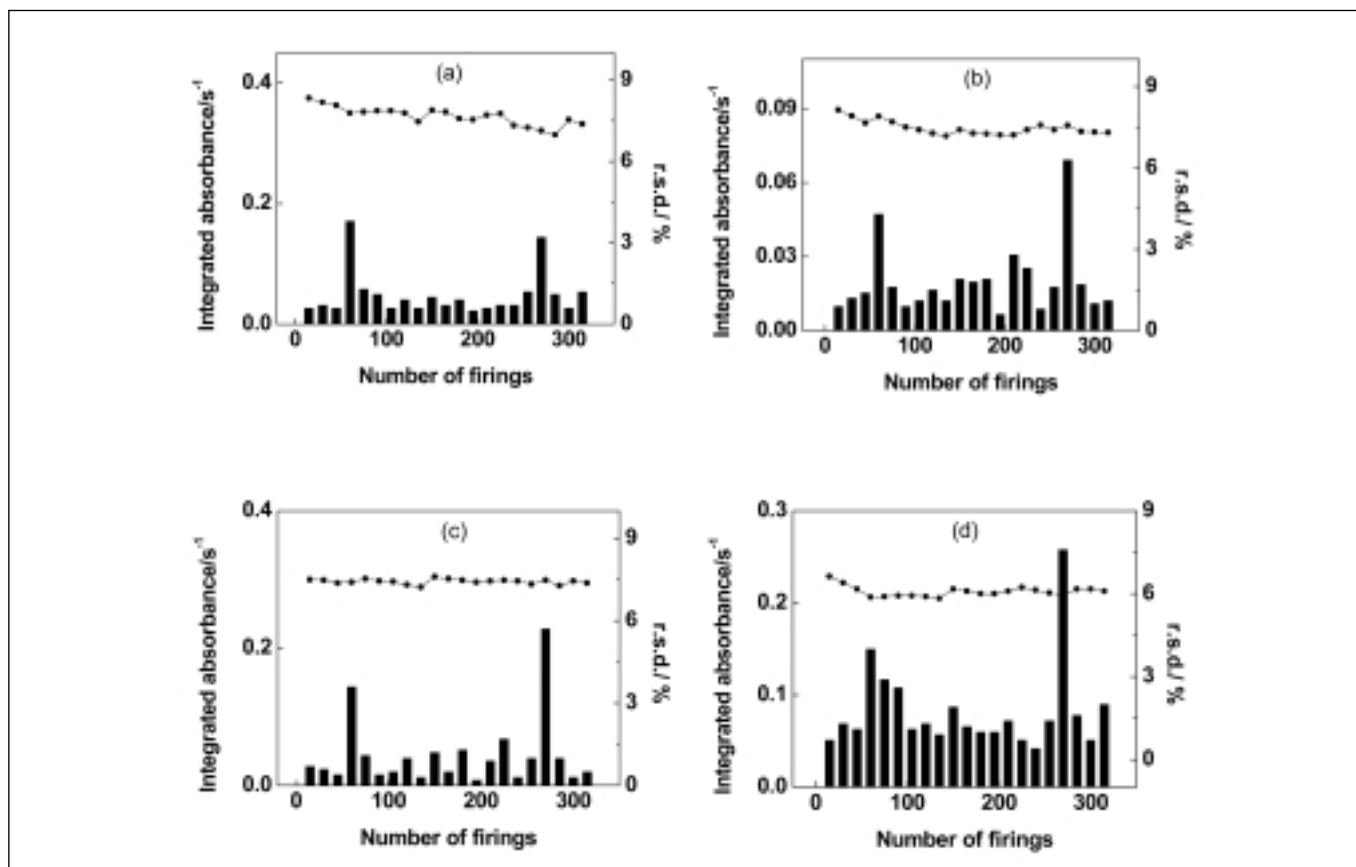


Fig. 5. Long-term stability curves of Ir-coated platform. Each point ( $\bullet$ ) represents average of 15 measurements for (a) As, (b) Bi, (c) Sb, and (d) Se and each column the RSD.

**TABLE III**  
**Comparative Results of the Simultaneous Determination of As, Bi, Sb, and Se in Standard Reference Materials<sup>a,b</sup> (SRM 1640; SRM 1643d) by the Proposed System**

SRM	Concentration ( $\mu\text{g L}^{-1}$ )							
	As	As <sup>a</sup>	Bi	Bi <sup>b</sup>	Sb	Sb <sup>a</sup>	Se	Se <sup>a</sup>
1640	26.81	26.67		—	14.22	13.79	23.41	21.96
	0.5%	1.5%			0.2%	3.0%	1.8%	2.3%
1643d	50.5	56.02	15	13	56.12	54.1	12.22	11.43
	1.4%	1.3%			0.4%	2.0%	2.9%	1.5%

<sup>a</sup> Certified values; <sup>b</sup> non-certified value (informative only).

the calculated characteristic masses were 32 pg As, 79 pg Bi, 35 pg Sb, and 130 pg Se and the corresponding limits of detection ( $3\sigma$ ) were 0.06, 0.16, 0.19, and 0.59  $\mu\text{g L}^{-1}$ , respectively. It should be noted that the simultaneous reduction of the four analytes usually leads to a drop in sensitivity in comparison to single-element analysis.

### CONCLUSION

A sample pretreatment method was developed for the simultaneous determination of As, Bi, Sb, and Se in mineral waters by hydride generation in graphite furnace atomic absorption spectrometry. The analysis of two water reference materials was accomplished and good agreement of the results was achieved between the experimental and certified values.

The alternative two-step sample treatment procedure comprises heating of the sample in HCl medium to reduce Se(VI) to Se(IV), followed by the addition of thiourea solution to reduce arsenic and antimony from the pentavalent to the trivalent states. The pretreated sample solution was processed in a flow system for in situ trapping and atomization in a graphite tube coated with Ir permanent modifier which remained stable up to 300 firings.

The simultaneous detection means less time per element and, consequently, lower analytical cost.

### ACKNOWLEDGMENTS

The authors thank the Fundação de Amparo à Pesquisa do Estado de São Paulo and Conselho Nacional de Desenvolvimento Científico e Tecnológico for financially supporting this work and for fellowships to J.A.G.N., C.D.F., and G.P.G.F.

*Received August 7, 2003.*

### REFERENCES

1. J. Dedina and D.L. Tsalev, *Hydride Generation Atomic Absorption Spectrometry*, Wiley-VCH, Chichester, UK (1995).
2. J. Moreda-Piñeiro, C. Moscoso-Pérez, P. López-Mahia, S. Muniategui-Lorenzo, E. Fernández-Fernández, and D. Prada-Rodríguez, *Anal. Chim. Acta* 431, 157 (2001).
3. F. Barbosa Jr., S.S. Souza, and F.J. Krug, *J. Anal. At. Spectrom.* 17, 382 (2002).
4. C. Rigby and I.D. Brindle, *J. Anal. At. Spectrom.* 14, 253 (1999).
5. S.J. Santosa, H. Mokudai, and S.J. Tanaka, *J. Anal. Atomic Spectrom.* 12, 409 (1997).
6. M. Segura, Y. Madrid, and C. Cámara, *J. Anal. At. Spectrom.* 14, 131 (1999).

7. G. Drasch, L.V. Meyer, and G. Kauert, *Fresenius' Z. Anal. Chem.* 304, 141 (1980).
8. R.E. Sturgeon, S.N. Willie, G.I. Sproule, P.T. Robinson, and S.S. Berman, *Spectrochim. Acta Part B* 44, 667 (1989).
9. D.L. Tsalev, A. D'Ulivo, L. Lampugnani, L.M. Di Marco, and R. Zamboni, *J. Anal. At. Spectrom.* 10, 1003 (1995).
10. H. Matusiewicz and R.E. Sturgeon, *Spectrochim. Acta Part B* 51, 377 (1996).
11. J.P. Matousek, R. Iavetz, K.J. Powell, and H. Louie, *Spectrochim. Acta Part B* 57, 147 (2002).
12. P. Bermejo-Barrera, J. Moreda-Piñeiro, A. Moreda-Piñeiro, and A. Bermejo-Barrera, *Anal. Chim. Acta* 368, 281 (1998).
13. S. Garbós, M. Walcerz, E. Bulska, and A. Hulanicki, *Spectrochim. Acta Part B* 50, 1669 (1995).
14. J. Murphy, P. Jones, G. Schlemmer, I.L. Shuttler, and S.J. Hill, *Anal. Commun.* 34, 359 (1997).
15. J. Murphy, G. Schlemmer, I.L. Shuttler, P. Jones, and S.J. Hill, *J. Anal. At. Spectrom.* 14, 1593 (1999).
16. M. Elsayed, E. Björn, and W. Frech, *J. Anal. At. Spectrom.* 15, 697 (2000).
17. J. Stripeikis, P. Costa, M. Tudino, and O. Troccoli, *Anal. Chim. Acta* 408, 191 (2000).
18. C. Brunori, M.B. Calle-Guntiñas, R. Morabito, *Fresenius J. Anal. Chem.* 360, 26 (1998).
19. R.M. Olivas and O.F.X. Donard, *Talanta* 45, 1023 (1998).
20. *The FIAS-Furnace Technique, User's Guide*, PerkinElmer Life and Analytical Sciences, Shelton, CT, USA (2000).
21. J. Bowman, B. Fairman, and T. Catterick, *J. Anal. At. Spectrom.* 12, 313 (1997).
22. P. Pohl and W. Zyrnicki, *Anal. Chim. Acta* 468, 71 (2002).

# Determination of Al, Cd, and Pb in Brazilian Sugar Cane Spirit, Cachaça, by ETAAS Using Matrix-matched Calibration

Marcus H. Canuto<sup>a</sup>, Helmuth G. L. Siebald<sup>b</sup>, Milton Batista Franco<sup>c</sup>, and \*José Bento Borba Silva<sup>b</sup>

<sup>a</sup>Departamento de Ciências Básicas, Faculdades Federais Integradas de Diamantina, FAFEID, Rua da Glória 152, 39100-187, Diamantina, MG, Brazil

<sup>b</sup>Departamento de Química, Universidade Federal de Minas Gerais, Av. Antônio Carlos 6627, 31270-901, Belo Horizonte, MG, Brazil

<sup>c</sup>Laboratório de Absorção Atômica, Centro de Desenvolvimento de Tecnologia Nuclear/CDTN/CNEW, Belo Horizonte, MG, Brazil

## ABSTRACT

In this work, a method is described for the determination of aluminium, cadmium, and lead in the Brazilian sugar cane spirit, cachaça, by electrothermal atomic absorption spectrometry (ETAAS) using matrix-matched calibration, i.e., calibration curves obtained at 40% (v/v) in ethanol-water media (the average alcohol content in cachaça). The methodology was applied to the determination of these three metals in 53 cachaça samples obtained from 53 different Jequitinhonha High Valley producers, in the Minas Gerais State, Brazil. All metals were determined with or without permanent chemical modifiers such as Zr+Rh and Ir+Rh. The selection of pyrolysis and atomization temperatures was determined in the presence of the matrix.

Best results were obtained without the use of chemical modifiers for Al and Cd. For Pb, the

results without a modifier were similar to those obtained using Zr + Rh (500 and 250 µg, respectively) or with Ir + Rh (500 and 250 µg) as the permanent modifier. For aluminum, without the use of a chemical modifier, the best pyrolysis and atomization temperatures were 1000 and 2500°C, respectively, with a characteristic mass ( $m_0$ ) of 9.0 pg (recommended 10 pg). It can therefore be assumed that cachaça itself in some way acts as modifier because it allows the use of higher temperatures for the three studied analytes.

Two samples of cachaça, spiked with different amounts of Al, showed recoveries between 87.5% and 103.0%, with a relative standard deviation (RSD) ( $n=3$ ) of less than 5%. The detection limit (LOD) ( $k=3$ ,  $n=10$ ) was 2.0 µg L<sup>-1</sup>. The Al results for the 53 samples varied from non-detectable to 22.4 µg L<sup>-1</sup>.

For cadmium, without the use of a modifier, the best pyrol-

ysis and atomization temperatures were 1000 and 1400°C, respectively, with  $m_0$  0.5 pg (equal to recommended). Two samples spiked with cadmium presented recoveries from 103.1–114.6%, with an RSD of less than 4%; the LOD was 0.07 µg L<sup>-1</sup>. In the 53 samples, the Cd values varied from non-detectable to 0.7 µg L<sup>-1</sup>.

For lead, without use of a modifier, the best pyrolysis and atomization temperatures were 900 and 1900°C, respectively, with  $m_0$  11.0 pg (recommended 10 pg). Two samples spiked with different amounts of the metal showed recoveries from 95.1–118.8%, with an RSD ( $n=3$ ) less than 6%; the LOD was 0.6 µg L<sup>-1</sup>. For 53 samples, the Pb results varied from non-detectable to 526.0 µg L<sup>-1</sup>.

For the three studied analytes, Al, Cd, and Pb, the calibration curves for matrix matching had an  $r$  (lineal regression coefficient) higher than 0.99.

## INTRODUCTION

Aluminum is an abundant metal in the earth and does not have any positive function in the human metabolism. Even low Al concentrations (above 5.0 µg L<sup>-1</sup>) are associated with diseases such as renal insufficiency, encephalopathy, pulmonary fibrosis, microcytic anemia, and sleeping disturbances, while high Al concentrations in the brain are known to cause Alzheimer's disease (1,2).

\*Corresponding author.  
E-mail: bentojb@terra.com.br

Cadmium is an element not essential to human life and potentially poisonous in low concentrations. The first mention of its poisonous effects in human beings was by Sovet in 1858 (3). Only over the last decades has there been a significant increase in the number of studies performed regarding this metal. In 1950 in Japan (3) illnesses such as osteomalacia and proteinuria were caused by the ingestion of Cd-polluted foods. Cadmium became then one of the metals more researched, and observations

showed it to be an element of slow excretion, long biological life (decades) in muscles, kidneys, liver, as well as in the whole human organism. It was also verified that as a result of the ingestion of Cd-polluted foods, the metal could cause renal damage and disturbances in the metabolism of calcium (3).

Lead is an element that has been used in various ways for over 4000 years. Today's industrial areas are the main cause of Pb contamination of foods due to its presence in soil.



The pollution of vegetables, for instance, is generated by absorption of the metal by the roots from the soil. The aquatic organisms accumulate lead in their system from the water and sediments they live in. Lead can also be incorporated into foods during processing steps, or in domestic preparation, especially when ceramic, lead-crystal, or metallic utensils are used (3). Blood lead concentrations above  $100 \text{ mg L}^{-1}$  appear to provide the first symptoms of chronic toxicity indicated by changes in the nervous system, loss of memory, difficulty in learning, saturnism and if not monitored, can result in the patient's death (3). In agreement with the Brazilian Legislation, the maximum allowable lead concentration for alcoholic beverages is  $0.05 \text{ mg L}^{-1}$  (4). The high toxicity of aluminum, lead, and cadmium requires that these metals be quantified in all foods and beverages. In Brazil, cachaça is the most popular drink and consumed in great amounts. Unfortunately, this highly sought after drink is polluted with these metals. Cachaça is produced from sugar cane and the plant can be contaminated from these poisonous elements if present in the soil as well as the water used in the production process. Another source of contamination are the utensils used during production, which are usually stainless steel or copper stills that are very often repaired with welding devices and materials containing lead and cadmium (5).

Electrothermal atomic absorption spectrometry (ETAAS) is probably the most popular technique used for the determination of low level concentrations of aluminum, cadmium, and lead, among others, in a variety of samples (6). For metals determination in cachaça, some authors have proposed the alcoholic extraction for use in calibration with aqueous solutions, although this is a slow process when a large number of samples

needs to be analyzed (7). Honorato et al. (8) compared the use of aqueous calibration with the standard additions method for copper determination in cachaça by flame atomic absorption spectrometry (FAAS). It was found that standard additions was the most appropriate methodology. Barbaste et al. (9) determined lead and cadmium concentrations in 152 wine samples from the Canary Islands, Spain, by inductively coupled plasma mass spectrometry (ICP-MS). The concentrations of cadmium found by these authors varied from  $0.20\text{--}1.73 \text{ mg L}^{-1}$ , while for lead the concentrations were found to be from  $3.89\text{--}159.5 \text{ mg L}^{-1}$ .

In this work, a methodology was developed for the determination of aluminum, cadmium, and lead in cachaça samples by ETAAS using matrix matched calibration. The metals were determined with and without permanent chemical modifiers and the results obtained with both techniques are compared (10–13). This is a novel methodology for cachaça, because flame atomic absorption spectrometry (FAAS) is the commonly used technique, which requires preconcentration of the sample with consequent loss of accuracy.

## EXPERIMENTAL

### Instrumentation

All measurements were carried out with a PerkinElmer® AAnalyst™ 300 atomic absorption spectrometer, equipped with graphite furnace, AS-72 autosampler, and deuterium arc lamp as background correction (PerkinElmer Life and Analytical Sciences, Shelton, CT, USA). Integrated absorbance (peak area) was used exclusively for signal evaluation. The hollow cathode lamp for Al (PerkinElmer Part No. 3050103) was operated at 15 mA and slit 0.7 nm. The electrodeless lamps for Cd and Pb (PerkinElmer Part No. 3050615 and 3050657,

respectively) were operated at 170 mA with a slit of 0.7 nm for Cd, and at 360 mA with a slit of 0.7 nm for Pb. A PerkinElmer EDL System 2 (Part No. 03030952) was used. The volume added into the graphite tube was  $20 \text{ }\mu\text{L}$  for the sample and the matrix-matched calibration solutions. When permanent modifiers were used, the tubes were treated as described previously (9–13). Argon, 99.996% (White Martins, Belo Horizonte, MG, Brazil), was used as the sheath gas. Pyrolytically coated graphite tubes without platform (Hitachi, Part No. 190–6003) were used for all studies. The graphite furnace temperature programs for the determination of Al, Cd, and Pb were optimized and are listed in Table I.

### Reagents and Solutions

All chemicals used were of analytical reagent grade, unless otherwise specified. Water was deionized in a Milli-Q™ system (Millipore, Bedford, MA, USA). The ethanol used to prepare the matrix-matched calibration curves was from Aldrich (Milwaukee, WI, USA, Part No. 20.699–7).

The following  $1000 \text{ }\mu\text{g mL}^{-1}$  stock solutions were used: aluminum standard solution (Fluka, Buchs, Switzerland, Part No 06155), Titrisol cadmium standard solution (Merck, Darmstadt, Germany); lead standard solution (Merck, Part No. 90361929), all in  $\sim 0.3 \text{ mol L}^{-1}$  nitric acid; rhodium from Fluka (Part No. 84033) and zirconium from Aldrich (Part No. 27,497–6).

All glassware was washed thoroughly with a detergent solution, rinsed with water, maintained in a bath with nitric acid 50% (v/v) for a period of at least one hour, and finally rinsed several times with deionized water prior to use. The autosampler cups were submitted to the same treatment.

## Procedure

The matrix-matched calibration curves were prepared for the three elements Al, Cd, and Pb (elements in aqueous solutions containing 40% (v/v) in ethanol, since the average alcohol content in cachaça is 40% (v/v)). The accuracy of the proposed methodology was verified by recovery of cachaça samples spiked with 30, 50, and 70  $\mu\text{g L}^{-1}$  for Al; 0.75, 1.25, and 1.75  $\mu\text{g L}^{-1}$  for Cd; and 15, 25, and 35  $\mu\text{g L}^{-1}$  for Pb. The recovery studies were performed within two days against matrix-matched calibration curves. The limit of detection (LOD,  $\mu\text{g L}^{-1}$ ) was calculated using the equation  $\text{LOD} = 3 \times S_{\text{BI}}/b$ , where SBI is the standard deviation of 10 measurements of the blank [aqueous solution 40% (v/v) in ethanol] and b is the slope of the matrix-matched calibration.

## RESULTS

### Pyrolysis and Atomization Temperature Curves

In order to investigate the behavior of pyrolysis and atomization of aluminum, cadmium, and lead in the cachaça samples, the respective temperature curves were obtained for each metal with and without the use of a modifier. The permanent modifier Zn+Rh and Ir+Rh were chosen based on the good results obtained previously with the use of such mixtures for these metals.

The best results for Al and Cd were obtained without the use of a chemical modifier. For Pb, the results without a modifier were similar to using Zr+Rh (500 and 250  $\mu\text{g}$ , respectively) or Ir + Rh (500 and 250  $\mu\text{g}$ ) as the permanent modifier, for this reason we have opted for not using a chemical modifier for the determination of the metals. For aluminum, the best pyrolysis and atomization temperatures were 1000 and 2500°C, respectively, with  $m_0$  9.0  $\mu\text{g}$  (rec-

**TABLE I**  
Temperature Program for the Determination of Al, Cd, and Pb in Cachaça Samples Without Modifier

Step	Temperature (°C)	Ramp (s)	Hold (s)	Ar Flow Rate (mL min <sup>-1</sup> )
1	90	5	10	250
2	140	5	10	250
3	1000 <sup>a,b</sup> , 900 <sup>c</sup>	5	10	250
4*	2500 <sup>a</sup> , 1400 <sup>b</sup> , 1900 <sup>c</sup>	0	5	0
5	20	1	5	250

\*Reading in this step.

<sup>a</sup> = Al; <sup>b</sup> = Cd; and <sup>c</sup> = Pb

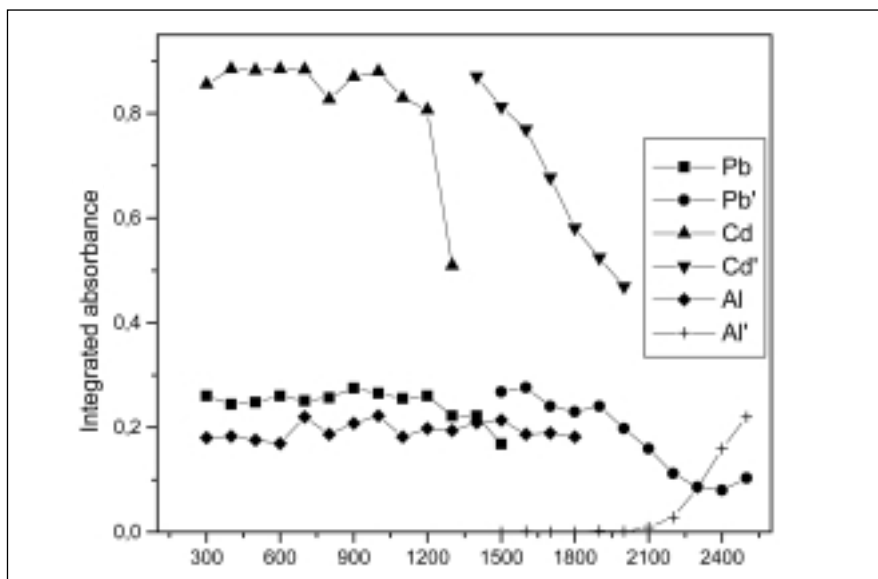


Fig. 1. Pyrolysis and atomization temperature curves for 0.4 ng of Al, 40 pg of Cd, and 0.4 ng of Pb in cachaça samples without the use of a modifier.

ommended 10  $\mu\text{g}$ ). For cadmium, without use of a modifier, the best pyrolysis and atomization temperatures were 1000 and 1400°C, respectively, with  $m_0$  0.5  $\mu\text{g}$  (equal to recommended). For lead, without use of a modifier, the best pyrolysis and atomization temperatures were 900 and 1900°C, respectively, with  $m_0$  11.0  $\mu\text{g}$  (recommended 10  $\mu\text{g}$ ).

It is interesting to note that for the three studied metals (especially cadmium), the curves of the pyrolysis temperature (Figure 1), without use of a modifier, form a plateau, which for cadmium and lead for

instance remains steady up to 1200°C, while for aluminum it remains steady up to 1800°C. This fact is amazing because usually without the use of a modifier, Cd begins to be lost during pyrolysis at 300°C, while for Pb this happens at around 500°C and 700°C for aluminum. It can therefore be assumed that the cachaça sample in some way acts as modifier because it allows the use of higher temperatures for the three studied analytes. This fact is being researched by our group.

**TABLE II**  
**Recoveries Obtained for Cachaça Samples Spiked With Al, Cd, and Pb**

Analyte	A ( $\mu\text{g L}^{-1}$ )	Add	Recovery (%)	B ( $\mu\text{g L}^{-1}$ )	Add	Recovery (%)
Al	4.9	30.0	102.6	8.4	30.0	90.0
		50.0	100.3		50.0	80.0
		70.0	87.5		70.0	102.9
Cd	nd	0.75	109.6	nd	0.75	112.4
		1.25	114.6		1.25	103.1
		1.75	103.7		1.75	108.7
Pb	8.6	15.0	118.8	49.6	15.0	86.4
		25.0	95.1		25.0	96.4
		35.0	105.7		35.0	95.8

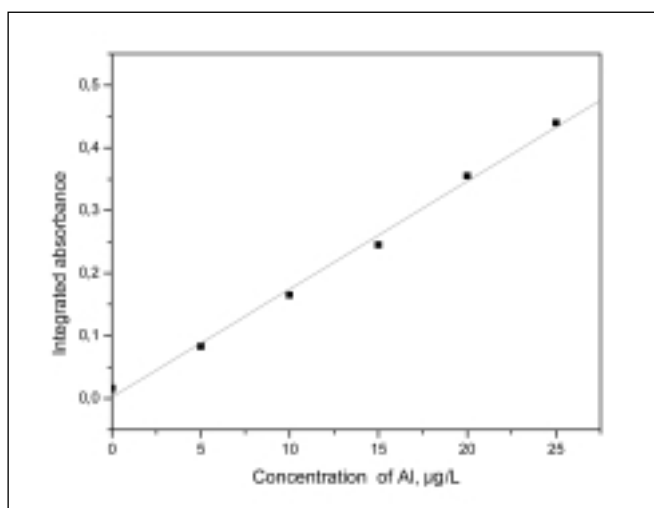


Fig. 2. Matrix-matched calibration curve for aluminum.

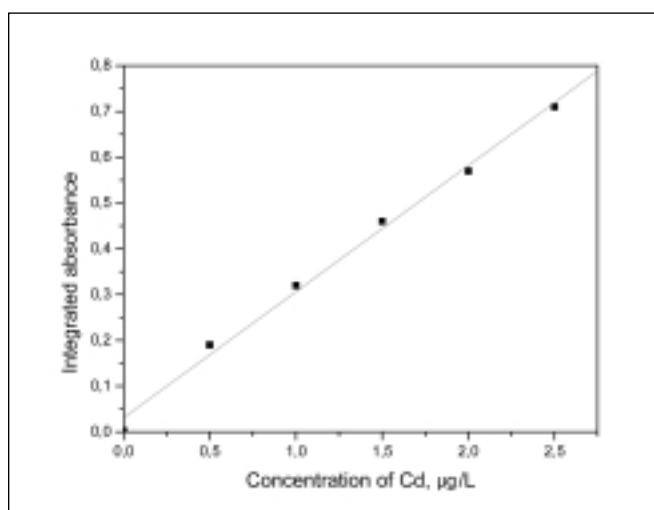


Fig. 3. Matrix-matched calibration curve for cadmium.

### Analytical Figures of Merit

Two cachaça samples spiked with different amounts of Al showed recoveries between 87.5 and 103.0% (Table II), with an RSD ( $n=3$ ) of less than 5%; the LOD ( $k=3, n=10$ ) was  $2.0 \mu\text{g L}^{-1}$ . For the 53 samples from 53 different producers, the Al results varied from non detectable to  $22.4 \mu\text{g L}^{-1}$ . The Brazilian Legislation does not regulate allowable Al value limits for alcoholic beverages.

Two samples spiked with cadmium presented recoveries from 103.1–114.6% (Table II), with an RSD of less than 4%; the LOD was  $0.07 \mu\text{g L}^{-1}$ . For the 53 samples, the Cd values varied from non-detectable to  $0.7 \mu\text{g L}^{-1}$ . The Brazilian Legislation does not regulate allowable Cd value limits in alcoholic beverages.

Two samples spiked with different amounts of lead showed recoveries from 95.1–118.8% (Table II), with an RSD ( $n=3$ ) of less than 6%; the LOD was  $0.6 \mu\text{g L}^{-1}$  Pb. For the 53 samples, the Pb results varied from non-detectable to  $526.0 \mu\text{g L}^{-1}$ .

In agreement with the Brazilian Legislation, the maximum allowable lead concentration for alcoholic beverages is  $0.05 \text{ mg L}^{-1}$  (4,13). It was observed that in some of the stills (lead-tin) used for cachaça production, the weldings were made with soft solder, which can be a probable source of Pb contamination of the cachaça samples analyzed.

For the studied analytes, Al, Cd, and Pb, calibration curves for matrix matching presented in the Figures 2, 3 and 4, respectively had  $r$  (lineal regression coefficient) higher than 0.99.

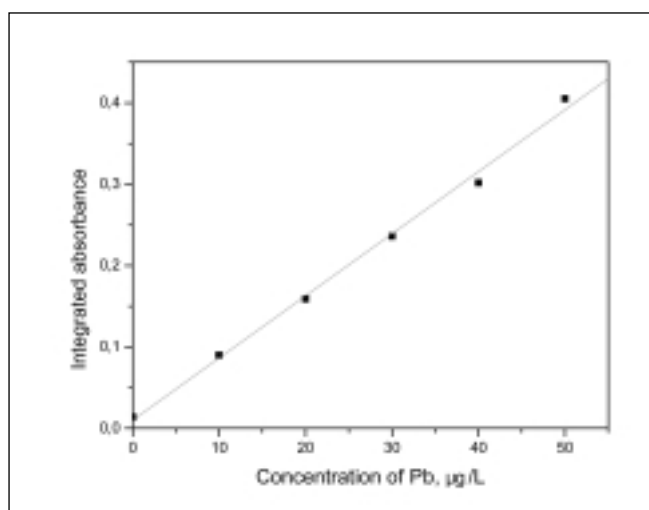


Fig. 4. Matrix-matched calibration curve for lead.

## CONCLUSION

It can be concluded that aluminum, cadmium, and lead in cachaça samples can be determined with good accuracy and precision by ETAAS without using a modifier and using matrix-matched calibration; it is possible that cachaça itself acts as a modifier. The recoveries for samples spiked with Al, Cd, and Pb showed values close to 100%, thus assuring good accuracy. It must be noted that 16 samples of cachaça (in 53 samples analyzed) showed lead concentration higher than  $50 \mu\text{g L}^{-1}$ , the maximum allowable lead concentration for alcoholic distilled beverages, in agreement with the Brazilian Legislation (4, 13) and this contamination found in some of the cachaça samples is of grave concern, particularly when used for human consumption.

## ACKNOWLEDGMENTS

The authors are grateful to Conselho Nacional de Desenvolvimento Científico e Tecnológico (CNPq), Fundação de Amparo a Pesquisa do Estado de Minas Gerais (FAPEMIG) and Coordenadoria de Aperfeiçoamento do Ensino Superior (CAPES) for financial support.

*Received October 9, 2003.*

## REFERENCES

1. A. Korolkovas, Química Farmacéutica, Guanabara Koogan S. A., Rio de Janeiro (1986).
2. J. Descotes, Immuno-toxicology of Drugs and Chemicals, Elsevier, Amsterdam (1988).
3. S. Oga. Fundamentos de Toxicologia. Atheneu Editora, São Paulo (1996).
4. Brasil, Ministério da Saúde. Secretaria de Vigilância Sanitária. Portaria No. 685 de 27 de agosto de 1998.
5. H. G. L. Siebald M. H. Canuto, G. M. de Lima, J. B. B. Silva. Informe Agropecuário 23, 217 (2002).
6. B. Welz, M. Sperling. Atomic Absorption Spectrometry, 3rd Edition, Wiley, Germany (1999).
7. M. Olalla, M. C. Gonzalez, C. Cabrera, R. Gimenez, and M. C. Lopez. J. of AOAC 85 (4), 960 (2002).
8. F. A. Honorato, R. S. Honorato, M. F. Pimentel, and M. C. Araújo, Analyst 127(11), 1520 (2002).
9. M. Barbaste, B. Medina, and J. P. Perez-Trujillo, Food Addit. Contam. 20 (2), 141 (2003).
10. C. G. Magalhães, K. L. A. Lelis, C. A. Rocha, and J. B. B. Silva, Anal. Chim. Acta 464, 323 (2002).
11. K. L. A. Lelis, C. G. Magalhães, C. A. Rocha, and J. B. B. Silva, Anal. and Bioanal. Chem. 347, 323 (2002).
12. M. B. O. Giacomelli, M. C. Lima, V. Stupp, J. B. B. Silva, and P. B. Barrera, Spectrochim. Acta Part B. 57, 2151 (2002).
13. M. H. Canuto, G. M. Lima, and H. G. Siebald. J. B. B. Silva, J. Anal. At. Spectrom. 18 (7), 787 (2003).
14. Brasil Ministério da Agricultura. Portaria nº. 371, 1974, Diário Oficial da República Federativa do Brasil, Brasília (17 de julho, 1974).

# Flow Injection On-line Sorption Preconcentration Coupled With Cold Vapor Atomic Fluorescence Spectrometry and On-line Oxidative Elution for the Determination of Trace Mercury in Water Samples

Li-Ping Yu and Xiu-Ping Yan\*

State Key Laboratory of Functional Polymer Materials for Adsorption and Separation, and Central Laboratory, Research Center for Analytical Sciences, College of Chemistry, Nankai University, Tianjin 300071, P.R. China

## INTRODUCTION

The toxicological and environmental effects of mercury compounds have become of increasing concern with regard to human health and the global ecosystem. The determination of mercury in our natural environment has been recognized as important for both regulatory and control purposes. For example, in the areas governed by the European Commission (EC), mercury has to be monitored in potable waters to ensure compliance with an EC Directive (1). Naturally, the concentration level of mercury in water samples is very low. Typical total dissolved mercury concentration in natural waters is in the range of 0.2–100 ng L<sup>-1</sup> and in some cases even lower (2), which means that direct and accurate determination of mercury in the aquatic environment is difficult. Thus, development of simple, sensitive, and reliable methods for the trace level determination of mercury in natural water samples is of particular significance.

A number of analytical techniques including cold vapor atomic absorption spectrometry (CV-AAS), cold vapor atomic fluorescence spectrometry (CV-AFS), optical emission spectrometry (OES), inductively coupled plasma mass spectrometry (ICP-MS), electroanalysis, and neutron activation

## ABSTRACT

A rapid, sensitive, and cost-effective method was developed for the determination of trace mercury in water samples by on-line coupling of flow injection (FI) sorption preconcentration with oxidative elution to cold vapor atomic fluorescence spectrometry (CV-AFS). Trace Hg(II) in aqueous solution was preconcentrated by on-line formation of mercury diethyldithiocarbamate complex (Hg-DDTC) and adsorption of the resulting neutral complex on the inner walls of a PTFE knotted reactor (KR). A mixture of 16% (v/v) HCl and 10% (v/v) H<sub>2</sub>O<sub>2</sub> was used as the eluent to remove the adsorbed Hg-DDTC from the KR, then convert on-line the Hg-DDTC into Hg(II) prior to its reduction to elemental mercury by KBH<sub>4</sub> for subsequent on-line CV-AFS detection. The tolerable concentrations of Cd(II), Zn(II), As(III), Se(IV), Fe(III), Co(II), Ni(II), and Cu(II) for the determination of 0.1 µg L<sup>-1</sup> Hg(II) were 0.1, 10, 0.1, 0.1, 0.7, 1, 0.3, and 0.2 mg L<sup>-1</sup>, respectively. With a sample loading flow rate of 3.1 mL min<sup>-1</sup> for a 60-s preconcentration, a detection limit (3σ) of 4.4 ng L<sup>-1</sup> was achieved at a sample throughput of 36 samples h<sup>-1</sup>. The precision (RSD, n = 11) was 1.7% at the 0.1-µg L<sup>-1</sup> Hg(II) level. The method was successfully applied to the determination of mercury in a certified reference material, GBW(E) 080392, and a number of local natural water samples.

analysis have been developed for mercury determination at the (ultra)trace levels. The cold vapor generation method followed by an element-selective detector has been the preferred technique (3). The cold vapor generation technique permits the efficient separation and preconcentration of analytes from sample matrices, thereby reducing or eliminating potential chemical and/or spectral interferences commonly encountered with direct solution analysis (3) and significantly increasing the signal of mercury (4).

Historically, the most extensively used technique for the measurement of mercury has been CV-AAS.

In recent years, cold vapor atomic fluorescence spectrometry (CV-AFS) has also been utilized for the detection of mercury (5–7). AFS is well suited for the determination of mercury as it absorbs and fluoresces at the same wavelength (6). Nevertheless, the low mercury concentration levels in natural waters are not compatible with the detection limit of the AFS technique even with mercury vapor generation.

When the concentration of analytes in the samples is too low to be determined directly, preconcentration and separation steps are always necessary. To improve the sensitivity and selectivity, off-line preconcentration and separation procedures, such as ion exchange, solvent extraction, and coprecipitation, are generally used before

\*Corresponding author.  
E-mail: xpyan@nankai.edu.cn,  
xpyan308@hotmail.com  
Fax: (86)22-23503034

determination. Such procedures, operated in the batch mode, are time-consuming and labor-intensive. They also require large sample volumes, and suffer great risk of contamination and analyte loss. However, with on-line operation using flow injection (FI) techniques, the drawbacks of a batch-wise operation can be overcome to a great extent, while preconcentration can be further enhanced (8). To date, various batch-type procedures have been adapted to FI on-line preconcentration for atomic spectrometry (8). However, the majority of on-line preconcentration systems are based on sorption principles. These systems include those using micro-columns packed with chelating ion-exchange resins, reversed phase silica gel sorbents with octadecyl functional groups ( $C_{18}$ ), and open tube knotted reactors (KRs) made from polytetrafluoroethylene (PTFE) tubing (8,9).

There are a number of publications dealing with FI on-line micro-column packed with silica gel, which are either immobilized with  $C_{18}$  (10–13), loaded with 2-mercaptobenzimidazol (8), fictionalized with methylthiosalicylate (TS-gel) (14), or packed with an anion-exchange resin (Dowex) immobilized with 1,5-Bis[2-pyridyl]-3-sulphophenyl methylene] thiocarbonylhydrazide (PSTH) (15) for preconcentration of mercury with on-line detection by CV-ICP-OES (14,15), CV-AAS (12,13), CV-ICP-MS (10), and CV-AFS (7,11). Recently, flow injection (FI) on-line preconcentration, based on the sorption of organometallic complexes on the inner walls of a PTFE knotted reactor (KR), has been successfully applied for trace element determination (9,16–19). Compared with conventional micro-column systems, the KR sorption system allows the analysis to be conducted at low cost, owing to the nearly unlimited lifetime and ease of con-

struction of the KR, which requires no packing materials and permits the use of higher sample loading rates for achieving higher sensitivity due to the low hydrodynamic impedance in the KR (9,16–19). The most widely used complexing agents for metal preconcentration in a KR have been diethyldithiocarbamate (DDTC) and ammonium pyrrolidine dithiocarbamate (APDC) (9). Recently, 2-(5-bromo-2-pyridylazo)-5diethylaminophenol (5-Br-PADAP) was employed as the complexing agent for the determination of mercury in drinking water with FI on-line KR sorption preconcentration coupled with CV-AAS (20). Although the detection limit was as low as  $5 \text{ ng L}^{-1}$ , a sample loading time of up to 5 minutes was required for the preconcentration of 25 mL aqueous solution, and the sample throughput was only  $11 \text{ h}^{-1}$  (20).

In the cold vapor generation system, organomercury compounds cannot be reduced to metallic mercury by  $\text{SnCl}_2$  or not completely by  $\text{NaBH}_4$  (21–29). It is generally agreed that all forms of mercury (organic and complexing forms) present in the sample have to be converted to Hg(II) prior to reduction to elemental mercury (24,25,28,29). A bewildering variety of combinations of strong acids ( $\text{HCl}$ ,  $\text{H}_2\text{SO}_4$ ,  $\text{HNO}_3$ ), oxidants ( $\text{H}_2\text{O}_2$ ,  $\text{KMnO}_4$ ,  $\text{K}_2\text{Cr}_2\text{O}_7$ ,  $\text{K}_2\text{S}_2\text{O}_8$ ,  $\text{KBr-KBrO}_3$ ), elevated temperatures, UV irradiation, and microwave exposure has been used and recommended for this purpose (21–29). However, such methods can be quite lengthy owing to the many steps required and subject to the inherent risk of contamination, volatilization, and adsorption losses (27). On-line oxidation offers a rapid and simple approach to decompose the organomercury/mercury complex prior to the reduction procedure, which is a distinct advantage over conventional pretreatment methods.

In light of the favorable characteristics of low cost, ease of operation, high selectivity, and sensitivity, coupling of FI on-line KR sorption preconcentration and separation to CV-AFS is expected to be an attractive technique for routine determination of trace mercury in natural water samples.

In this work, a rapid, sensitive, and cost-effective method was developed for trace mercury determination in natural water samples by coupling FI on-line KR sorption preconcentration, and on-line oxidative elution with CV-AFS detection. The Hg(II) in the water sample was retained on the inner walls of the KR in the form of the Hg-DDTC complex. The retained analyte was then eluted on-line with an  $\text{HCl-H}_2\text{O}_2$  solution for subsequent CV-AFS detection. Potential factors that affect sorption, rinsing, elution, and cold vapor generation were investigated in detail. Under optimum conditions, a detection limit ( $3\sigma$ ) of  $4.4 \text{ ng L}^{-1}$  was achieved at a sample throughput of 36 samples  $\text{h}^{-1}$  with the consumption of only 3.1 mL of aqueous solution.

## EXPERIMENTAL

### Instrumentation

The measurements were performed with a Model XGY-1011A non-dispersive atomic fluorescence spectrometer (Institute of Geophysical and Geochemical Exploration, Langfang, P.R. China). A mercury hollow cathode lamp (Ningqiang Light Sources Co. Ltd., Hengshui, P.R. China) was used as the radiation source. A laboratory-made gas-liquid separator (GLS) was used to isolate the generated mercury vapor from the reaction solution, and an argon flow was used to transport the mercury vapor into the atomizer (7-mm id  $\times$  14-cm quartz tube) of AFS (22). The argon flow was controlled by a rotameter. The optimized operating

parameters of the AFS instrument are given in Table I.

A Model FIA-3100 flow injection analyzer (Vital Instrumental Co. Ltd., Beijing, P.R. China) was used throughout this work. The FIA-3100 consists of two peristaltic pumps and a standard rotary injection valve (8-channel 16-port multifunctional injector). The knotted reactors (KRs) for preconcentration were laboratory-made from PTFE-tubing of (i.d./o.d.) = (0.50 mm/1.60 mm) by tying interlaced knots. Tygon® peristaltic pump tubing was employed to carry the sample, eluent, and reagents. PTFE tubing with 0.5 mm i.d. was used for all connections, which were kept as short as possible to minimize dead volumes.

### Reagents

All reagents were at least of analytical grade. Doubly deionized water (DDW) was used throughout. All glassware was soaked in a 10% (v/v) nitric acid solution for at least 24 hours and rinsed with DDW before use.

A stock standard solution of inorganic mercury (1000 mg L<sup>-1</sup> Hg) was prepared by dissolving 1.354 g of HgCl<sub>2</sub> (The Second Chemicals Co., Beijing, P.R. China) in 10 mL concentrated nitric acid and then diluted to 1000 mL with DDW. Working standard solutions were freshly prepared by stepwise dilution of the stock solution.

A 0.04% (m/v) KBH<sub>4</sub> solution was prepared daily by dissolving KBH<sub>4</sub> (Tianjin Institute of Chemicals Institute, Tianjin, P.R. China) in 0.5% (m/v) KOH (Taixing Chemicals Co., Tianjin, P.R. China) solution. The complexing agent solution was prepared by dissolving sodium diethyldithiocarbamate (DDTC) (Guangzhou Chemicals Co., Guangzhou, P.R. China) in acetic acid-ammonia buffer solution (pH 9.0).

The eluent solution was prepared daily by adding 10 mL 30% (m/m) hydrogen peroxide (Taixing Chemicals Co., Tianjin, P.R. China) to 100 mL 16% (v/v) hydrochloric acid solution (Taixing Chemicals Co., Tianjin, P.R. China).

### Sample Collection and Preparation

To prevent any exogenous contamination, low density polyethylene (LDPE) bottles used for sampling were soaked in a 10% (v/v) nitric acid solution, then rinsed with DDW and dried at room temperature before use. One lake water, one river water, one slush water, and three seawater samples were collected locally. Immediately after sampling, the samples were filtered through 0.45-mm pore size membrane filters and then acidified to the optimum acidity for preconcentration with nitric acid. A certified reference material, GBW(E) 080392 (simulated natural water)

was used for quality control in the determination of mercury in natural water samples.

### Procedures

The FI manifold for the on-line KR sorption preconcentration coupled with CV-AFS is shown in Figure 1.

The FI procedure ran through a cycle of three sequences.

In sequence 1, pump 2 was active while the injector valve turned to the fill position. In this sequence, the Hg (II)-DDTC complex was formed on-line and sorbed onto the inner walls of the KR, the effluent from the KR flowing to waste.

After preconcentration for 60 s, and with the valve maintained in the same position, sequence 2 is started, in which pump 2 was stopped and pump 1 was activated. The washing solution (DDW) was sucked through the KR to remove the residual components from the surface of the retained analyte.

In sequence 3, the valve was turned to the injection position while pump 1 was still running so that the HCl-H<sub>2</sub>O<sub>2</sub> solution was pumped to elute the sorbed analyte and also to provide the required acidic medium for subsequent cold vapor generation. Meanwhile, a flow of KBH<sub>4</sub> solution was introduced to merge with the HCl-H<sub>2</sub>O<sub>2</sub> solution containing the eluted analyte just before entering the gas-liquid separator to generate mercury vapor. The generated gaseous mixture was transported to the atomizer with an argon flow at 400 mL min<sup>-1</sup>. At the same time, the atomic fluorescence signal was detected by AFS. The total time required for a single determination lasted 100 s. The optimized flow rate and time for the three sequences are summarized in Table II.

**TABLE I**  
**Optimized Operating Parameters for XGY-1011A Atomic Fluorescence Spectrometer**

Parameters	Setting
Lamp	Hg Hollow Cathode Lamp
Lamp Current	50 mA
Quartz Furnace Temperature	Room Temperature
Quartz Furnace Height	7 mm
Negative High Voltage of Photomultiplier	270 V
Integration Time	15 s

## RESULTS AND DISCUSSION

### Selection of Eluent

Choice of a proper eluent is critical to the successful coupling of FI on-line KR sorption preconcentration to CV-AFS. In addition to the sufficiently strong elution capability required, the eluent employed in FI on-line KR sorption preconcentration and separation for CV-AFS should facilitate the ensuing cold vapor generation reaction. A diluted HCl solution is generally considered a favorable medium for

hydride generation/cold vapor generation, so it was tested for its suitability as the eluent in the present FI on-line KR sorption preconcentration CV-AFS system.

The effect of HCl concentration on the signal intensity of mercury was examined as the first step in search for an appropriate eluent. As shown in Figure 2, the signal intensity of  $2.0 \mu\text{g L}^{-1}$  Hg(II) increased as the concentration of HCl increased up to 15% (v/v) and then leveled off until 24% (v/v). However, the fluorescence intensity in the range

of the HCl concentration studied was quite weak, suggesting that the efficiency of cold vapor generation was rather low.

To improve the efficiency of cold vapor generation, the eluted Hg-DDTC should be converted to Hg(II) prior to cold vapor generation. For this purpose,  $\text{H}_2\text{O}_2$ , an effective oxidant under relatively mild conditions of pH and temperature, was included in the eluent for on-line elution, which provides a safe and reliable oxidative digestion

**TABLE II**  
**Operational Sequences for the FI On-line Sorption Preconcentration System for AFS Determination of Mercury**

Sequence	Function	Time (s)	Pumped Medium	Flow Rate ( $\text{mL min}^{-1}$ )		Valve Position
				Pump 1	Pump 2	
1 (Figure 1a)	Sample Loading	60	Sample	Off	3.1	Fill
			DDTC (0.02% m/v)		3.4	
2 (Figure 1a)	KR Rinsing	20	DDW	3.0	Off	Fill
3 (Figure 1b)	Analyte Elution	20	16% (v/v) HCl-10% (v/v) $\text{H}_2\text{O}_2$	4.2	Off	Inject
			0.04% m/v $\text{KBH}_4$	4.2		

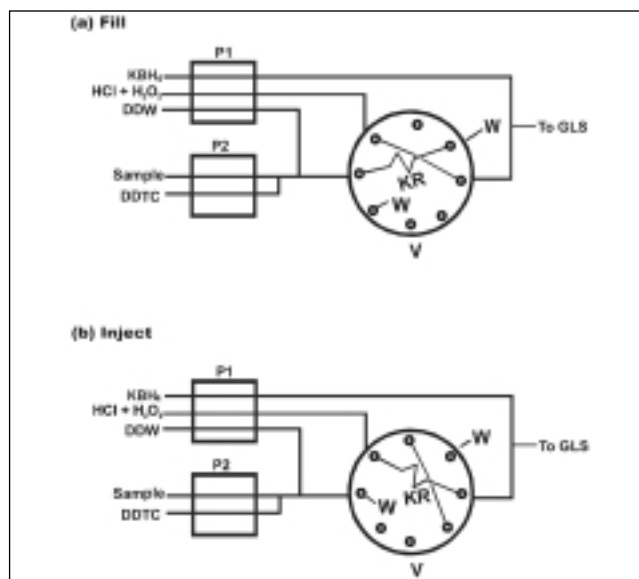


*Fig. 1. FI manifold and operational sequences for the on-line KR preconcentration coupled with CV-AFS: P1, P2, peristaltic pump; W, waste; KR, knotted reactor (150-cm long  $\mu$  0.5-mm i.d. PTFE tubing); V, injector valve (the inner is the rotor); GLS, gas-liquid separator; injector valve position (a) fill, (b) inject.*

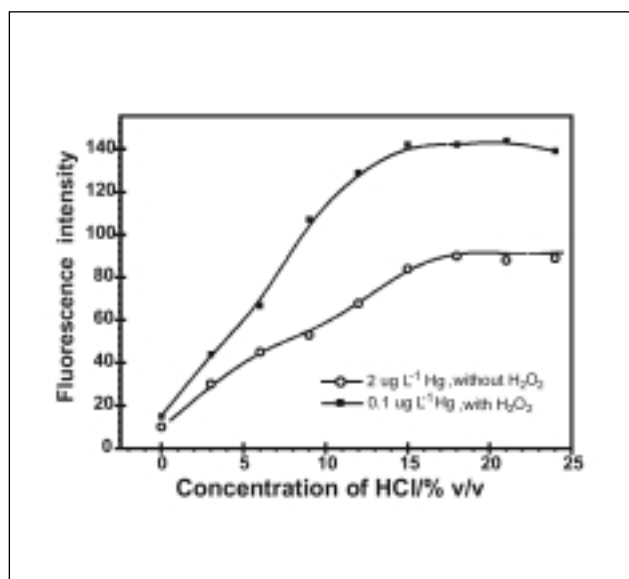


*Fig. 2. Effect of HCl concentration in the eluent on the determination of  $0.1 \mu\text{g L}^{-1}$  Hg(II) with inclusion of 10% (v/v)  $\text{H}_2\text{O}_2$  in the eluent, and  $2.0 \mu\text{g L}^{-1}$  Hg(II) without  $\text{H}_2\text{O}_2$  in the eluent. All other conditions as in Figure 1 and Tables I, II, and IV.*



without risk of contamination and analyte loss. From Figure 2, it can be concluded that  $H_2O_2$  played an important role in improving the efficiency of cold vapor generation. The addition of 10% (v/v)  $H_2O_2$  in the eluent resulted in about 30-fold increase in the sensitivity for mercury determination.

The effect of  $H_2O_2$  concentration in the eluent was also investigated to determine the optimal  $H_2O_2$  concentration for efficient elution and cold vapor generation. As shown in Figure 3, the fluorescence intensity significantly increased with increasing the  $H_2O_2$  concentration up to 4% (v/v), then leveled off in the  $H_2O_2$  concentration range of 4–16% (v/v). Accordingly, a solution of 16% (v/v) HCl and 10% (v/v)  $H_2O_2$  was chosen as the eluent for further experiments. The effect of the eluent solution flow rate was studied, and the best CV-AFS signal intensity was achieved at  $4.2 \text{ mL min}^{-1}$ .

### Sample Acidity

The effect of sample acidity on the preconcentration of  $0.1 \mu\text{g L}^{-1}$  Hg(II) was tested at a fixed DDTC concentration of 0.05% (m/v). As shown in Figure 4, the optimum sample acidity ranged from 3% to 10% (v/v)  $HNO_3$ . It was wide enough for easy control. The lower sensitivity at lower acidity [ $<3\%$  (v/v)  $HNO_3$ ] probably resulted from an unfavorable complex formation between Hg(II) and DDTC and/or an unfavorable adsorption of the resulting Hg-DDTC complex on the inner surface of the KR. For further experiments, an acidity of 4% (v/v)  $HNO_3$  was used.

### Concentration of DDTC

The influence of DDTC concentration on the preconcentration of  $0.1 \mu\text{g L}^{-1}$  Hg(II) was tested when sample and reagent flow rates were kept at  $3.1$  and  $3.4 \text{ mL min}^{-1}$ , respectively. The result is shown in Figure 5. In the absence of DDTC, little Hg(II) was sorbed on the walls of the KR. The signal intensity significantly increased with an increase in the concentration of

DDTC up to 0.01% (m/v). These results indicate that it was the Hg(II)-DDTC rather than the Hg(II) that was sorbed on the inner walls of the KR. However, the fluorescence intensity changed slightly in the range of 0.01–0.04% (m/v) DDTC and reduced remarkably with a further increase in DDTC concentration, probably due to the competition of excessive complexing reagent for the active sites on the inner walls of the KR. Accordingly, a DDTC concentration of 0.02% (m/v) was employed for further work.

### $KBH_4$ Concentration

The effect of  $KBH_4$  concentration on the signal intensity is shown in Figure 6. As the  $KBH_4$  concentration increased, the fluorescence intensity of mercury increased rapidly and reached a plateau from 0.01 to 0.10% (m/v)  $KBH_4$ . Low  $KBH_4$  concentrations [ $<0.01\%$  (m/v)] probably gave an incomplete reduction of the analyte, leading to low signal intensity. Higher concentrations of  $KBH_4$  [ $>0.10\%$  (m/v)] would cause

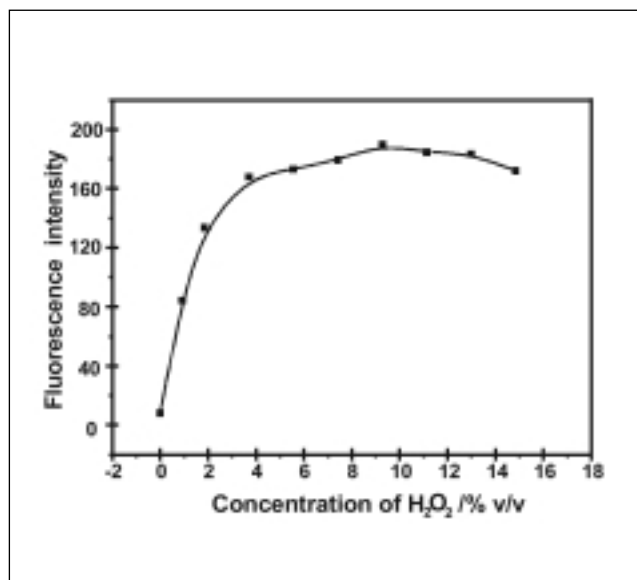


Fig. 3. Effect of  $H_2O_2$  concentration included in the eluent [16% (v/v) HCl] on the determination of  $0.1 \mu\text{g L}^{-1}$  Hg(II). All other conditions as in Figure 1 and Tables I, II, and IV.

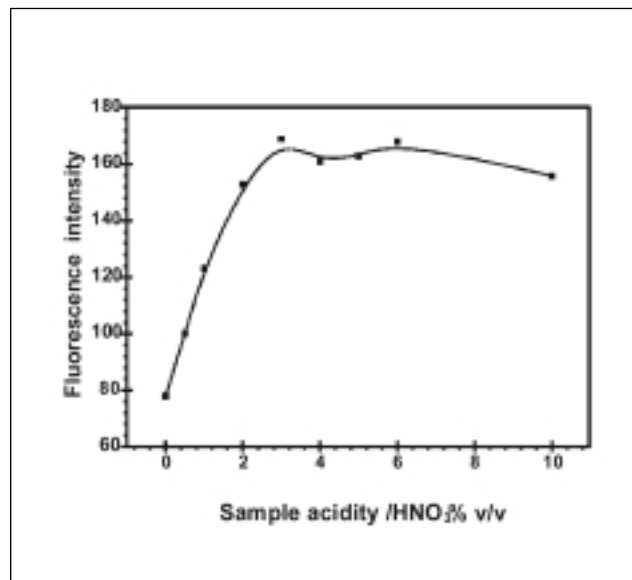


Fig. 4. Effect of sample acidity [ $HNO_3\%$  (v/v)] on the preconcentration of  $0.1 \mu\text{g L}^{-1}$  Hg(II). All other conditions as in Figure 1 and Tables I, II, and IV.

serious effervescence. As a result, water vapor and/or mist of reagents might condense on the transfer line and consequently trap the volatile mercury, resulting in a significant decrease of the signal intensity. In order to avoid any possible interference, a  $\text{KBH}_4$  concentration of 0.04% (m/v) was selected.

### Sample Loading Flow Rate and Preconcentration Time

The influence of sample loading flow rate on the preconcentration of  $0.1 \mu\text{g L}^{-1}$  Hg(II) was evaluated at a fixed sample loading time of 60 s. It was found that the signal intensity of  $0.1 \mu\text{g L}^{-1}$  Hg(II) increased linearly with the sample loading flow rate up to at least  $6.0 \text{ mL min}^{-1}$ . Studies on the effects of sample preconcentration time showed a linear relationship until the sample loading time increased up to at least 300 s. To achieve a reasonable sample frequency, a preconcentration time of 60 s was selected. Thereby, a complete cycle of the entire FI procedure lasted for 100 s, resulting in a sample throughput of 36 samples  $\text{h}^{-1}$ .

### KR Rinsing

After sample loading into the KR, the residual solution in the KR may contain dissolved salts, which could cause interferences with the determination of Hg(II). Thus, a rinsing step was used to remove the residual matrix in the KR before elution. In this work, air, DDW, and diluted  $\text{HNO}_3$  solution were tested as the rinsing solution. Air was found not able to remove the residual matrix completely. When diluted  $\text{HNO}_3$  solution was used as the rinsing solution, the signal decreased with an increase in the concentration of  $\text{HNO}_3$ . However, DDW was found to remove the residual matrix effectively while not stripping off the sorbed analyte. Accordingly, DDW was chosen as the rinsing solution.

### KR Tubing Length

The influence of KR tubing length on the preconcentration of  $0.1 \mu\text{g L}^{-1}$  Hg(II) was investigated for a sample loading time of 60 s. It was observed that the signal intensity increased with an increase in

the KR tubing length from 50 to 400 cm and then decreased from 400 to 500 cm. The result provided the ability to achieve high sensitivity by properly increasing the KR tubing length. However, longer KR needed longer rinsing and elution time. It was found that a KR length of 150 cm was long enough to obtain a high preconcentration efficiency and to reach a short time cycle.

### Interferences

Commonly encountered matrix components in natural water, i.e., alkali and alkaline earth elements, cause no interferences due to the group-specific character of DDTC and the efficient rinsing step. In addition, six typical transition metal ions, Cd(II), Fe(III), Co(II), Ni(II), Cu(II), and Zn(II), and two hydride-forming elements, As(III) and Se(IV), were chosen to examine the interferences in the determination of  $0.1 \mu\text{g L}^{-1}$  Hg(II) under the conditions given in Tables I, II, and IV. The results are shown in Table III. The tolerable concentrations of

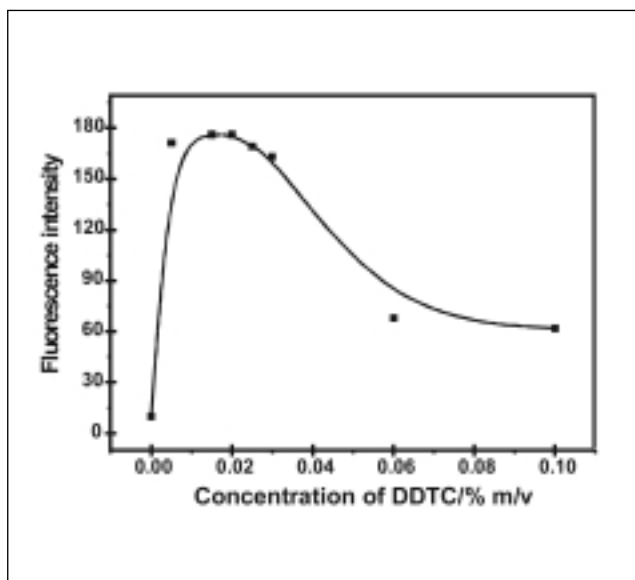


Fig. 5. Effect of DDTC concentration on the preconcentration of  $0.1 \mu\text{g L}^{-1}$  Hg(II). All other conditions as in Figure 1 and Tables I, II, and IV.

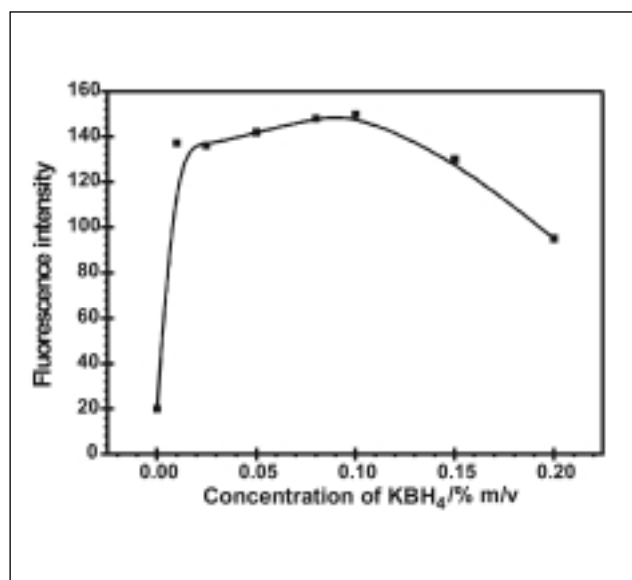


Fig. 6. Effect of  $\text{KBH}_4$  concentration on the determination of  $0.1 \mu\text{g L}^{-1}$  Hg(II). All other conditions as in Figure 1 and Tables I, II, and IV.

**TABLE III**  
**Effect of Potential Interfering Species on the Determination of 0.1  $\mu\text{g L}^{-1}$  Hg(II) Under the Conditions Given in Tables I, II and IV**

Foreign Ion	Conc. ( $\text{mg L}^{-1}$ )	Recovery (mean $\pm \sigma$ , n =5) (%)
Cd(II)	0.05	96 $\pm$ 2
	0.1	85 $\pm$ 1
	0.5	69 $\pm$ 2
Fe(III)	0.2	98 $\pm$ 1
	0.7	83 $\pm$ 2
Co(II)	0.2	100 $\pm$ 1
	1	86 $\pm$ 1
	3	70 $\pm$ 2
Ni(II)	0.1	99 $\pm$ 1
	0.3	87 $\pm$ 2
	0.4	79 $\pm$ 2
Cu(II)	0.05	96 $\pm$ 2
	0.2	85 $\pm$ 1
	0.5	69 $\pm$ 2
Zn(II)	2	98 $\pm$ 1
	10	97 $\pm$ 1
	20	78 $\pm$ 2
As(III)	0.05	97 $\pm$ 1
	0.1	87 $\pm$ 2
	0.2	77 $\pm$ 2
Se(IV)	0.05	95 $\pm$ 1
	0.1	83 $\pm$ 2
	0.2	70 $\pm$ 2

Cd(II), Zn(II), As(III), Se(IV), Fe(III), Co(II), Ni(II), and Cu(II) for the determination of 0.1  $\mu\text{g L}^{-1}$  Hg(II) were found to be 0.1, 10, 0.1, 0.1, 0.7, 1, 0.3, and 0.2  $\text{mg L}^{-1}$ , respectively, much higher than their concentrations usually found in natural water samples. In addition, no significant interferences from the organomercury species up to 0.5  $\text{mg L}^{-1}$  were observed in the preconcentration of Hg(II) under the conditions given in Tables I, II, and IV.

**TABLE IV**  
**Characteristic Performance Data of the FI On-line Preconcentration for CV-AFS Determination of Mercury**

Preconcentration Time	60 s
Sample Throughput	36 samples $\text{h}^{-1}$
Sample Consumption	3.1 mL
Reagent Consumption	
0.02% (m/v) DDTC	3.4 mL
0.04% (m/v) $\text{KBH}_4$	1.4 mL
16% (v/v) HCl-10% (v/v) $\text{H}_2\text{O}_2$	1.4 mL
Working Range	10–2000 $\text{ng L}^{-1}$
Detection Limit ( $3\sigma$ )	4.4 $\text{ng L}^{-1}$
Precision (RSD, n=11)	1.7% (0.1 $\mu\text{g L}^{-1}$ )
Calibration Function (7 standards, n=11, C in $\mu\text{g L}^{-1}$ )	$A = 1347.52C + 7.64$
Correlation Coefficient	0.9991

#### Analytical Performance of the FI On-line Preconcentration CV-AFS System

The analytical characteristic data of the proposed FI on-line KR sorption preconcentration system for CV-AFS determination of mercury are summarized in Table IV. Under the optimum conditions, a detection limit ( $3\sigma$ ) of 4.4  $\text{ng L}^{-1}$  was achieved at a sample throughput of 36 samples  $\text{h}^{-1}$  with the consumption of only 3.1 mL of aqueous solution. The precision (%RSD) for 11 replicate determinations of 0.1  $\mu\text{g L}^{-1}$  Hg(II) was 1.7%.

Table V compares the analytical performance data of the present method with those of several typical FI on-line sorption preconcentration systems for atomic (mass) spectrometric determination of mercury. Generally speaking, the present method offers low detection limits, good precision, high sample throughput, and low sample consumption. For example, the present system using DDTC as the complexing agent and on-line

oxidative elution [in comparison to a previous FI on-line KR sorption preconcentration CV-AAS system using 5-Br-PADAP as the complexing agent for mercury determination (24)] permits a much higher sample throughput (36  $\text{h}^{-1}$  vs 11  $\text{h}^{-1}$ ), requires a smaller sample solution (3.1 mL vs 25 mL), and offers better precision (1.7% at the 0.1- $\mu\text{g L}^{-1}$  level vs 2.8% at the 1- $\mu\text{g L}^{-1}$  level) with comparable detection limits (4.4  $\text{ng L}^{-1}$  vs 5  $\text{ng L}^{-1}$ ).

The accuracy of the present method was checked by analyzing a certified reference material, GBW(E) 080392 (simulated natural water). As shown in Table VI, the concentration of mercury determined by the present method using simple aqueous standards for calibration was in good agreement with the certified values.

The present FI method was also applied to the determination of trace mercury in several local natural water samples. The analytical results obtained by the present

**TABLE V**  
**Comparison of Analytical Characteristic Data Obtained by Selected FI On-line Sorption Preconcentration Systems for Cold Vapor Atomic (mass) Spectrometric Determination of Mercury**

Technique Employed	Sorbent	Complexing Agent	Reductant	Eluent	Sample Volume Needed	D.L.	Sample Throughput (samples h <sup>-1</sup> )	Precision (%RSD)	Ref.
CV-AFS	KR	DDTC	KBH <sub>4</sub>	16% (v/v) HCl +10% (v/v) H <sub>2</sub> O <sub>2</sub>	3.1 mL	4.4 ng L <sup>-1</sup>	36	1.7% (0.1 µg L <sup>-1</sup> )	This work
CV-ICP-AES	Micro-column packed with TS-gel	no	NaBH <sub>4</sub>	5% thiourea +1% HNO <sub>3</sub>	8 mL	5 µg L <sup>-1</sup>	40	2.1% (10 µg L <sup>-1</sup> )	(18)
CV-ICP-MS	Micro-column packed with C <sub>18</sub>	DDTP <sup>a</sup>	NaBH <sub>4</sub>	Methanol	2.3 mL	5 µg L <sup>-1</sup>	21	3% (0.2 µg L <sup>-1</sup> )	(14)
CV-ICP-AES	Micro-column packed with PSTH immobilized resin (Dowex)	no	SnCl <sub>2</sub>	2 mol L <sup>-1</sup> HNO <sub>3</sub>	9 mL	4 µg L <sup>-1</sup>	40	3.6% (10 µg L <sup>-1</sup> )	(19)
CV-AFS	Micro-column packed with C <sub>18</sub>	APDC	SnCl <sub>2</sub>	Ethanol	45 mL	14.9 ng L <sup>-1</sup>	4	5.9% (? µg L <sup>-1</sup> )	(15)
CV-AAS	Micro-column packed with C <sub>18</sub>	DDTC	NaBH <sub>4</sub>	Ethanol	25 mL	16 ng L <sup>-1</sup>	–	3.4% (0.5 µg L <sup>-1</sup> )	(16)
CV-AAS	Micro-column packed with C <sub>18</sub>	DDTP	NaBH <sub>4</sub>	Ethanol	24 mL	10 ng L <sup>-1</sup>	12	–	(17)
CV-AFS	Micro-column packed with 2-mercapto benzimidazol loaded silica gel	no	SnCl <sub>2</sub>	0.05 mol L <sup>-1</sup> KCN	1000 mL	0.07 ng L <sup>-1</sup>	–	8.8% (? µg L <sup>-1</sup> )	(8)
CV-AAS	KR	5-Br-PADAP	NaBH <sub>4</sub>	3 mol L <sup>-1</sup> HCl	25 mL	5 ng L <sup>-1</sup>	11	2.8% (1 µg L <sup>-1</sup> )	(24)

<sup>a</sup> DDTP = O,O-diethyldithiophosphoric acid

**TABLE VI**  
**Analytical Results for Determination of Mercury in Water Samples and a Certified Reference Material Sample**

Sample	Hg Conc. in Original Sample (µg L <sup>-1</sup> )		Hg Added (µg L <sup>-1</sup> )	Recovery (%) (mean ± σ, n=5)
	Certified	Determined (mean ± σ, n=5)		
GBW(E) 080392				
Simulated Natural Water	10.0 ± 0.5	10.1 ± 0.07	–	–
Slush Water	–	0.055 ± 0.005	0.100	99 ± 3
Lake Water	–	0.077 ± 0.003	0.100	105 ± 5
River Water	–	0.106 ± 0.002	0.100	93 ± 5
Seawater 1	–	0.171 ± 0.002	0.200	102 ± 5
Seawater 2	–	0.128 ± 0.002	0.200	99 ± 4
Seawater 3	–	0.073 ± 0.004	0.200	94 ± 2

method using a simple aqueous standard calibration technique were given in Table VI. The recoveries of mercury spike from these natural water samples varied from 93 to 105%, indicating that the presence of concomitants did not interfere in the determination of mercury and the proposed method is suitable for natural water analysis.

## CONCLUSION

The results of this work have demonstrated that the developed FI on-line KR sorption preconcentration CV-AFS technique with on-line decomposition of Hg-complex is rapid, sensitive, and cost-effective for routine determination of mercury in natural water samples. Although the CV-AFS system is not appropriate for the direct determination of mercury complex subsequent to KR preconcentration procedure, the same technique became a useful tool in providing meaningful results when an on-line oxidative elution process was employed with a mixture of 16% (v/v) HCl and 10% (v/v) H<sub>2</sub>O<sub>2</sub> as the eluent. Under the optimum conditions, a detection limit (3σ) of 4.4 ng L<sup>-1</sup> was achieved at a sample throughput of 36 samples h<sup>-1</sup> with the consumption of 3.1 mL sample solution. The method was successfully applied to the determination of mercury in a certified reference material and a number of local natural water samples.

## ACKNOWLEDGMENTS

This work was supported by the National Natural Science Foundation of P.R.China (No. 20275019, 20025516).

*Received September 2, 2003.*

## REFERENCES

1. J. Allibone, E. Fatemian, and P.J. Walker, *J. Anal. At. Spectrom.* 14, 235 (1999).
2. D. Cossa, J. Sanjuan, J. Cloud, P.B. Stockwell, and W.T. Corns, *J. Anal. At. Spectrom.* 10, 287 (1995).
3. Y. Cai, *Trends Anal. Chem.* 19, 62 (2000).
4. C.-C. Wan, C.-S. Chen, and S.-J. Jiang, *J. Anal. At. Spectrom.* 12, 683 (1997).
5. M.J. Bloxham, S.J. Hill, and P.J. Worsfold, *J. Anal. At. Spectrom.* 11, 511 (1996).
6. L. Rahman, W.T. Corns, D.W. Bryce, and P. B. Stockwell, *Talanta* 52, 833 (2000).
7. H. Bagheri and A. Gholami, *Talanta* 55, 1141 (2001).
8. Z.-L. Fang, *Flow Injection Atomic Absorption Spectrometry*, Wiley, Chichester, U. K., 1995.
9. X.-P. Yan and Y. Jiang, *Trends Anal. Chem.* 20, 552 (2001).
10. E.L. Seibert, V.L. Dressler, D. Pozebon, and A.J. Curtius, *Spectrochim. Acta, Part B*, 56, 1963 (2001).
11. L. Gámiz-Gracia and M.D. Luque de Castro, *J. Anal. At. Spectrom.* 14, 1615 (1999).
12. M.F. García, R.P. García, N.B. García, and A. Sanz-Medel, *Talanta* 41, 1833 (1994).
13. A. da C.P. Monteiro, L.S.N. de Andrade, and R.C. de Campos, *Fresenius' J. Anal. Chem.* 371, 353 (2001).
14. P. Cañada Rudner, J.M. Cano Pavón, F. Sánchez Rojas, and A. García de Torres, *J. Anal. At. Spectrom.* 13, 1167 (1998).
15. P. Cañada Rudner, A. García de Torres, J.M. Cano Pavón, and F. Sánchez Rojas, *Talanta* 46, 1095 (1998).
16. Z.-L. Fang, S.-K. Xu, L.-P. Dong, and W.-Q. Li, *Talanta* 41, 2165 (1994).
17. X.-P. Yan, W. Van Mol, and F. Adams, *Analyst* 121, 1061 (1996).
18. X.-P. Yan, X.-B. Yin, X.-W. He, and Y. Jiang, *Anal. Chem.* 74, 2162 (2002).
19. X.-P. Yan, M.J. Hendry, and R. Kerich, *Anal. Chem.* 72, 1879 (2000).
20. J.C.A. Wuilloud, R.G. Wuilloud, J.A. Gásquez, R.A. Olsina, and L.D. Martínez, *At. Spectrosc.* 22, 398 (2001).
21. G. Tao, S.N. Willie, and R.E. Sturgeon, *Analyst* 123, 1215 (1998).
22. W.R. Hatch and W.L. Ott, *Anal. Chem.* 40, 2085 (1968).
23. R. Ahmed, K. May, and M. Stoeppler, *Fresenius' J. Anal. Chem.* 326, 510 (1987).
24. L. Ping and P.K. Dasgupta, *Anal. Chem.* 61, 1230 (1989).
25. D.C. Baxter, W. Frech, *Anal. Chim. Acta* 236, 377 (1990).
26. C.P. Hanna, J.F. Tyson, and S. McIntosh, *Anal. Chem.* 65, 653 (1993).
27. J. Murphy, P. Jones, and S. J. Hill, *Spectrochim. Acta, Part B*, 51, 1867 (1996).
28. T. Guo, J. Baasner, M. Gradl, and A. Kistner, *Anal. Chim. Acta* 320, 171 (1996).
29. B. Welz, D.L. Tsalev, and M. Sperling, *Anal. Chim. Acta* 261, 91 (1992).
30. X.-B. Yin, X.-P. Yan, Y. Jiang, and X.-W. He, *Anal. Chem.* 74, 3720 (2002).

# Books on the AAS, ICP-OES, ICP-MS techniques:



## 1. Concepts, Instrumentation and Techniques in Atomic Absorption Spectrophotometry

Authors: Richard D. Beatty and Jack D. Kerber

Order No. AA-914C (free of charge)

Ordering information: <http://www.las.perkinelmer.com> or contact your local PerkinElmer representative.

This book contains theoretical concepts and definitions of the science of atomic spectroscopy: atomic emission, atomic absorption, and atomic fluorescence. It also discusses high sensitivity sampling systems and the advantages and limitations of the cold vapor mercury, hydride generation, and graphite furnace atomic absorption techniques.

Also discussed are spectral and non-spectral interferences, including the goals and use of the stabilized temperature platform furnace (STPF) system.

## 2. Analytical Graphite Furnace AAS – A Laboratory Guide

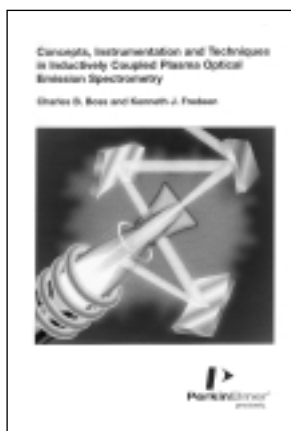
Authors: G. Schlemmer and B. Radziuk

Order No. B051-1731

Ordering and price information: <http://www.las.perkinelmer.com> or contact your local PerkinElmer representative.

This book provides insight into the theoretical and practical aspect of graphite furnace AA making it the perfect reference resource for all laboratories wanting to use their graphite furnace more effectively.

Using an easy-to-follow style, the reader is guided from method development to calibration and validation of the instrument to the use of accessories and software in modern graphite furnace AA.



## 3. Concepts, Instrumentation and Techniques in Inductively Coupled Plasma Optical Emission Spectrometry

Authors: Charles B. Boss and Kenneth J. Fredeen

Order No. 005446B (free of charge)

Ordering information: <http://www.las.perkinelmer.com> or contact your local PerkinElmer representative.

This book presents the general characteristics of ICP-OES and ICP-OES instrumentation. It discusses ICP-OES methodologies including their application for the analysis of samples in the various industries such as agriculture and foods, biological and clinical, geological, environmental and water, metals, and organics.

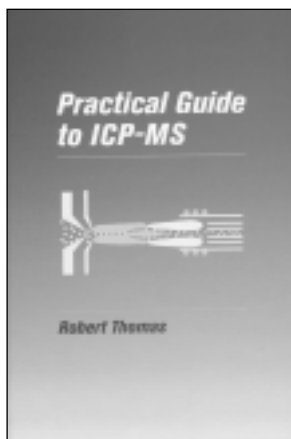
## 4. Practical Guide to ICP-MS

Author: Robert Thomas, Scientific Solutions ([www.scientificsolutions1.com](http://www.scientificsolutions1.com))

Published in 2004 by Marcel Dekker

Ordering and price information:

[www.dekker.com/servlet/product/productid/5319-4](http://www.dekker.com/servlet/product/productid/5319-4)



The brand new reference book presents this powerful trace-element technique as a practical solution to real-world problems. The basic principles of ion formation/transportation/detection, common interferences, peak quantitation, sample preparation, contamination issues, routine maintenance and application strengths of ICP-MS are described in a way that is easy to understand for both experienced users and novices of the technique. In addition ICP-MS is compared with AA and ICP-OES in the areas of detection capability, dynamic range, sample throughput, ease of use and cost of ownership. The book concludes with an excellent chapter on the most important testing criteria when evaluating commercial instrumentation.

## Editor

Anneliese Lust  
E-mail:  
anneliese.lust@perkinelmer.com

## Technical Editors

Glen R. Carnrick, AA  
Dennis Yates, ICP  
Kenneth R. Neubauer, ICP-MS

## SUBSCRIPTION INFORMATION

*Atomic Spectroscopy*  
P.O. Box 3674  
Barrington, IL 60011 USA  
Fax: +1 (847) 304-6865

### 2004 Subscription Rates

- U.S. \$60.00 includes third-class mail delivery worldwide; \$20.00 extra for electronic file.
- U.S. \$80.00 includes airmail delivery; \$20 extra for electronic file.
- U.S. \$60.00 for electronic file only.
- Payment by check (drawn on U.S. bank in U.S. funds) made out to: "*Atomic Spectroscopy*"

### Electronic File

- For electronic file, send request via e-mail to:  
atsponline@yahoo.com

### Back Issues/Claims

- Single back issues are available at \$15.00 each.
- Subscriber claims for missing back issues will be honored at no charge within 90 days of issue mailing date.

### Address Changes to:

Atomic Spectroscopy  
P.O. Box 3674  
Barrington, IL 60011 USA

### Copyright © 2004

PerkinElmer, Inc.  
All rights reserved.  
www.perkinelmer.com

### Microfilm

*Atomic Spectroscopy* issues are available from:  
University Microfilms International  
300 N. Zeeb Road  
Ann Arbor, MI 48106 USA  
Tel: (800) 521-0600 (within the U.S.)  
+1 (313) 761-4700 (internationally)

## Guidelines for Authors

*Atomic Spectroscopy* serves as a medium for the dissemination of general information together with new applications and analytical data in atomic absorption spectrometry.

The pages of *Atomic Spectroscopy* are open to all workers in the field of atomic spectroscopy. There is no charge for publication of a manuscript.

The journal has around 1500 subscribers on a worldwide basis, and its success can be attributed to the excellent contributions of its authors as well as the technical guidance of its reviewers and the Technical Editors.

The original of the manuscript should be submitted to the editor by mail plus electronic file on disk or e-mail in the following manner:

1. Mail original of text, double-spaced, plus graphics in black/white.
2. Provide text and tables in .doc file and figures in doc or tif files.
3. Number the references in the order they are cited in the text.
4. Submit original drawings or glossy photographs and figure captions.
5. Consult a current copy of *Atomic Spectroscopy* for format.

6. Or simply e-mail text and tables in doc file and graphics in doc or tif files to the editor:  
[anneliese.lust@perkinelmer.com](mailto:anneliese.lust@perkinelmer.com)  
or [annelieselust@aol.com](mailto:annelieselust@aol.com)

All manuscripts are sent to two reviewers. If there is disagreement, a third reviewer is consulted.

Minor changes in style are made in-house and submitted to the author for approval.

A copyright transfer form is sent to the author for signature.

If a revision of the manuscript is required before publication can be considered, the paper is returned to the author(s) with the reviewers' comments.

In the interest of speed of publication, a pdf file of the type-set text is e-mailed to the corresponding author before publication for final approval.

Additional reprints can be purchased, but the request must be made at the time the manuscript is approved for publication.

Anneliese Lust  
Editor, *Atomic Spectroscopy*  
PerkinElmer  
Life and Analytical Sciences  
710 Bridgeport Avenue  
Shelton, CT 06484-4794 USA

*PerkinElmer* is a registered trademark, and *AAAnalyst* and *Optima 3000* are trademarks of *PerkinElmer, Inc.*  
*SCIEX* and *ELAN* are registered trademarks of *MD Sciex*, a division of *MDS Inc.*  
*IBM* is a registered trademark of *International Business Machine Corporation.*  
*Intel* is a registered trademark of *Intel Corporation.*  
*Milli-Q* is a trademark of *Millipore Corporation.*  
*Suprapur* is a registered trademark of *Merck & Co.*  
*Tygon* is a trademark of *Norton Co.*  
*Xenix* is a trademark of *Microsoft Corporation.*  
Registered names and trademarks, etc. used in this publication even without specific indication thereof are not to be considered unprotected by law.

↓  
Atomic Absorption

# Just touch and go.



## There, that's all the training you need.

Walk up to the AAnalyst 200 and let the touch screen guide you through everything from setup to analysis. It practically tells you what to do—and in your own language. All instrument controls are right there on the screen, available at your fingertips. Even troubleshooting and repairs are easier, with quick-change parts you simply snap out and snap in. No service visit, no down time. As rugged and reliable as ever, our newest AAnalyst is a better way to do AA. Experience it for yourself. Talk to a PerkinElmer inorganic analysis specialist today.



U.S. 800-762-4000 (+1) 203-925-4600